

**IMPACT OF SILVER NANOPARTICLES ON THE NUTRITIONAL
PROPERTIES OF *Spirulina platensis***

SHAROLYNNE LIANG XIAO TONG

MASTER OF SCIENCE

**FACULTY OF SCIENCE
UNIVERSITI TUNKU ABDUL RAHMAN
JANUARY 2023**

**IMPACT OF SILVER NANOPARTICLES ON THE NUTRITIONAL
PROPERTIES OF *Spirulina platensis***

By

SHAROLYNNE LIANG XIAO TONG

A dissertation submitted to Faculty of Science

Universiti Tunku Abdul Rahman

in partial fulfillment of the requirements for the degree of

Master of Science

January 2023

ABSTRACT

IMPACT OF SILVER NANOPARTICLES ON THE NUTRITIONAL PROPERTIES OF *Spirulina platensis*

SHAROLYNNE LIANG XIAO TONG

Spirulina platensis (*S. platensis*) is farmed worldwide due to its nutrient-rich properties and provides multiple benefits to human health. However, the wide usage of silver nanoparticles (Ag NPs) causes pollution which may affect the nutritional quality of *S. platensis*. Hence, this study aimed to investigate the interaction and accumulation of Ag NPs on *S. platensis*, and determine the changes in biomass and nutritional value of *S. platensis* due to the exposure to Ag NPs. The cellular interaction and accumulation of Ag NPs on *S. platensis* were examined through Fourier transformed infrared (FTIR) spectroscopy and scanning electron microscope (SEM). The loss in biomass together with the macromolecules, pigments, and phenolic compounds of *S. platensis* was investigated upon treating with various concentrations of Ag NPs (5, 10, 25, 50 and 100 µg/mL) for 24, 48 72 and 96 h. The EDX analysis confirmed the surface accumulation of Ag NPs on *Spirulina* cells, while SEM images evidenced the surface alterations and damage of the treated cells. The functional groups such as hydroxyl, amine, methyl, amide I, amide II, carboxyl, carbonyl, and phosphate groups from the cell wall of the *S. platensis* were identified to be possibly involved in the interaction of Ag NPs with *S. platensis*. The results showed that the treatment of *S. platensis* with Ag NPs

caused a dose and time-dependent reduction in biomass, macronutrients, pigments and phenolic compounds. The highest detrimental effects were found at 96 h with the reported values of 65.71 ± 2.79 , 67.21 ± 3.98 , 48.99 ± 4.39 and $59.62 \pm 3.96\%$ reduction in biomass, proteins, carbohydrates and lipids, respectively, along with 82.99 ± 7.81 , 67.55 ± 2.63 , 75.03 ± 1.55 , and $63.43 \pm 2.89\%$ loss in chlorophyll-*a*, carotenoids, C-phycoerythrin, and total phenolic compounds of *S. platensis* for 100 $\mu\text{g/mL}$ of Ag NPs. Hence, the study confirmed that the exposure of Ag NPs is detrimental to *S. platensis* where the interaction and accumulation of Ag NPs on *S. platensis* caused reduction in biomass, macromolecules, pigments, and total phenolic compounds.

ACKNOWLEDGEMENT

I would like to send my warm and heartiest appreciation to those who have contributed to the successful completion of this project. A million thanks to those who involved themselves directly and indirectly in all aspects to complete this study.

First and foremost, I would like to express my sincere gratitude to my supervisor, Dr. Sinouvassane Djearamane, for his continuous guidance, encouragement, patience and advice throughout the project. I would like to thank my co-supervisor, Dr. Anto Cordelia Tanislaus Antony Dhanapal, for her guidance, support and advice, and to express my gratitude my external supervisor, Professor. Dr. Wong Ling Shing, INTI International University, for his opinions and feedback throughout the work. I have learned a lot from my supervisors and have broadened my perspective in this studied area.

This research was supported by Universiti Tunku Abdul Rahman (Grant no: IPSR/RMC/UTAR RF/2019-C1/S03), and the Ministry of Higher Education (Grant no: FRGS/1/2020/STG03/INTI/01/1). I would like to express this appreciation to the university UTAR for providing this opportunity to complete my project with sufficient facilities and equipment. Also, thank you to the laboratory officers in UTAR which guided me in the operation and utilization of the equipment and also sharing of their knowledge in this project.

DECLARATION

I SHAROLYNNE LAING XIAO TONG hereby declare that the dissertation is based on my original work except for quotations and citations which have been duly acknowledged. I also declare that it has not been previously or concurrently submitted for any other degree at UTAR or other institutions.



(SHAROLYNNE LAING XIAO TONG)

Date: 21 January 2023

APPROVAL SHEET

This dissertation entitled “**IMPACT OF SILVER NANOPARTICLES ON THE NUTRITIONAL PROPERTIES OF *Spirulina platensis***” was prepared by SHAROLYNNE LAING XIAO TONG and submitted as partial fulfillment of the requirements for the degree of Master of Science at Universiti Tunku Abdul Rahman.

Approved by:



(Dr. Sinouvassane Djearamane)
Supervisor
Department of Biomedical Science
Faculty of Science
Universiti Tunku Abdul Rahman

Date: 21 January 2023



(Dr. Anto Cordelia Tanislaus Antony Dhanapal)
Co-Supervisor
Department of Chemical Science
Faculty of Science
Universiti Tunku Abdul Rahman

Date: 21 January 2023



(Prof. Dr. Wong Ling Shing)
External Supervisor
Life Science Division
Faculty of Health and Life Science
INTI International University

Date: 21 January 2023

FACULTY OF SCIENCE
UNIVERSITI TUNKU ABDUL RAHMAN

Date: 21 January 2023

SUBMISSION OF DISSERTATION

It is hereby certified that **SHAROLYNNE LIANG XIO TONG** (ID No: **19ADM05983**) has completed this dissertation entitled “IMPACT OF SILVER NANOPARTICLES ON THE NUTRITIONAL PROPERTIES OF *Spirulina platensis*” under the supervision of Dr. Sinouvassane Djearamane (Supervisor) from the Department of Biomedical Science, Faculty of Science, Dr. Anto Cordelia Tanislaus Antony Dhanapal (Co-Supervisor) from the Department of Chemical Science, Faculty of Science, and Prof. Dr. Wong Ling Shing (External Supervisor) from the Life Science Division, Faculty of Health and Life Science, INTI International University.

I understand that the University will upload softcopy of my dissertation in pdf format into UTAR Institutional Repository, which may be made accessible to UTAR community and public.

Yours truly,



(SHAROLYNNE LIANG XIAO TONG)

TABLE OF CONTENTS

	Page
ABSTRACT	iii
ACKNOWLEDGEMENT	v
DECLARATION	vi
APPROVAL SHEET	vii
SUBMISSION OF DISSERTATION	viii
TABLE OF CONTENTS	ix
LIST OF TABLES	xii
LIST OF FIGURES	xiii
LIST OF ABBREVIATIONS	xv
CHAPTER	
1 INTRODUCTION	1
1.1 Research Background	1
1.2 Research Objective	6
2 LITERATURE REVIEW	7
2.1 Microalgae	7
2.2 <i>Spirulina platensis</i>	8
2.3 Nutritional Values of <i>Spirulina platensis</i>	9
2.4 Metallic Nanoparticles (MNPs)	11
2.5 Silver Nanoparticles (Ag NPs)	15
2.6 MNPs in the Aquatic Ecosystem	17
2.7 Effects of MNPs on Microalgae	25
2.7.1 Growth rate	25
2.7.2 Macromolecules	26
2.7.3 Pigments	28
2.7.4 Phenolic Compounds	29
2.8 Ag NPs and its Toxicity	30

3	MATERIALS AND METHODS	36
3.1	Overview of Research Methodology	36
3.2	Characterization of Ag NPs	37
3.3	Cultivation of Microalgae	37
3.4	Exposure of Microalgae to Ag NPs	37
3.5	Cellular Interaction and Cellular Accumulation of Ag NPs on Algal Cells	38
3.5.1	Attenuated Total Reflectance Fourier Transformed Infrared (ATR-FTIR) Spectroscopy	38
3.5.2	SEM-EDX Analysis	38
3.6	Effects of Ag NPs on Growth Pattern and Biomass	39
3.7	Effects of Ag NPs to Proteins, Carbohydrates and Lipids	40
3.7.1	Proteins	40
3.7.2	Carbohydrates	41
3.7.3	Lipids	42
3.8	Effects of Ag NPs to Chlorophyll- <i>a</i> , Carotenoids and C-Phycocyanin	43
3.8.1	Chlorophyll- <i>a</i> and Carotenoids	43
3.8.2	C-Phycocyanin	43
3.9	Effects of Ag NPs to Total Phenolic Compounds	44
3.10	Statistical analysis	45
4	RESULTS	46
4.1	Characterization of Ag NPs	46
4.2	Cellular Interaction and Cellular Accumulation of Ag NPs on Algal Cells	48
4.2.1	ATR-FTIR Spectroscopy	48
4.2.2	SEM-EDX Analysis	50
4.3	Effects of Ag NPs on Growth Pattern and Biomass	52
4.4	Effects of Ag NPs to Proteins, Carbohydrates and Lipids	55
4.4.1	Proteins	55
4.4.2	Carbohydrates	56
4.4.3	Lipids	57
4.5	Effects of Ag NPs to Chlorophyll- <i>a</i> , Carotenoids and C-Phycocyanin	58

4.5.1 Chlorophyll- <i>a</i>	58
4.5.2 Carotenoids	59
4.5.3 C-Phycocyanin	60
4.6 Effects of Ag NPs to Total Phenolic Compounds	61
5 DISCUSSION AND CONCLUSION	63
5.1 Cellular Interaction and Cellular Accumulation of Ag NPs on Algal Cells	63
5.1.1 ATR-FTIR Spectroscopy	63
5.1.2 SEM-EDX Analysis	64
5.2 Effects of Ag NPs on Growth Pattern and Biomass	65
5.3 Effects of Ag NPs to Proteins, Carbohydrates and Lipids	67
5.4 Effects of Ag NPs to Chlorophyll- <i>a</i> , Carotenoids and C-Phycocyanin	70
5.5 Effects of Ag NPs to Total Phenolic Compounds	72
5.6 Toxicity Mechanism of NPs	74
5.7 Conclusion	75
5.8 Limitation and Recommendation	76
REFERENCES	78
LIST OF PUBLICATIONS AND CONFERENCE PRESENTATIONS	100
APPENDICES	106

LIST OF TABLES

Table		Page
2.1	Effects of MNPs on microalgae.	21
2.2	Effects of Ag NPs on microalgae.	34
4.1	Possible involvement of functional groups from the cell wall of <i>S. platensis</i> in the binding of Ag NPs on algal cell surface.	48

LIST OF FIGURES

Figures	Page
4.1 Characterization of Ag NPs under (A) SEM with 50,000X magnification, (B) EDX spectrum and (C) XRD pattern.	47
4.2 ATR-FTIR spectrum of control (black line) and 100 µg/mL Ag NPs treated <i>S. platensis</i> at 96 h (blue line).	59
4.3 SEM images of control and 100 µg/mL Ag NPs treated <i>S. platensis</i> at 96 h. (A) control at 1000X magnification; (B) control at 2000X magnification; (C, E) 100 µg/mL Ag NPs treated <i>S. platensis</i> at 1000X magnification; (D, F) 100 µg/mL Ag NPs treated <i>S. platensis</i> at 2000X magnification.	51
4.4 EDX image and spectrum of control (A) and 100 µg/mL Ag NPs treated <i>S. platensis</i> at 96 h (B).	52
4.5 <i>S. platensis</i> cultures treated with different concentrations of Ag NPs at each time interval (24, 48, 72 and 96 h).	53
4.6 Growth pattern of <i>S. platensis</i> treated with different concentrations of Ag NPs at each time interval.	54
4.7 Percentage of loss in biomass concentration of <i>S. platensis</i> relative to control from 24 to 96 h upon treatment of Ag NPs.	54
4.8 Percentage of loss in proteins of <i>S. platensis</i> relative to control from 24 to 96 h upon treatment of Ag NPs.	55
4.9 Percentage of loss in carbohydrates of <i>S. platensis</i> relative to control from 24 to 96 h upon treatment of Ag NPs.	56
4.10 Percentage of loss in lipids of <i>S. platensis</i> relative to control from 24 to 96 h upon treatment of Ag NPs.	57
4.11 Percentage of loss in chlorophyll- <i>a</i> of <i>S. platensis</i> relative to control from 24 to 96 h upon treatment of Ag NPs.	59
4.12 Percentage of loss in carotenoids of <i>S. platensis</i> relative to control from 24 to 96 h upon treatment of Ag NPs.	60

4.13	Percentage of loss in C-phycoyanin of <i>S. platensis</i> relative to control from 24 to 96 h upon treatment of Ag NPs.	61
4.14	Percentage of loss in total phenolic compounds of <i>S. platensis</i> relative to control from 24 to 96 h upon treatment of Ag NPs.	62
5.1	Toxicity mechanism of NPs to algal cell membrane and organelles (Chen et al., 2019).	75

LIST OF ABBREVIATIONS

Ag	Silver
Ag NPs	Silver Nanoparticles
Ag ₂ O	Silver oxide
ANOVA	Analysis of variance
ATR-FTIR	Attenuated Total Reflectance Fourier Transformed Infrared
Au	Gold
BSA	Bovine serum albumin
CaCl ₂ ·2H ₂ O	Calcium chloride dihydrate
CeO ₂	Cerium(IV) oxide
Co	Cobalt
CoCl ₂ ·6H ₂ O	Cobalt(II) chloride hexahydrate
Cr	Chromium
Cu	Copper
CuO	Copper(II) oxide
CuSO ₄ ·4H ₂ O	Copper(II) sulfate tetrahydrate
CuSO ₄ ·5H ₂ O	Copper(II) sulfate pentahydrate
EAA	Essential amino acid
EDX	Energy dispersive X-ray
ENPs	Engineered nanoparticles
FCR	Folin-Ciocalteu phenol reagent
Fe ₂ O ₃	Iron(III) oxide
FeCl ₃ ·6H ₂ O	Iron(III) chloride hexahydrate
FTIR	Fourier transform infrared
GLA	Gamma linoleic acid
H ₃ BO ₃	Boric acid
HCl	Hydrochloric acid

HIV-1	Human immunodeficiency virus type 1
ICP-OES	Inductively coupled plasma-optical emission spectroscopy
K_2HPO_4	Dipotassium hydrogen phosphate
K_2SO_4	Potassium sulfate
Mg	Magnesium
MgO	Magnesium oxide
$MgSO_4 \cdot 7H_2O$	Magnesium sulfate heptahydrate
$MnCl_2 \cdot 4H_2O$	Manganese(II) chloride tetrahydrate
MNPs	Metallic nanoparticles
MRI	Magnetic resonance imaging
Na_2CO_3	Sodium carbonate
$Na_2EDTA \cdot 2H_2O$	Disodium ethylenediaminetetraacetate dihydrate
$Na_2HPO_4 \cdot 7H_2O$	Sodium phosphate dibasic heptahydrate
$Na_2MoO_4 \cdot 2H_2O$	Sodium molybdate dihydrate
NaCl	Sodium chloride
$NaH_2PO_4 \cdot H_2O$	Sodium phosphate monobasic monohydrate
$NaHCO_3$	Sodium bicarbonate
$NaK \text{ tartrate} \cdot 4H_2O$	Potassium sodium tartrate tetrahydrate
$NaNO_3$	Sodium nitrate
NaOH	Sodium hydroxide
NiO NPs	Nickel oxide nanoparticles
NPs	Nanoparticles
Pb	Lead
PBS	Phosphate buffered saline
POD	Peroxidase
PRINT	Particle replication in non-wetting templates
Pt	Platinum
ROS	Reactive oxygen species

SEM	Scanning electron microscope
SEM-EDX	Scanning electron microscope-energy dispersive X-ray
SERS	Surface-enhanced Raman spectroscopy
SOD	Superoxide dismutase
TEM	Transmission electron microscope
Ti	Titanium
TiO ₂	Titanium oxide
TiO ₂ NPs	Titanium oxide nanoparticles
XPS	X-ray photoelectron spectroscopy
XRD	X-ray diffractometry
Zn	Zinc
ZnCl ₂	Zinc chloride
ZnO NPs	Zinc oxide nanoparticles
ZnO	Zinc oxide
ZnSO ₄ ·7H ₂ O	Zinc sulfate heptahydrate

CHAPTER 1

INTRODUCTION

1.1 Research Background

Nanotechnology involves the study and utilization of atoms or molecules with dimensions less than 100 nm. Richard Zsigmondy, a chemistry Nobel Prize winner from 1925, was the one who initially coined the term “nanometer” specifically to describe particle size. Later, Richard Feynman, the 1965 Nobel Prize Laureate in physics, introduced modern nanotechnology with the concept of manipulating matter at the atomic level. Nanotechnology is a fast growing and dynamic field of study, with utilities across all the other scientific disciplines such as wound dressings, wood flooring, electronics, biological sensors, water treatments, and also cosmetic industries. The wide applications and unique features of NPs clearly explained the huge market potential for nanoparticles (NPs) (Banerjee and Roychoudhury, 2019). The global nanomaterials market size was predicted to have \$9.68 billion in 2021, and the demand for nanomaterials will likely increase due to the growing usage of NPs. Precedence Research (2022) estimates that the global market for nanomaterials would be valued \$43.1 billion by 2030, growing at a spectacular compound annual growth rate of 18.05% between 2022 and 2030.

Among the other manufactured engineered nanomaterials (ENMs) such as gold platinum, zinc, and others, silver nanoparticles (Ag NPs) are estimated to have a worldwide production of about 360 to 450 tons per year by 2025 and will increase

to produce around 800 tons per year in the future (Narsing Rao and Dhulappa, 2022). According to the Allied Market Research report released in 2022, Ag NPs global market was valued \$1.5 billion in the year of 2020, and is expected to reach \$6.6 billion by 2030, with a compound annual growth rate of 15.6% from year 2021 to 2030 (Moon et al., 2022), which implies that Ag NPs are widely utilized on a global scale. Due to the strong antimicrobial property, Ag NPs comprise the largest family of materials utilised in food, biomedical, and personal care goods (Vance et al., 2015) and are also rapidly being utilised in wound dressings, textiles, wood flooring, food storage containers, medicine, cosmetics, electronics, and optical equipment as a broad-spectrum antimicrobial agent (Karlsson et al., 2015; Panda, 2021; Tolaymat et al., 2010).

The increased prevalence of ENMs inevitably lead to NPs pollution of soil and aquatic environment including groundwater (Lohse et al., 2017; Lone et al., 2013). The effluents from wastewater treatment plants and combustion of waste products are stated to be the major entry points of NPs into the aquatic environment (Dalai et al., 2012; Li and Lenhart, 2012; Liang et al., 2020). Typically, about 5 to 95% of the total quantity of Ag NPs in commercial products may be released into wastewater treatment plant (Mueller and Nowack, 2008). According to reports, the Connecticut undeveloped headwaters, rivers from industrial areas, and rivers from urban areas each contained between 5 to 100 ng/L of Ag NPs (Bilberg et al., 2012). While, the concentration of Ag NPs in Texas river, Trinity river (Wen et al., 1997) and Rhine river (Blaser et al., 2008) ranged from 0.01 to 62 ng/L, 0.4 to 6.4 ng/L and 4 to 40 ng/L, respectively. Syafiuddin et al. (2018) investigated the

concentrations of Ag NP in the water environment in Malaysia and reported to have the range of 0.13 to 10.16 mg/L and 0.13 to 20.02 mg/L of Ag NPs in rivers and sewage treatment plants respectively. Ag NPs also were reported to cause toxicity towards several aquatic organisms including bacteria (Morones et al., 2005; Sondi and Salopek-Sondi, 2004), algae (Navarro et al., 2008b; Oukarroum et al., 2012; Park et al., 2010), and fish (Griffitt et al., 2009; Laban et al., 2010; Lee et al., 2007). The transport and subsequent accumulation of NPs in higher aquatic species through the food chain may be facilitated by the ingestion of NPs by lower trophic organisms (Croteau et al., 2011; Miao et al., 2010; Zhao and Wang, 2010). Thus, the ecosystem as a whole, will likely be influenced by Ag NPs within lower trophic organisms (Burchardt et al., 2012).

Spirulina, one of the many nutritional supplements that are commercially accessible, has recently been the subject of extensive food science and biochemistry research. *Spirulina* is an unrivalled source of protein, unsaturated fatty acids, minerals, and vitamins, and is made up of biomass produced by cyanobacteria of the *Arthrospira* genus, most typically *Arthrospira platensis*. As *Spirulina* can be produced and harvested very easily, *Spirulina* has been used largely as a food supplement by cultures living near alkaline lakes for centuries, including areas like Lake Texcoco in Mexico and Lake Chad in Africa. *Spirulina* is harvested in these areas using tiny nets, and it is then processed to create an appetising blue-green cake (Reboleira et al., 2019; Wan et al., 2021). The Kanembu people who live around the shores of Lake Chad are popular in harvesting *Spirulina*. The harvested *Spirulina* are drained with cloth. The drained algae are then sun-dried to enable

longer storage before being sold in neighbourhood markets. Until now, *Spirulina* continues to be a significant source of protein in African regions that are deficient in nutrients and vitamins (Belay, 2007). The strong links between *Spirulina* ingestion and therapeutic advantages in a wide range of illnesses have been demonstrated via considerable research, including cancer, viral infections, cardiovascular and inflammatory illnesses, hypercholesterolemia, and glycemia (Deng and Chow, 2010). *Spirulina* is currently grown in many nations, either in greenhouses or outside ponds, as a result of growing knowledge of its functional and nutritional benefits. The cultivated *Spirulina* is used as a supplement for poultry and other land animals, as a primary ingredient in fish and shrimp diets, and in human and animal feed (Habib et al., 2008).

Spirulina is a well-known nutrient microalga that grows in water bodies with high salt concentration ranging from 8.5 to 200 g/L and alkaline pH (9.5 to 11) which is also known as marine microalgae (Moraes et al., 2013). *Spirulina* contains about 55-70% proteins, 15-25% carbohydrates, 6-13% nucleic acids, 5-6% lipids, and 2.2-4.8% minerals (Reboleira et al., 2019). Vitamins such as B1, B2, B3 and B12, photosynthetic pigments, and minerals like calcium, copper, iron, magnesium, phosphate, sodium, and zinc are also rich in *Spirulina* species (Wan et al., 2021). Among all the *Spirulina* species, *Spirulina platensis* is more popular and mostly used for nutritional and therapeutic purposes (Kameshwari et al., 2020), which made the cultivation of *S. platensis* become industrialized in a number of countries (del Rio-Chanona et al., 2015). *S. platensis* has been commercially produced for decades and is used as food coloring, aquaculture, medicines, nutraceuticals, and

vitamin supplements (Abdulqader et al., 2000; de Marco Castro et al., 2019). Nevertheless, the contamination of NPs on the nutrient microalgae throughout the development stage in the water bodies may cause negative effects in the nutritional value of the nutrient rich microalgae through physiological and biochemical changes, thereby causing deleterious impacts in its nutritional quality and food chain (Lone et al., 2013).

S. platensis has the capacity to effectively accumulate NPs in its algal biomass (Al-Dhabi, 2013; Comotto et al., 2014; Dazhi et al., 2003; Djearmane et al., 2018a; Zinicovscaia et al., 2017). Researches have reported the negative effects of heavy metals on the nutritional values of *S. platensis* (Gupta et al., 2014; Zinicovscaia et al., 2017). Rzymiski et al. (2019) highlighted the continuous need to monitor the microalga supplements in order to fully eliminate those of low quality and to ensure the consumer safety. Although *S. platensis* is one of the most popular microalgae used for diet and supplements, and Ag NPs is one of the most frequently used ENMs, the detrimental impact of Ag NPs on the nutritional values of *S. platensis* are not yet reported. Hence, this study appraised the detrimental effects of Ag NPs on the nutritional values of *S. platensis*. Findings of this study will be helpful to detect the contamination of Ag NPs in the nutrient microalga *S. platensis* and thus will help to produce and provide the consumers with high-quality *Spirulina* nutritional supplements with uncompromised nutritional values. In other terms, the consumption of NPs contaminated nutrient microalgae will compromise the supply of expected nutrients and may also cause health hazards to the consumers due to the accumulated NPs.

1.2 Research Objectives

The present study designed to evaluate the detrimental effects of Ag NPs on the nutritional values of *S. platensis* through investigating the interaction and cellular accumulation of Ag NPs in *S. platensis* and the corresponding changes in biomass, macromolecules (proteins, carbohydrates, lipids), pigments (chlorophyll-*a*, carotenoids, C-phycoerythrin) and phenolic compounds in *S. platensis*. The specific objectives of this study are:

- 1) To study the cellular interaction and cellular accumulation of Ag NPs in *S. platensis* and the subsequent morphological alterations of *S. platensis* with the presence of Ag NPs.
- 2) To evaluate the changes in the biomass of *S. platensis* due to the presence of Ag NPs.
- 3) To investigate the effects of Ag NPs to macromolecules, pigments, and phenolic compounds of *S. platensis*.

CHAPTER 2

LITERATURE REVIEW

2.1 Microalgae

Microalgae are unicellular photosynthetic organisms that use light energy to convert atmospheric carbon dioxide into organic carbon. Microalgae have a quick generation period and can develop exponentially in optimum environmental conditions (Devi et al., 2014). Microalgae have been processed for food and supplements for over a thousand years because of their strong nutritional qualities, including proteins, vitamins (A, B1, B2, B6, B12, C and E), minerals (potassium, iron, magnesium, calcium and iodine), and other nutrients (Koyande et al., 2019; Molino et al., 2018). Some of the widely used microalgae species that are with high nutritional qualities such as *S. platensis*, *Dunaliella terticola*, *Chlorella sp.*, *Dunaliella saline*, *Skeletonema*, *Nannochloris*, *Nitzschia*, *Schizochytrium*, *Tetraselmis*, *Haematococcus*, *Botryococcus*, *Phaeodactylum*, *Porphyridium*, *Chaetoceros*, *Cryptocodinium*, and *Isochrysis* (Sathasivam et al., 2019). Microalgae with rich source of essential nutrient have become a major source of food, especially in Asian countries such as China, Japan and Korea (Jibri et al., 2016).

2.2 *Spirulina platensis*

Arthrospira is generally known as *Spirulina* due to its spiral or helical shape, is a type of cyanobacterium species that belongs to the Microcoleaceae family. Cyanobacteria is a Gram-negative bacterium that has been categorized as blue-green algae because they produce the blue-green pigment phycocyanin, which gives them their distinctive colour. *Spirulina* is an obligate photoautotrophic filamentous species and is prokaryotic in structure that has a lamellar photosynthetic system, ribosomes, many inclusions, and a multilayered cell wall. Natural alkaline waters with high mineral content and temperatures between 25 and 40°C are ideal for cyanobacteria growth. The filament of cyanobacteria can grow to a length of 0.5 mm, due to its helical shape and the existence of gas vacuoles inside the cells, floating mats are formed (Ali and Saleh, 2012; Fais et al., 2022).

S. platensis generates filamentous, helicoidal trichomes as it grows and divides by binary fission and oxygenic photosynthesis (Jung et al., 2021). The blue-green non-heterocystous filaments of *S. platensis* which are composed of vegetative cells that undergo binary fission in a single plane, have clearly discernible transverse cross-walls under light microscopy. The gliding motility of filaments, which are single and free-floating, is visible. The trichomes of *Spirulina* are covered in a thin sheath and exhibit more or less barely perceptible constrictions at the cross-walls (Ali and Saleh, 2012). The apices are either barely or completely unattenuated. Apical cells can be capitated and calyptrate, and they can be broadly spherical or pointy. The width of the trichomes which ranges from around 6 to 12 µm in a variety of shapes and is made up of cylindrical cells that are shorter than broad (Ciferri, 1983).

The helix geometry of *Spirulina* can be impacted by environmental factors, particularly temperature, physical conditions, and chemical conditions (van Eykelenburg, 1979). The reversible change from helix to spiral shape when moving the filaments from liquid to solid medium is one significant modification of this geometry. Although the degree of helicity can vary significantly across different strains of the same species and within a single strain, the helical form of the trichome is thought to be a permanent and constant feature retained in culture (Mühling et al., 2003). Variations in trichome geometry may be seen even in naturally occurring monospecific populations. Furthermore, spontaneous culture variations that are straight or nearly straight have been observed numerous times (Venkataraman, 1997; Zeng and Vonshak, 1998). A strain cannot change back to its helical shape after it has converted to the straight form, whether naturally or as a result of physical or chemical treatments like UV light or chemicals. This is as a result of a mutation that occurs in some trichomes under specific growth circumstances. Straight trichomes are frequently found in *Spirulina* cultures, which may indicate that plasmids carry the helicity trait. When a few filaments in a culture of a helically coiled strain happen to become straight, they often start to dominate (Ali and Saleh, 2012).

2.3 Nutritional Values of *Spirulina platensis*

Spirulina platensis has a well-balanced derived composition of various biochemical properties ranging from vitamins, minerals (8%), proteins (60% - 70%), phenolic compounds, γ -linolenic acid (49%), phycocyanin (15%), and constituent of

phytochemicals (Bensehaila et al., 2015; Molino et al., 2018; Stanic-Vucinic et al., 2018). In addition, the microalgae is well known for its higher content of carotenoids (456.00 mg/100g of dry weight), about 80% are beta-carotene and others made up of secondary carotenoids like xanthophyll typically higher than found in carrots (Bensehaila et al., 2015; Koru, 2012; Shao et al., 2019). *S. platensis* is also rich in complete essential amino acids (EAA), gamma linoleic acid (GLA) (Jaime et al., 2005; Koyande et al., 2019) and antioxidants due to the accumulation of various types of phytochemicals to neutralize the oxidative stress caused by reactive oxygen species (ROS) (Richmond, 2003; Siddiqui and Prasad, 2017). High nutritional values with natural antioxidant properties, and the low production cost of *S. platensis* has created the opportunity for *S. platensis* to be exploited as an alternative food source and as dietary supplements due to its therapeutic effects (Molino et al., 2018; Richmond, 2003). As compared to leguminous plant, *Spirulina*'s protein content is 20% higher and it can be consumed whole (Bensehaila et al., 2015). The photosynthetic ability of *S. platensis* renders production of valuable nutrients like high levels of essential amino acids, fatty acids, and carotenoids at an economical level has place *S. platensis* in the frontline as a product for commercialization especially in today's nutraceutical, food supplement, and pharmaceutical sector as well as for the renewable bioenergy (Koyande et al., 2019; Shao et al., 2019).

Since *Spirulina* is regarded as a nutritional supplement in the United States, the production of *Spirulina* supplements is not actively regulated, and no purity or standards that are enforced. *Spirulina* supplements are graded as "possibly safe",

provided they are free of contamination but “likely unsafe” if contaminated (Jung et al., 2019). Researchers in public health have expressed the concern about the lack of customer assurance in the purity of *Spirulina* supplements. Since the likelihood of contamination in microalgae is higher in open pond systems than in closed bioreactors, increased quality control for algal products produced in open ponds is required (Lane, 2022). The heavy metal contamination of *Spirulina* supplements has also raised concerns. According to the Chinese State Food and Drug Administration, *Spirulina* supplements sold in China were frequently contaminated with lead, mercury, and arsenic, most likely as a result of water pollution (Al-Dhabi, 2013; Jung et al., 2019). Therefore, it is crucial to only use *Spirulina* from the manufacturers who produce the supplements under strict and standardized guidelines.

2.4 Metallic Nanoparticles (MNPs)

Metallic nanoparticles (MNPs) are objects with a submicron size that are made of pure metals such as silver (Ag) , gold (Au), zinc (Zn), titanium (Ti), copper (Cu) and others; or their compounds such as oxides, hydroxides, sulfides, chlorides and fluorides (Mahana et al., 2021). The antimicrobial, optical characteristics and biocompatibility properties of MNPs made them to be the widely used in biomedicine. The nanosized of MNPs enable them to communicate with the biomolecules on the microalgae cell surfaces and inside the cells in a variety of ways that may be decoded and assigned to different biochemical and physiochemical characteristics of the cells (Mody et al., 2010). For example, TiO₂

NPs are commonly used in sunscreens, iron oxide used in magnetic resonance imaging (MRI), silica used as vaccine adjuvants, and CeO₂ used in catalyst and automobile industry (Karlsson et al., 2015).

Depending on the method used, MNPs can be obtained in the shape of nanoparticles, nanospheres or nano capsules. MNPs can be made from a wide range of materials including proteins, polysaccharides and synthetic polymers. The choice of matrix materials will be influenced by elements such as the required size of NPs, surface characteristics, level of biodegradability, biocompatibility, toxicity, and antigenicity of the finished product (Mohanraj and Chen, 2007). The three most popular techniques to produce NPs are ionic gelation or coacervation of hydrophilic polymers, polymerization of monomers, and dispersion of preformed polymers (Mohanraj and Chen, 2007). There are further ways to create MNPs, including the use of supercritical fluid technology and the particle replication in non-wetting templates (PRINT) technique, which has been claimed to have complete control over particle size, shape, and content (Rolland et al., 2005). Besides chemically synthesized, MNP can also be synthesized using living organisms like bacteria, fungi, and plants (Li et al., 2012).

There are some advantages and disadvantages of MNPs. MNPs have several benefits, including the ability to improve Rayleigh scattering, surface-enhanced Raman scattering, high plasma absorption, and the ability to ascertain chemical information on metallic nanoscale substrates (Li et al., 2007). One of the disadvantages of MNPs is the particle instability. MNPs can undergo transformation as they are thermodynamically unstable and lie in the region of high

energy local minima. This leads to deterioration of quality, poor corrosion resistance, and the main concern is retaining the structure of MNPs become difficult. The chance of impurity in MNPs can also be high as NPs are highly reactive. NPs are synthesized in the form of encapsulation in solution form, where this become a challenge to overcome impurities in NPs. MNPs are also reported to be toxic, carcinogenic and cause irritation as they become transparent to the cell dermis (Granqvist and Buhrman, 1976; Nagasamy Venkatesh et al., 2018).

MNPs can be characterized using different approach like infrared spectroscopy to obtain information on the organic layers surrounding the MNPs and to understand the surface structure of MNPs. The size, shape, crystallinity, and interparticle interaction of the NPs can be studied using a transmission electron microscope (TEM). The interaction of the incident electron beam with the specimen in a scanning electron microscope (SEM) results in secondary electrons, which can be used to determine the purity of MNPs samples. A practical and often used method for figuring out the crystalline structure of MNPs is X-ray diffractometry (XRD). The Debye-Scherrer method can also be employed with the XRD line to determine the particle size. Besides, Fourier transform infrared (FTIR) spectroscopy is commonly used as compared to IR spectroscopy to determine the functional groups attached to the surface of MNPs. The oxidation state of the surface of MNPs can be detected using X-ray photoelectron spectroscopy (XPS) (Kumar and Dixit, 2017; Nagasamy Venkatesh et al., 2018).

MNPs are generally used in different functions such as optimal, thermal, electrical and others. Imaging sensors, displays, solar cells, photocatalysts, biomedical

devices, optical detectors, and lasers are a few examples of MNPs employed in optical functions. These devices heavily depend on size, shape, surface area, doping, and interactions of MNPs with the environment. Polymers filled with nanotubes leads to improvement in the mechanical functions and is highly depends on the filter type and the way which the nanotubes are conducted. MNPs can be used to made electronic wiring as they have lower boiling point where the MNPs particle size less than 10 nm has a lower melting point than bulk materials. MNPs also can be used to make high temperature superconductivity materials. By combining NPs with metals or ceramics, the mechanical properties of MNPs can be increased. Some MNPs such as Pt and Au NPs can have magnetic properties in nanosized but not in bulk size, provide chances to adjust the physical characteristics of NPs (Nagasamy Venkatesh et al., 2018).

In short, MNPs are highly demanded in this 21st century as they can be synthesized in various methods and the process of MNPs synthesis is important as it can affect the properties of the MNPs being synthesized. MNPs can play a vital role in individualized medicine although more research is needed, and noble MNPs can be effective in therapeutic and diagnostic agents as MNPs show new properties at the atomic and nanosized scale. It cannot be denied the demand of MNPs used in healthcare, industry and cosmetic is increasing, however, safety measures also need to be taken to protect human health and the surrounding environment.

2.5 Silver Nanoparticles (Ag NPs)

Silver nanoparticles (Ag NPs) are tiny Ag particles, ranging in size from 1 to 100 nm. Some materials, despite being widely referred as “Ag”, include a significant amount of Ag₂O due to the large proportion of surface to bulk Ag atoms (Mody et al., 2010). There is currently work being done to include Ag NPs into a variety of medical products, such as surgical masks, bone cement, and other items. Additionally, Ag NPs has been demonstrated that using ionic Ag to cure wounds in the proper dosages (Atiyeh et al., 2007; Lansdown, 2006; Qin, 2005). Ag NPs have taken over from silver sulfadiazine as the preferred agent for treating wounds (Atiyeh et al., 2007). On the surfaces of home appliances, Samsung has also developed and sold a substance called Silver Nano that contains Ag NPs. Moreover, Ag NPs have drawn a lot of interest in biological imaging employing surface-enhanced Raman spectroscopy (SERS) because of their appealing physiochemical features. In reality, individual Ag NPs are excellent candidates for molecular labelling due to their surface plasmon resonance and huge effective scattering cross-section (Schultz et al., 2000).

Ag NPs are typically created by reducing a silver salt with a reducing agent such as sodium borohydride with the presence of colloidal stabilizer. Polyvinyl alcohol, polyvinylpyrrolidone, bovine serum albumin (BSA), citrate, and cellulose are the most often employed colloidal stabilizers. The creation of Ag NPs by ion implantation requires the use of starch as a stabilizer and β -d-glucose as a reducing sugar in more recent innovative approaches (Stepanov et al., 2002). All the produced NPs are not equal, as it has been demonstrated that the effectiveness of

NPs is influenced by the size and form of the NPs. Elechiguerra et al. (2005) reported that Ag NPs interact with HIV-1 in a size-dependent manner, with particles only in the 1–10 nm range adhering to the virus, and, further propose that the preferential attachment of Ag NPs to the gp120 glycoprotein knobs mediates their interaction with the HIV-1 virus. Furno et al. (2004) also reported a similar finding where they created biomaterials by utilizing supercritical carbon dioxide to impregnate silicone covered with Ag₂O NPs. These cutting-edge biomaterials were created with the intention of lowering antimicrobial infection. Although the findings were inconsistent, the process permits the first ever Ag impregnation of medicinal polymers and holds out the prospect of producing an antibacterial biomaterial.

Ag NPs is likely known for their antibacterial properties in the medical and healthcare area where in the inclusion of Ag NPs into numerous products has been studied. Urnukhsaikhan et al. (2021) reported that Ag NPs exhibited antibacterial activity on both Gram-negative (*Escherichia coli*) and Gram-positive bacteria (*Micrococcus luteus*) with 5.5 ± 0.2 mm to 6.5 ± 0.3 mm and 7 ± 0.4 mm to 7.7 ± 0.5 mm inhibition zone. Besides, the antibacterial activity of Ag NPs against different Gram-negative bacteria was also determined. The minimum inhibitory concentration (MIC) and minimum bactericidal concentration (MBC) of Ag NPs against *Salmonella typhimurium*, *Salmonella enteritidis*, *E. coli* and *Klebsiella pneumoniae* were 3.9, 3.9, 7.8, 3.9 and 7.8, 3.9, 7.8, 3.9 $\mu\text{g/mL}$, respectively (Loo et al., 2018). Although the exact toxicity mechanism for Ag NPs has not been completely identified, there are multiple antibacterial actions that have been

proposed. Firstly, the release of Ag ions can attach to the bacterial cell wall and cytoplasmic membrane through the electrostatic attraction and affinity to sulfur proteins, which will lead to the disruption of bacterial envelop due to the enhanced cytoplasmic membrane permeability (Khorrami et al., 2018). Secondly, the generation of ROS. The ROS can cause disruption in the bacterial cell membrane and DNA alteration as sulfur and phosphorous are the vital components of DNA. The interaction of Ag ions with the components can affect the replication of DNA, cell reproduction, and subsequently cause cell death (Ramkumar et al., 2017). Ag ions can also inhibit the synthesis of bacterial proteins by denaturing the ribosomes in the cytoplasm (Durán et al., 2016). Moreover, Ag NPs can be involved in the bacterial signal transduction by dephosphorylate tyrosine residues on the peptide substrates and lead to cell apoptosis and termination of cell multiplication (Li et al., 2019).

2.6 MNPs in the Aquatic Ecosystem

The anthropogenic revolution began with the agricultural revolution 10,000 years ago and continued with the industrial revolution in the 1700s and the information revolution that followed after is consistent with the technological development of each revolution and era. These revolutions were able to and now are able to meet the demands of the world's expanding population, with a cost associated with pollution and global warming (Al-Homaidan et al., 2014; Anastopoulos and Kyzas, 2015). This has a negative and irreversible impact on the environment, as well as on the health, economy, and society (Al-Homaidan et al., 2014). However,

regardless of the difficulties that have yet to discover a long-term solution to the pollution, microalgae are the front-runners in tackling this situation (Anastopoulos and Kyzas, 2015). The increased use of metals and MNPs in the commercial industry is causing metals and MNPs contamination of soil and aquatic environment (Lohse et al., 2017; Lone et al., 2013). Algae are the most vulnerable aquatic species to NPs as they are toxicant-sensitive and would have impacts on those higher organisms through the intake of NPs contaminated biomass (Banerjee and Roychoudhury, 2019; Neale et al., 2015; Tang et al., 2018; Zhang et al., 2016).

MNPs at low concentrations are non-toxic to microalgae for their cellular functions as small amount of the MNPs can act as the essential minerals for the growth of microalgae (Aravantinou et al., 2015). Some of the elements act as the components for photosynthetic electron transport proteins, photosynthetic water oxidizing centers, or constituents of vitamins (Andersen, 2005). They also can serve as cofactors for enzymes in carbon dioxide fixation (Moroney et al., 2001), DNA transcription and phosphorous acquisition (Sunda, 2012) or N₂ assimilation (Bothe et al., 2010) and nitrate reduction (Vega et al., 1971). Microalgae has the ability to withstand high level of nanoparticle despite the increasing toxicity level of concentrations through its bioaccumulation process (Govindaraju et al., 2008; Li et al., 2017). This is due to its ability to create a resistance towards such incidence, which enables for such high level of concentration of chemicals to be accumulated (Govindaraju et al., 2008; Richmond, 2003). Although low dose of the metals and MNPs can promote the growth of microalgae, however, high dose of metals and MNPs can cause toxicity (Liang et al., 2020). Multiple studies had reported the

toxicity of metals and MNPs to microalgae and subsequently affects their nutritional values. Although metals and MNPs generally shows negative effects on microalgae, however, some research also observed stimulatory outcomes during the cultivation of microalgae, depending on the metals or MNPs used and also the species used in the study. Table 2.1 shows the effects of MNPs on microalgae.

Lau et al. (2022) studied on different type of NPs (carbon-based, metal oxide based and noble metal-based) found out that the NPs tested improved the growth and photosynthesis efficiency of microalgae at low concentrations, ranging between 1 and 15 mg/L, depending on the type of NPs. While, high concentrations caused inhibition of microalgae growth and reduced photosynthesis efficiency. Saçan et al. (2007) studied the effect of lead and aluminum on *Dunaliella. tertiolecta*, and El-Sheekh et al. (2003) studied cobalt on *Monoraphidium minutum* and *Nitzschia perminuta*; reported that low concentration of the respective metals showed increased percentage on growth of respective microalgae. The stimulation of growth on *M. minutum* and *N. perminuta* at low concentration of cobalt may be due to the substitution of cobalt for zinc in some metalloenzymes. Besides the stimulation of growth, El-Sheekh et al. (2003) also reported the increased production of chlorophyll at low concentration of cobalt due to the substitution of cobalt for zinc and increase production of carotenoids. Moreover, microalgae tend to adjust their cellular metabolism and store more large molecules such as proteins and lipids when they are under stress condition (He et al., 2017) which may be the reason for the increased production of macromolecules at lower NPs concentrations.

The increased in the carbohydrate production may be a protective mechanism in response of environmental stress (Bolouri-Moghaddam et al., 2010).

A study by Lone et al. (2013) reported that the treatment of ZnO NPs resulted in 93.5% loss of chlorophyll-*a* and 50% decrease in carotenoids of *S. platensis* on day 10 and Mary Leema et al. (2010) reported that the salt stress on *S. platensis* from the treatment with sea water resulted in 53.1% fall of chlorophyll-*a*, 37.5% decrease in carotenoids and 32.1% loss in phycocyanin during day 25. Gupta et al. (2014) observed a concentration and time dependent fall in chlorophyll-*a* of *S. platensis* with a significantly maximum reduction of 63.9% at 10 mg/L of chromium (Cr) on day 9. Treatment with selenium (100 mg/L) resulted in 90% decrease in phycocyanin pigment of *S. platensis* on day 3 (Zinicovscaia et al., 2017) and the treatment of *Spirulina* cells with 1 mg/L of copper caused 50% decrease in algal biomass on the day 7 (Deniz et al., 2011). The exposure of TiO₂ NPs on *S. platensis* resulted in 74.1% decrease in biomass on day 15 with 100 mg/L of TiO₂ NPs (Comotto et al., 2014). ZnO NPs demonstrated the highest level of toxicity among other metal and metal oxide NPs in *Pseudokirchneriella subcapitata* with a significant reduction of growth (EC₅₀) at 42 mg/L (Aruoja et al., 2009) and 4.6 mg/L in *Thalassiosira pseudonana* (Wong et al., 2010). The EC₅₀ values of NiO NPs on *Chlorella vulgaris* was reported to be 32.28 mg/L when exposed for 72 h. The toxicity of NiO NPs caused plasmolysis, disruption of cell membrane, and disarray in the thylakoid structures of *C. vulgaris*. It was also reported that the organisms in the higher food chain that take the NiO NPs contaminated algae were susceptible to the toxic effects of NiO NPs (Gong et al., 2011).

Table 2.1: Effects of MNPs on microalgae.

NPs	Size (nm)	Microalgae strain	Time (h)	Concentration (mg/L)	Effects	Reference
C	<2	<i>Scenedesmus obliquus</i>	96	40	No significant effect on cell growth; Reduction in chlorophyll (28%), proteins (7%) and lipids (41%); Increased in soluble sugars (12%)	(He et al., 2017)
Co	<100	<i>Microcystis sp.</i>	120	5	Reduction in biomass concentration (69%), chlorophyll (84%) and carotenoids (69%)	(Anusha et al., 2017a)
Co	<100	<i>Oscillatoria sp</i>	120	5	Reduction in biomass concentration (88%), chlorophyll (82%) and carotenoids (73%)	(Anusha et al., 2017a)
Cu	89	<i>C. vulgaris</i>	192	50	Reduction in chlorophyll- <i>a</i> (72%), carotenoids (76%), proteins (50%), lipids (20%) and carbohydrates (38%)	(Sibi et al., 2017)
CuO	<100	<i>Chlamydomonas reinhardtii</i>	72	1000	EC ₅₀ = 250.45 mg/L, NOEC ≤100 mg/L Reduction in total chlorophyll (74%) and carotenoids (82%); Increase in ROS level (190%) and lipid peroxidation (73%)	Melegari et al., 2013

Table 2.1: Effects of MNPs on microalgae (continued).

NPs	Size (nm)	Microalgae strain	Time (h)	Concentration (mg/L)	Effects	Reference
CuO	<100	<i>Nannochloropsis oculata</i>	72	200	MTT assay shows 70% toxicity to cells; Reduction growth rate (98%), chlorophyll (52%), carotenoids (46%), LDH activity (5.7-fold); Increased in H ₂ O ₂ level (2.64-fold), MDA level (6.02-fold), phenolic compounds (1.79-fold) and oxidative enzymes (CAT 2.48-fold, APX 2.18-fold and PPO 4.89-fold)	(Fazelian et al., 2019)
Fe ₂ O ₃	<30	<i>S. obliquus</i>	96	100	Reduction in cell density (17%); Reduction in chlorophyll (10%) and lipids (21%); Increased in proteins (15%) and soluble sugars (62%)	(He et al., 2017)
Mg	82	<i>C. vulgaris</i>	192	200	Reduction in chlorophyll- <i>a</i> (32%), carotenoids (61%) and proteins (36%); Increment in lipids (52%) and carbohydrates (36%)	(Sibi et al., 2017)
MgO	<50	<i>S. obliquus</i>	96	100	Complete growth inhibition; Reduction in chlorophyll (88%) and lipids (76%); Increased in proteins (55%) and soluble sugars (107%)	(He et al., 2017)

Table 2.1: Effects of MNPs on microalgae (continued).

NPs	Size (nm)	Microalgae strain	Time (h)	Concentration (mg/L)	Effects	Reference
Pb	76	<i>C. vulgaris</i>	192	100	Reduction in chlorophyll- <i>a</i> (39%) and carotenoids (78%); Increment in proteins (23%), lipids (77%) and carbohydrates (19%)	(Sibi et al., 2017)
TiO ₂	14	<i>C. vulgaris</i>	504	100	Reduction in biomass concentration (17%) and intracellular phenolic content (17%); Extracellular phenolic content reduced 7% but is not significant	(Comotto et al., 2014)
TiO ₂	14	<i>Haematococcus pluvialis</i>	504	100	Reduction in biomass concentration (18%) and intracellular phenolic content (12%). Slight increase in extracellular phenolic concentration	(Comotto et al., 2014)
TiO ₂	<100	<i>S. platensis</i>	120	100-500	NPs concentration of 100 to 500 mg/L did not show significant biomass reduction using cells at stationary phase. While, 74% growth inhibition observed NPs was exposed since beginning of culture. Increased production of extracellular polyphenols with decrease in intracellular polyphenols, and 66% reduction in lipids	(Casazza et al., 2015a)

Table 2.1: Effects of MNPs on microalgae (continued).

NPs	Size (nm)	Microalgae strain	Time (h)	Concentration (mg/L)	Effects	Reference
TiO ₂	14	<i>S. platensis</i>	504	100	Reduction in biomass concentration (74%) and intracellular phenolic compounds (24%); Extracellular phenolic content increased 127%	(Comotto et al., 2014)
ZnO	92	<i>C. vulgaris</i>	192	200	Reduction in chlorophyll- <i>a</i> (49%) and carotenoids (69%); Increment in proteins (17%), lipids (72%) and carbohydrates (45%)	(Sibi et al., 2017)
ZnO	45	<i>C. vulgaris</i>	72	200	Reduction in growth rate (62%), biomass concentration (56%) and chlorophyll- <i>a</i> (68%)	(Djearamane et al., 2019b)
ZnO	52	<i>H. pluvialis</i>	96	200	Reduction in cell viability (53%), biomass concentration (49%), chlorophyll- <i>a</i> (63%), carotenoids (43%) and astaxanthin (48%)	(Djearamane et al., 2019a)
ZnO	45	<i>S. platensis</i>	96	200	Reduction in cell viability (87%), algal biomass (76%), chlorophyll- <i>a</i> (92%), carotenoids (76%) and phycocyanin (74%)	(Djearamane et al., 2018a)

2.7 Effects of MNPs on Microalgae

2.7.1 Growth rate

Growth rate of microalgae is the percentage of change in the biomass concentration of microalgae in a specific time. Numerous variables, including temperature, light intensity, carbon dioxide, pH, and the make-up of the culture medium, have an impact on the growth rate of microalgae (Papapolymerou et al., 2018). The two main factors among all the environmental factors that are affecting the rate of growth and biomass concentration of microalgae are the optimal temperature and the requirement of light for different species of microalgae (Li et al., 2012). Microalgae that are cultivated under stressful conditions such as inadequate nutrients in culture medium, and excessively low or high light intensities and temperatures can cause the decreased production of microalgae biomass and growth rate (Wijffels et al., 2010). Multiple studies have reported the growth inhibition of different strains and species of microalgae due to the exposure of MNPs. The general inhibitory mechanism of MNPs that was proposed by researchers includes the generation of ROS (Suman et al., 2015; Xia et al., 2015); mechanical damages induced by MNPs (Castro-Bugallo et al., 2014); release of metal ions (Aravantinou et al., 2015; Lee and An, 2013); light shading effect (Sadiq et al., 2011); interaction of MNPs with growing medium (Manier et al., 2013); and the synergistic effects of all these different factors (Manzo et al., 2013). The concentration of MNPs used and exposure time interval are also the factors that are affecting the toxicity of MNPs, where higher concentration and exposure time can result in higher inhibition in the growth of microalgae. The level of toxicity of MNPs also highly depends on

the type of MNPs used and species tested (Griffitt et al., 2008). Microalgae treated with high dose of MNPs may show reduced growth rate, this may be because of the destruction of cell membrane that result in the uncontrolled intake or release of electrolytes, which may also affect the photosynthetic apparatus and biological macromolecules synthesis (Anusha et al., 2017a).

2.7.2 Macromolecules

The macromolecules or macronutrient composition of microalgae is proteins, carbohydrates and lipids. The production of these macromolecules is highly influenced by the environmental and cultural conditions like temperature, light intensity, pH, and nutrient make-up of the culture medium (Metsoviti et al., 2019; Zhu et al., 2015). In some algae species like *B. braunii*, the increase of light intensity caused a higher lipid content and reduced protein and carbohydrate content (Ruangsomboon, 2012), while, in some other species like *Nannochloropsis* sp. (Sukenik et al., 1989) and *Ankistrodesmus falcatus* (George et al., 2014), low light intensity resulted in a high lipid content. The toxicity of ions produced in large concentrations, which results in the oxidation of biological macromolecules, is frequently linked to the breakdown and destruction of biological macromolecules. Macromolecules can be degraded when the medium or environment is unsuitable for the growth of microalgae and therefore unable to support the essential cellular functions in the cell (Zinicovscaia et al., 2017). The impact of MNPs on the central cell metabolism can be understood through the total protein, carbohydrate and lipid concentration of microalgae (Romero et al., 2020). Microalgae might alter their

biochemical make-up and tend to adjust their cellular metabolism to store more large molecules such as proteins, carbohydrates and lipids as a physiological reaction to keep harmful components out of the primary metabolic pathways when they are under stress condition (Huang et al., 2016; Pham, 2019). Generally, the techniques used for the determination of total protein concentration in microalgae are based on the detection of peptide bonds, where the decrease in protein content denotes the lysing of biomass (Zinicovscaia et al., 2017). The primary photosynthetic products in microalgae that are stored in the chloroplast as starch grains are carbohydrates (Huang et al., 2016). The increased concentration of carbohydrates may be due to the protective mechanism in microalgae when they are under stress conditions, which will be triggered by the production of specific ROS scavengers. However, at higher concentrations, carbohydrates can also act directly as ROS scavengers. Glucose and sucrose are crucial for ROS signaling (Bolouri-Moghaddam et al., 2010). On the other hand, the reduced level of total carbohydrates during the exposure of MNPs may be due to the disruption of cell membrane that caused the uncontrolled release and intake of electrolytes (Anusha et al., 2017a). Microalgae can withstand toxicant concentrations that are lower most of the time. Since lipids are the primary constituents of the cell membrane, the composition of lipids can be altered in response to changes in the physiological state of cells (Zinicovscaia et al., 2017).

2.7.3 Pigments

Chlorophylls are primary photosynthetic pigments that are comprised with tetra pyrrole macrocycle rings and can be found in a variety of forms in distinct microalgae species (Miazek et al., 2015). The microalgae chlorophyll content is frequently used to represent the rate of photosynthesis or rate of cell division (Pham, 2019). Low concentrations of metals are necessary for the growth of microalgae; nevertheless, high concentrations of metals can impact the pace of growth and the ability of microalgae to produce chlorophyll. This is due to the possibility that too much metals will inhibit chlorophyll ability to function (El-Sheekh et al., 2003; Puspitasari et al., 2018). Majority of research found that low concentrations of metals and MNPs can enhance chlorophyll synthesis slightly, while, high concentrations cause the amount of chlorophyll reduced significantly (Djearamane et al., 2018a; El-Sheekh et al., 2003; Puspitasari et al., 2018). As cobalt and copper are necessary metals for the metabolism of microalgae cells and their respiration, the substitution of cobalt for zinc (El-Sheekh et al., 2003) and the substitution of copper for magnesium (Puspitasari et al., 2018) may be the cause of the enhanced chlorophyll synthesis at low NPs concentrations. Chlorophyll concentration decreases due to an inhibition of the electron transport chain in the donor center, whereas chlorophyll content increases due to an inhibition in the acceptor center (Sendra et al., 2017). The auxiliary photosynthetic pigments known as carotenoids are fat-soluble tetraterpenoids that can be divided into oxygen-containing xanthophyll (lutein, astaxanthin, and zeaxanthin) and no-oxygen-containing carotenoids (β -carotene) (Miazek et al., 2015). Water-soluble proteins called

phycobiliproteins act as auxiliary pigments in blue-green or red microalgae, giving the microalgae cells a blue or red colour that absorbs light energy and transmits it to chlorophyll *a*. (Boussiba and Richmond, 1980; Miazek et al., 2015). Allophycocyanin and c-phycocyanin are the blue pigments, and b-phycoerythrin and c-phycoerythrin are the red pigments (Miazek et al., 2015). Depending on the environmental conditions, the c-phycocyanin concentration present in microalgae cells may vary (Boussiba and Richmond, 1980).

2.7.4 Phenolic Compounds

Phenolic compounds are a diverse class of secondary metabolites that contain polyphenol structure consisting of two or more six-carbon aromatic rings (Tibbetts et al., 2015). Phenolic compounds are one of the most important classes of natural antioxidants that can mitigate or prevent the effects of oxidative stress (Aliakbarian et al., 2009; Ben Hamissa et al., 2012; Cardozo et al., 2007; Palmieri et al., 2012) by donating a hydrogen atom or an electron in order to form stable radical intermediates (Hajimahmoodi et al., 2010). The total phenolic compound of microalgae varies in different species and strain, which can be influenced by environmental factors (Machu et al., 2015a) and cultivation conditions like temperature, light intensity, and the availability of nutrients (Maadane et al., 2015; Maria N. Metsoviti et al., 2019). When the microalgae cells are subjected to environmental stress, antioxidant enzymes are produced to protect the algal cells from free radical damages (Li et al., 2006). In response to a stress state, the strong photocatalytic activity of titanium dioxide nanoparticles increases the formation of

phenolic compounds. Free radicals will destroy the generated phenolic compounds when they are discharged into the media, supporting the idea that the amount of extracellular phenolic compounds reduced during the exposure of NPs (Comotto et al., 2014).

2.8 Ag NPs and its Toxicity

Ag NPs are one of the mostly used nanomaterial in commercial applications due to its antimicrobial properties, where Ag NPs has been widely utilized in different commercial products across different field (da Costa and Hussain, 2020). The widespread application of Ag NPs results in the release of the NPs into the environment. Ag NPs are easily released from the products with NPs during use, particularly through washing and through waste water effluents (Bolaños-Benítez et al., 2020) and therefore it is possible that the NPs will eventually be introduced into the aquatic environment (Li and Lenhart, 2012). Under this context, Ag NP releases would undoubtedly result in cumulative exposure to the environment and people (Liu et al., 2018; Sufian et al., 2017). Multiple researches have reported cytotoxic potentials of Ag NPs in aquatic environment, especially on algae which serve as the foundation for aquatic biota food web (Kleiven et al., 2019; Ribeiro et al., 2015; Sørensen and Baun, 2015). Besides, Dewez and Oukarroum (2012), Navarro et al. (2008) and Ribeiro et al. (2015) have also stated the cytotoxic effects of Ag NPs on the photosynthetic process of microalgae. The toxicity of Ag NPs on some microalgae strains were summarized in Table 2.2.

Griffitt et al. (2008) reported that Ag NPs caused toxicity to freshwater alga *P. subcapitata*, freshwater flea *Daphnia pulex* and zebrafish *Danio rerio* with LD₅₀ values of 0.19, 0.040-0.067 and 7.0-7.2 mg/mL, respectively, when exposed to Ag NPs for 48 h. *C. reinhardtii* exposed to 1, 5, and 10 µmol/L of Ag NPs under both light and dark condition for 6 h was reported to have a higher inhibition on the electron transport activity of photosynthetic system under light exposure, which may be due to the light-induced production of ROS by Ag NPs directly affecting the biochemical processes of *C. reinhardtii* (Dewez and Oukarroum, 2012). Ag ions released from Ag NPs can caused reduction in the growth of cell, photosynthesis and production of chlorophyll in *Thalassiosira weissflogii* (Miao et al., 2009). Navarro et al. (2008b) also proved the higher toxicity of Ag NPs when compared to Ag ions on the photosynthetic reaction of *C. reinhardtii*. Temperature is also one of the factors affecting the toxicity of Ag NPs. Oukarroum et al. (2012) also demonstrated that *Dunaliella tertiolecta* and *C. vulgaris* treated with Ag NPs cultivated under 25°C and 31°C respectively, resulted in a higher altering effect on photosynthetic electron transport in higher temperature. Besides microalgae, Ag NPs are also reported to be toxic to aquatic vertebrates. Some researches on the toxicity of Ag NPs on zebrafish embryo showed the penetration of Ag NPs aggregates into the skin and circulatory system when treated with 10 to 20 mg/L of Ag NPs for 72 h (Yeo and Yoon, 2009); the deposition of Ag NPs in cell nucleus, blood and nervous system when treated with 5 to 100 mg/L Ag NPs (Asharani et al., 2008); and the defects in fin regeneration and infiltration of Ag NPs into

intracellular organelles when treated with 0.4 to 4 mg/L Ag NPs for 2 to 36 days (Yeo and Pak, 2008).

Ag in the macroscopic scale does not have adverse effects to human unless there is abnormal exposure. A review on the interaction of Ag NPs with tissues reported that Ag NPs can be bioaccumulated in the lungs and detected in the blood and other organs that proved the penetration and circulation of inhaled Ag NPs. Ag NPs can also damage the fundamental cellular structures when absorbed through the skin (Chen and Schluesener, 2008). DNA fragmentation was found in the bone marrow, spleen, liver, kidneys, and peripheral blood cells of rats (Zhurkov et al., 2017). Carlson et al. (2008) showed the detrimental effects of Ag NPs to human health through ingestion or usage of medical devices. Some other researches have also demonstrated the cytotoxicity of Ag NPs on mammalian cell lines (Hussain et al., 2005; Marin et al., 2015; Pandurangan and Kim, 2015), revealed the potential of Ag NPs to have an adverse effect on the reproductive system. The increased number of studies suggested that NPs may contribute to a number of chronic diseases that were previously likely to be contributed to the genetic factors. Smaller NPs have more reactivity, which can affect their ability to penetrate organisms. Blood-brain barriers can be crossed by NPs measuring 35 nm and less, while, NPs up to 100 nm can enter cell membranes (Sufian et al., 2017).

Multiple literature have suggested that the physiochemical features of Ag NPs like the size, shape, charge and surface coating play an vital role on the toxicity, stability, bio-uptake and the NP-biological interaction (Cho et al., 2018; Y. Li et al., 2015; Moon et al., 2019). Ag NPs with smaller size has higher dissolution than larger size

NPs and may be related to the increased reactive surface area per unit mass (Cunningham et al., 2021). Studies demonstrated that the dissolved Ag ions are toxic to microalgae and this serves as a point of reference for Ag NPs, which are known to undergo surface oxidation and release Ag ions (Burchardt et al., 2012; Navarro et al., 2008b). On the other hand, Cunningham et al. (2021) tested the toxicity of Ag NPs by blocking the dissolution of Ag NPs to form Ag ions, proved that the toxicity of Ag NPs is both size and concentration dependent. Burchardt et al. (2012) also suggested that Ag NPs may exert their toxicity by interacting directly with intracellular molecules and compartments, or, the Ag NPs uptake in microalgae encourage the intracellular release of silver ions close to molecular targets.

As microalgae *S. platensis* is one the of most popular algae used for diet and supplements, and also Ag NPs is one of the most frequently used ENPs, the effect of how Ag NPs will affect the nutritional properties of *S. platensis* is not widely reported. Multiple studies have reported that *S. platensis* has the capacity to effectively accumulate metals and MNPs in their biomass. However, the accumulative capacity of *S. platensis* for Ag NPs and the corresponding detrimental effects of Ag NPs on the nutritional values of *S. platensis* have not been reported yet.

Table 2.2: Effects of Ag NPs on microalgae.

Microalgae strain	Concentration	Time (h)	Size (nm)	Effects	References
<i>C. reinhardtii</i>	10-300 µg/L	72	4.5, 16.7, 46.7	EC ₅₀ value for 4.5 and 16.7 nm = <10 µg/L while 46.7 nm = >300 µg/L. The 4.5 nm NPs shows 1.6% reduction in chlorophyll- <i>a</i> at 24 h and 48 h, and 1.4 % reduction for 16.7 nm at 72 h. The 46.7 nm NPs did not show significant difference in the chlorophyll content.	(Sendra et al., 2017)
<i>C. reinhardtii</i>	10 µM	2	25	Exposure of 1 h show less toxic (EC ₅₀ = 3,300 nM and photosynthetic yield 84.68%) than 2 h exposure (EC ₅₀ = 1,049 nM and photosynthetic yield 100%).	(Navarro et al., 2008b)
<i>Phaeodactylum tricornutum</i>	10-300 µg/L	72	4.5, 16.7, 46.7	EC ₅₀ for 16.7 nm is 184 µg/L, while for both 4.5 and 46.7 nm did not reach the EC ₅₀ threshold. 1.5% reduction in chlorophyll- <i>a</i> content found in 4.5 nm NPs and in contrast, exposure to 16.7 nm NPs shows increased chlorophyll content. The 46.7 nm NPs did not show significant difference in the chlorophyll content.	(Sendra et al., 2017)

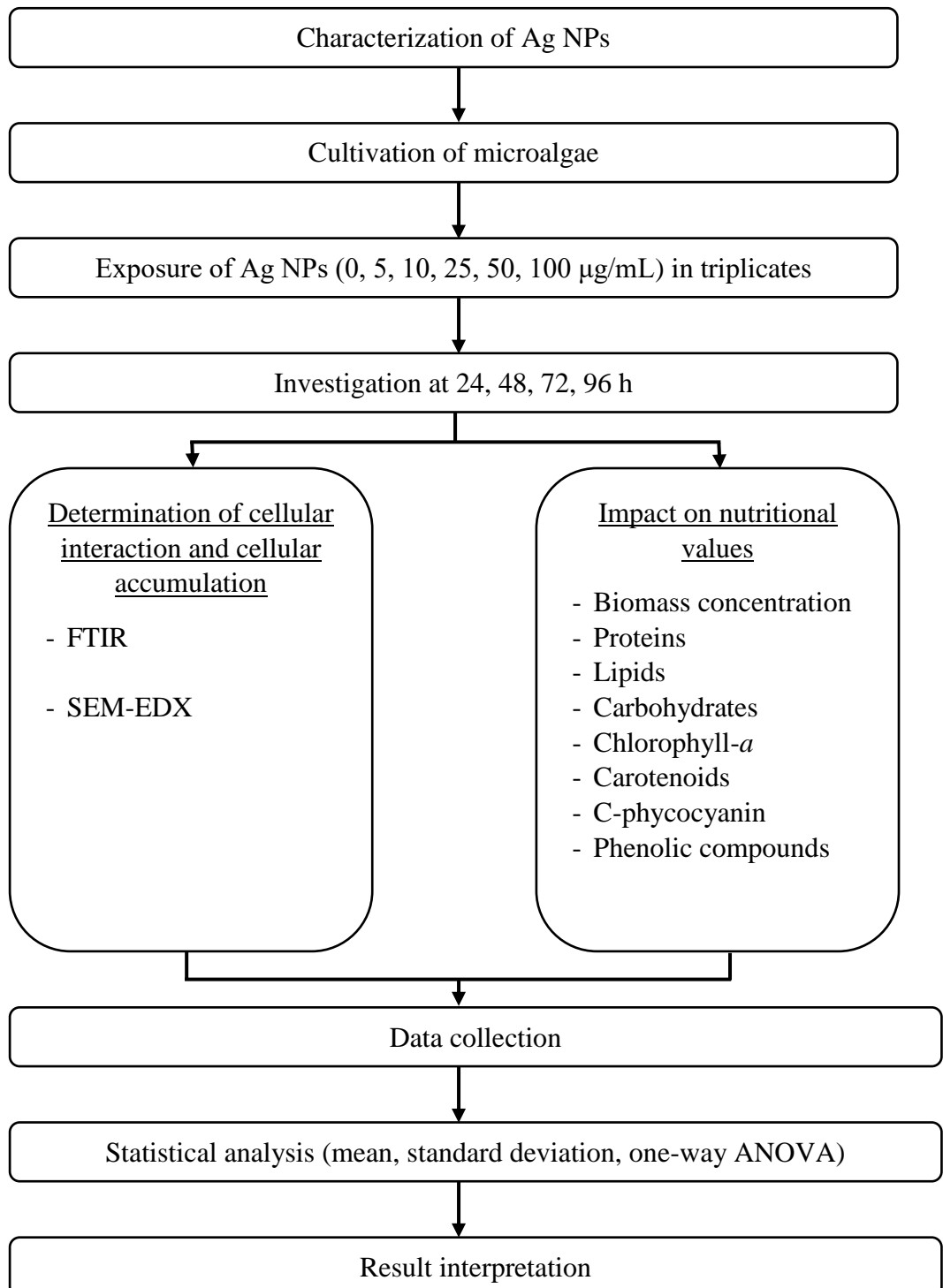
Table 2.2: Effects of Ag NPs on aquatic organisms (continued).

Microalgae strain	Concentration	Time (h)	Size (nm)	Effects	References
<i>P. subcapitata</i>	1-50 mg/L	72	10-40	NOEC, EC ₅₀ and EC ₁₀₀ values are 0.85, 1.62 and 5.0 mg/L, respectively, with a 100% drop in chlorophyll content.	(Książyk et al., 2015)
<i>P. subcapitata</i>	1000 µg/L	2	30	Reduction in growth rate (EC ₅₀ = 710 µg/L).	(Sørensen and Baun, 2015)
<i>Scenedesmus</i> sp.	200 µg/L	72	6-10	Complete growth inhibition (EC ₅₀ = 89.92 µg/L) with 22 and 5% reduction in chlorophyll- <i>a</i> and lipids.	(Pham, 2019)
<i>Skeletonema costatum</i>	5 mg/L	24	8	EC ₁₀ and EC ₅₀ values are 48 µg/L and 25.77 mg/L. Increased 30% and 16% of protein and lipid content with limited impact in carbohydrates.	(Huang et al., 2016)
<i>Synechococcus</i> sp.	10 µM	72	20, 40, 100	100% reduction in all sizes after 72 h exposure.	(Burchardt et al., 2012)
<i>T. pseudonana</i>	10 µM	72	20, 40, 100	20 nm and 40 nm Ag NPs inhibit growth by 50% and 60%, while 100 nm inhibit 40% of growth.	(Burchardt et al., 2012)
<i>Thalassiosira</i> sp.	200 µg/L	72	6-10	Almost 100% inhibition (EC ₅₀ = 107.21 µg/L) with 15% reduction in chlorophyll- <i>a</i> and 33% increment in lipid content.	(Pham, 2019)

CHAPTER 3

MATERIALS AND METHODS

3.1 Overview of Research Methodology



3.2 Characterization of Ag NPs

Scanning electron microscope (SEM, JSM-6701F, Joel, Japan), energy dispersive X-ray (EDX, JSM-6701F, Joel, Japan), and X-ray diffractometer (XRD, XRD-600, Shimadzu, Japan) were used to characterize Ag NPs powder (particle size <100 nm). The particle size was determined using SEM operated at acceleration voltage of 4.0 kV with working distance of 6.0 mm. The chemical composition of Ag NPs was confirmed by using SEM-EDX with an acceleration voltage of 10kV. The crystalline nature of Ag NPs was analysed using XRD operated at a voltage of 40 kV and current of 30 mA with Cu radiation $\lambda=1.5406$ in the scan range of $2\theta=20-80^\circ$.

3.3 Cultivation of Microalgae

The marine microalgae *S. platensis* stock culture (UTEX Number: LB1926) was obtained from University of Texas Culture Collection, Austin, Texas, United States of America. *S. platensis* was cultured using *Spirulina* medium and the algal cultures were maintained in Erlenmeyer flasks under 1200 lux illumination using cool white fluorescent lamp with 16 h light and 8 h dark at room temperature (21-23°C).

3.4 Exposure of Microalgae to Ag NPs

Stock culture solution with Ag NPs (200 $\mu\text{g}/\text{mL}$) was used to prepare culture solution with five different working concentrations of Ag NPs (5, 10, 25, 50, and 100 $\mu\text{g}/\text{mL}$) by diluting the stock solution using *Spirulina* culture medium.

S. platensis cells at exponential phase (Day 7) with initial concentration of 0.6 at OD₅₆₀ were exposed to 5, 10, 25, 50, and 100 µg/mL of Ag NPs in 1 L Erlenmeyer flask for duration of 24, 48, 72, and 96 h. The *Spirulina* cells cultured in culture medium without Ag NPs was used as negative control.

3.5 Cellular Interaction and Cellular Accumulation of Ag NPs on Algal Cells

3.5.1 Attenuated Total Reflectance Fourier Transformed Infrared (ATR-FTIR) Spectroscopy

ATR-FTIR spectroscopy was carried out to confirm the functional groups from the microalgal cell wall involved in the attachment of Ag NPs on the cell surface of microalgal cells. A 25 mL of algal suspension was treated with different concentration of Ag NPs at different incubation period was centrifuged (Velocity 14R, Dynamica Scientific Ltd., Australia) at 5,000 rpm for 10 min. The isolated pellet was then washed twice with 1x PBS and distilled water. The washed cells were freeze dried to remove moisture and subjected to ATR-FTIR (Spectrum Two, Perkin-Elmer, United States of America) analysis over the range of 4000 to 400 cm⁻¹ using the reflection technique.

3.5.2 SEM-EDX Analysis

SEM-EDX was carried out to identify the cellular accumulation of Ag NPs in the biomass of *S. platensis* and to study the morphological damages on the cells resulted from the treatment of Ag NPs. A 25 mL of Ag NPs treated algal cell suspension was centrifuged for 10 min at 5,000 rpm and the pelleted cells were washed with 0.1X PBS and distilled water for twice and freeze dried. The

freeze-dried algal cells were subjected to SEM-EDX (JSM-6701F, Joel, Japan) analysis.

3.6 Effects of Ag NPs on Growth Pattern and Biomass

The algal biomass concentration was estimated by measuring the optical density at 560 nm using a spectrophotometer (Gynesys 10S UV-Vis, Thermo Scientific, United States of America) along with the control. An additional control with only the Ag NPs for each concentration was measured and subtracted from the test reading to eliminate the interference from Ag NPs (Equation 1). The medium for algal growth, *Spirulina* medium, was used as blank for both the tests and also controls. The percentage change in the test as compared to the control (Equation 2) was analysed to observe the trend of algal growth after the treatment with different concentrations of Ag NPs at different time interval.

$$\text{OD of the culture at 560 nm} = \text{OD}_1 - \text{OD}_0 \text{ (Eq. 1)}$$

$$\text{OD}_0 = \text{OD of the medium with Ag NPs only}$$

$$\text{OD}_1 = \text{OD of cell culture with Ag NPs}$$

$$\% \text{ change in biomass} = \frac{(\text{OD}_{560} \text{ of negative control} - \text{OD}_{560} \text{ of cell culture}) \times 100}{\text{OD}_{560} \text{ of negative control}} \text{ (Eq.2)}$$

3.7 Effects of Ag NPs to Proteins, Carbohydrates and Lipids

3.7.1 Proteins

The proteins in microalgae was extracted using alkali method. A 10 mL of treated and untreated algal suspensions were centrifuged for 10 min at 5,000 rpm and supernatant was discarded. A 4.5 mL of 0.5 N sodium hydroxide (NaOH) was added to the pellet followed by incubation in an 80°C water bath (FCE20 Serials, Sastec, Malaysia) for 10 min for the extraction of protein. The mixture was centrifuged again after incubation and the protein content in the supernatant was estimated using Lowry method (Anusha et al., 2017b). A 1 mL of supernatant was transferred into a new tube and 2 mL of Lowry solution (Lowry reagent A:B:C = 48:1:1) was added and incubated for 10 min at room temperature. After incubation, 0.2 mL of 1 N Folin-Ciocalteu phenol reagent (FCR) was added into mixture, vortexed and incubated in dark for 30 min. The absorbance of the mixture was measured using microplate reader (FLUOstar Omega, BMG labtech, Germany) at 600 nm (Tan et al., 2020). Bovine serum albumin (BSA) was used to generate a standard curve to estimate the protein content in the supernatant. The percentage change in the tests relative to the control was calculated using Equation 3.

$$\% \text{ change in protein content} = (P_0 - P_1) \times 100 \% / P_0 \text{ (Eq. 3)}$$

P_0 = Proteins in untreated cells

P_1 = Protein in treated cells

3.7.2 Carbohydrates

The extraction of carbohydrates from the microalgae was performed using HCl extraction. A volume of 10 mL of algal samples were centrifuged at 5,000 rpm for 10 min and the supernatant was discarded. A volume of 5 mL of 2.5 N HCl was added to the pellet and incubated in 90°C water bath for 3 h and cooled to room temperature (Sharma et al., 2019). Sodium carbonate was added to the samples until no effervescence observed to neutralise the sample. The sample was then topped up to 50 mL with distilled water and centrifuged at 5,000 rpm for 10 min to settle down the solid particles (Agrawal et al., 2015). The carbohydrate content in the supernatant was estimated using the phenol-sulfuric acid method. A 1 mL of supernatant was transferred into a new tube, 1 mL of distilled water and 50 µL of 80% phenol was added and the mixture was vortexed. About 5 mL of concentrated sulphuric acid (96% H₂SO₄) was added to the mixture and vortexed. The mixture was then allowed to stand for 10 min and cooled down in a room temperature water bath for 10 min. The mixture was vortexed again and the absorbance of the mixture was measured using microplate reader (FLUOstar Omega, BMG labtech, Germany) at 490 nm (Nielsen, 2010). The carbohydrate content in the sample was calculated by using a standard graph plotted with glucose. The percentage change in the tests relative to the control was analysed using Equation 4.

$$\% \text{ change in carbohydrate content} = (C_0 - C_1) \times 100 \% / C_0 \text{ (Eq. 4)}$$

C_0 = Carbohydrates in untreated cells

C_1 = Carbohydrates in treated cells

3.7.3 Lipids

The total lipids in the samples were extracted using a modification of Bligh and Dyer method. About 40 mL of algal sample was centrifuged for 10 min at 5,000 rpm and 7.6 mL of chloroform/methanol/water (1/2/0.8, v/v/v) was added to re-suspend the pellet. The mixture was then sonicated for 1 min at 200 W and 45 kHz and vortexed for 30 s. About 2 mL of chloroform and water were added to the mixture to make the final ratio of chloroform/methanol/water to 1/1/0.9 (v/v/v). The mixture was vortexed again for 30 s and centrifuged for 5 min at 5,000 rpm to separate the mixture into three layers. The methanol layer at upper layer was removed and the chloroform layer at the bottom layer that contains lipid was transferred into a new pre-weighted tube. The extraction process was repeated twice with the remaining middle layer. The chloroform layers were combined in the same tube and evaporated at 80°C for 24 h in a drying oven (Rizwan et al., 2017). The weight of the lipid obtained was measured and analysed as compared to the control (Eq. 5).

$$\% \text{ change in the lipid content} = (L_0 - L_1) \times 100 \% / L_0 \text{ (Eq. 5)}$$

L_0 = Lipids in untreated cells

L_1 = Lipid in treated cells

3.8 Effects of Ag NPs to Chlorophyll-*a*, Carotenoids and C-Phycocyanin

3.8.1 Chlorophyll-*a* and Carotenoids

Chlorophyll-*a* and carotenoids were extracted using 90% methanol and measured spectrophotometrically. A volume of 5 mL of algal suspension was centrifuged at 5,000 rpm for 10 min and the supernatant was discarded. A 5 mL of 90% methanol was added to the pellet and vortexed. The mixture was then incubated in a 60°C water bath for 10 min. The mixture was centrifuged at 5,000 rpm for 5 min after incubation to settle down the solid particles. The absorbance of the supernatant was measured using microplate reader at 470, 652, and 665 nm (Kondzior and Butarewicz, 2018). The chlorophyll-*a* and carotenoids content were calculated using Equation 6, 7, 8. The percentage change in chlorophyll-*a* and carotenoids in algal suspensions treated with different concentrations and time intervals as compared to the control was analysed.

$$\text{Chlorophyll-}a \text{ (}Ca\text{)} = 16.82A_{665} - 9.28A_{652} \text{ (mg/mL) (Eq. 6)}$$

$$\text{Chlorophyll-}b \text{ (}Cb\text{)} = 36.92A_{652} - 16.54A_{665} \text{ (mg/mL) (Eq. 7)}$$

$$\text{Carotenoid (}Ct\text{)} = (1000A_{470} - 1.91Ca - 95.15Cb)/225 \text{ (mg/mL) (Eq. 8)}$$

3.8.2 C-Phycocyanin

C-phycocyanin in the samples was extracted using the ultrasonic treatment method. A 5 mL of algal sample was centrifuged at 5,000 rpm for 10 min and the collected pellet was washed with 5 mL of distilled water (Akbarnezhad et al., 2016). About 2 mL of 0.05 M phosphate buffer (pH 6.7) and 3 pieces of glass pearl were added to the washed pellet. The mixture was then vortexed and

sonicated in ultrasonic bath for 1 h (Djearamane et al., 2018b). After that, the mixture was centrifuged at 5,000 rpm for 5 min and the absorbance of the supernatant was measured at 615 and 652 nm using microplate reader. The C-phycocyanin content in the samples was calculated using Equation 9 (Bennett and Bogorad, 1973). The percentage changed relative to the control in the treated samples was calculated and analysed.

$$\text{C-Phycocyanin (C-PC)} = (A_{615} - 0.474A_{652})/5.34 \text{ (mg/mL)} \text{ (Eq. 9)}$$

3.9 Effects of Ag NPs to Total Phenolic Compounds

The extraction of phenolic compounds in algal samples was done using distilled water. A 5 mL of algal sample was centrifuged at 5,000 rpm for 10 min and the supernatant was discarded. A 5 mL of distilled water was added to the pellet and incubated in 80°C water bath for 10 min. The mixture was then cooled down to room temperature and centrifuged at 5,000 rpm for 5 min to settle down solid particle. The total phenolic content in the supernatant was estimated by the Folin-Ciocalteu method (Machu et al., 2015b). About 1 mL of supernatant was transferred into a new tube and 1 mL of Folin-Ciocalteu reagent (FCR) and 5 mL of distilled water were added. The mixture was vortexed and stand for 5 min in dark at room temperature. A 1 mL of 20% Na₂CO₃ was added and the solution was made up to 10 mL with distilled water. The solution was then vortexed and again incubated in dark for 1 h at room temperature. The absorbance of the solution was measured using microplate reader at 765 nm (Casazza et al., 2015b). Gallic acid was used to plot a standard curve to estimate the total

phenolic content in the algal samples. The percentage change in the tests relative to the control was calculated and analysed using Equation 10.

$$\% \text{ change in total phenolic compounds} = (P_0 - P_1) \times 100 \% / P_0 \text{ (Eq. 10)}$$

P_0 = Phenolic compounds in untreated cells

P_1 = Phenolic compounds in treated cells

3.10 Statistical analysis

Statistical analysis was performed to analyse the variance induced by Ag NPs on the algal cells. All the exposure tests were conducted in triplicates ($n=3$) and the data are presented as mean \pm standard deviation. Shapiro-Wilk test was used to test the normal distribution of the data. All the analysis on significant values ($p<0.05$) was conducted using one-way analysis of variance (ANOVA) followed by Tukey's post-hoc test for multiple comparisons.

CHAPTER 4

RESULTS

4.1 Characterization of Ag NPs

The size and shape of Ag NPs powder were observed using SEM, the elemental component of Ag NPs was confirmed using EDX, and XRD was performed to confirm the crystalline nature of Ag NPs as shown in Figure 4.1. Based on the SEM observation, cubic shaped NPs were in the agglomerated state and the average size of Ag NPs was measured to be 43.38 nm with a range of 26.8 nm to 65.9 nm. The EDX spectrum showed the presence of silver element in Ag NPs powder studied. The XRD pattern of Ag NPs displayed the strongest peaks at 34.41° , 38.23° and 44.34° and also the diffraction peaks at 39.91° , 57.71° , 64.58° , 68.91° and 77.53° . The XRD results obtained also confirmed the cubic structure and the light gray metallic colour of Ag NPs can be confirmed.

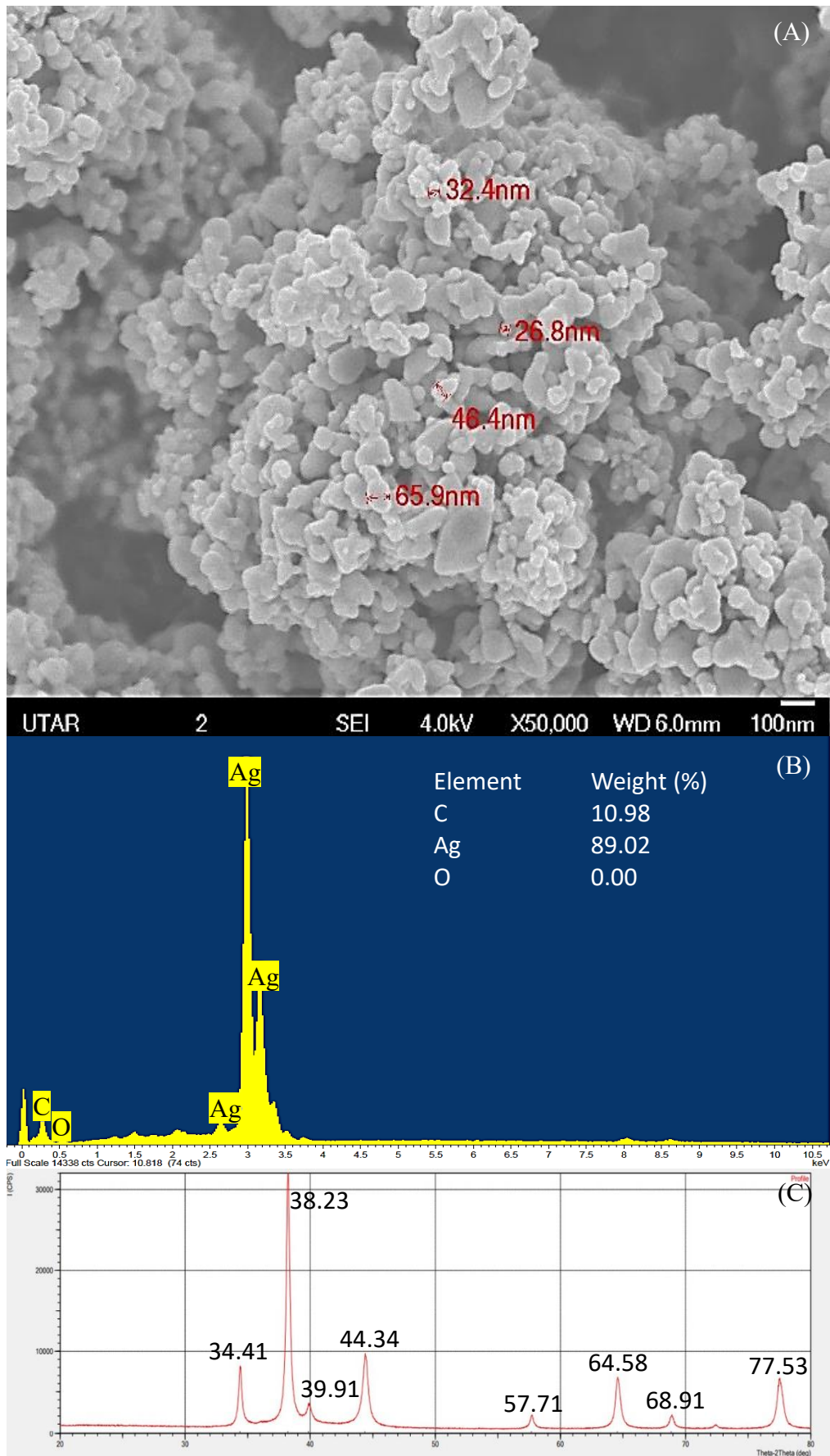


Figure 4.1: Characterization of Ag NPs under (A) SEM with 50,000X magnification, (B) EDX spectrum and (C) XRD pattern.

4.2 Cellular Interaction and Cellular Accumulation of Ag NPs on Algal Cells

4.2.1 ATR-FTIR Spectroscopy

The functional groups from the algal cell wall that were involved in the binding and cellular uptake of Ag NPs into the algal cells was confirmed using ATR-FTIR spectroscopy as shown in Figure 4.2. The peaks that were shifted between the algal samples treated with 100 µg/mL Ag NPs and the control at 96 h were compared and analysed. The possible functional groups that were involved in the surface binding and cellular uptake of Ag NPs on the algal cell wall are listed in Table 4.1.

Table 4.1: Possible involvement of functional groups from the cell wall of *S. platensis* in the binding of Ag NPs on algal cell surface.

Absorption (cm ⁻¹)	Functional group	Component
3282 – 3279	-OH, -NH	Hydroxyl, amine (protein)
2925 – 2923	-CH ₂	Methyl (lipid fraction)
1644 – 1638	C=O	Amide I (protein)
1537 – 1535	N-H, C=N	Amide II (protein)
1393 – 1387	C=O	Carbonyl (aldehyde, ketone, carboxylate)
1239 – 1235	P=O	Phosphodiester (nucleic acid, phospholipids)
1157 – 1152	C-O, C-C	Carbohydrate
1024	C-C, C-O, C-OH	Carboxyl, hydroxyl
524 – 520	-PO, -CH	Phosphate

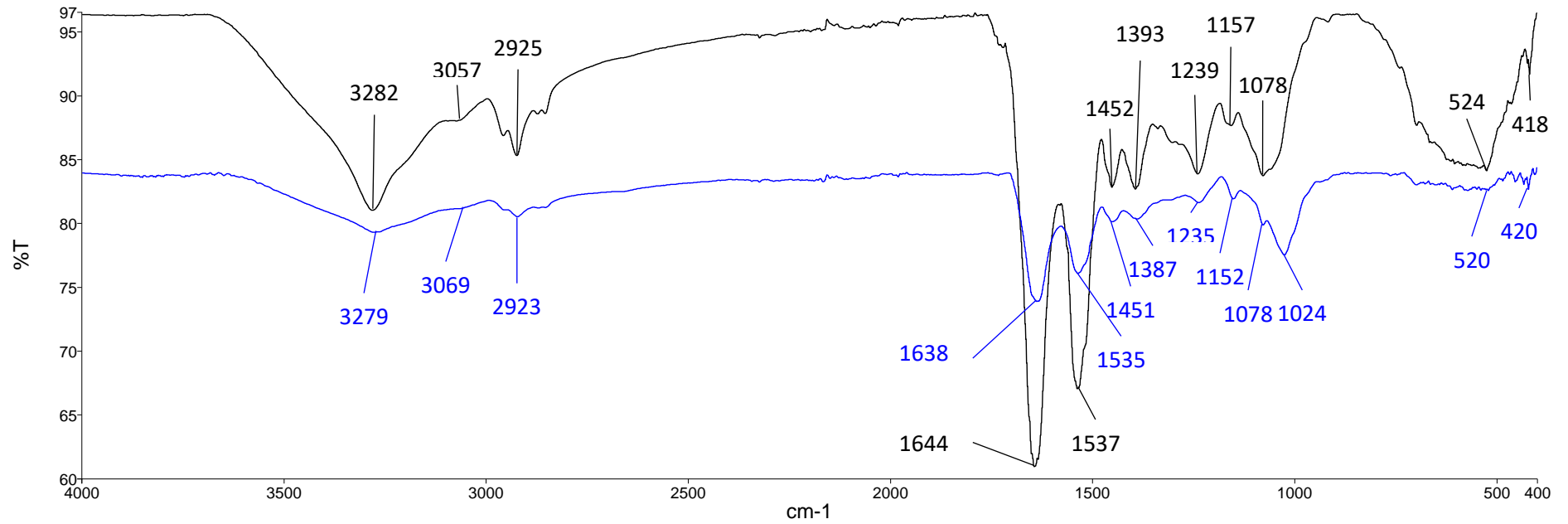


Figure 4.2: ATR-FTIR spectrum of control (black line) and 100 µg/mL Ag NPs treated *S. platensis* at 96 h (blue line).

4.2.2 SEM-EDX Analysis

The SEM images of control and 100 µg/mL Ag NPs treated *S. platensis* cells are shown in Figure 4.3. Figure 4.3(A and B) shows the smooth cylindrical cells with intact cell membrane without the treatment of Ag NPs. While, the cells treated with Ag NPs shows the attachment of NPs on cell surface, agglomeration of Ag NPs, fragmentation and distortion of *Spirulina* cells. The EDX spectrum of Ag NPs treated cells (Figure 4.4) showed the presence of Ag, which was not present in the control cells, which confirmed the accumulation of Ag NPs on *S. platensis*. The carbon and oxygen element signals may be due to the X-ray emission from *S. platensis* cell wall (Zinicovscaia et al., 2017).

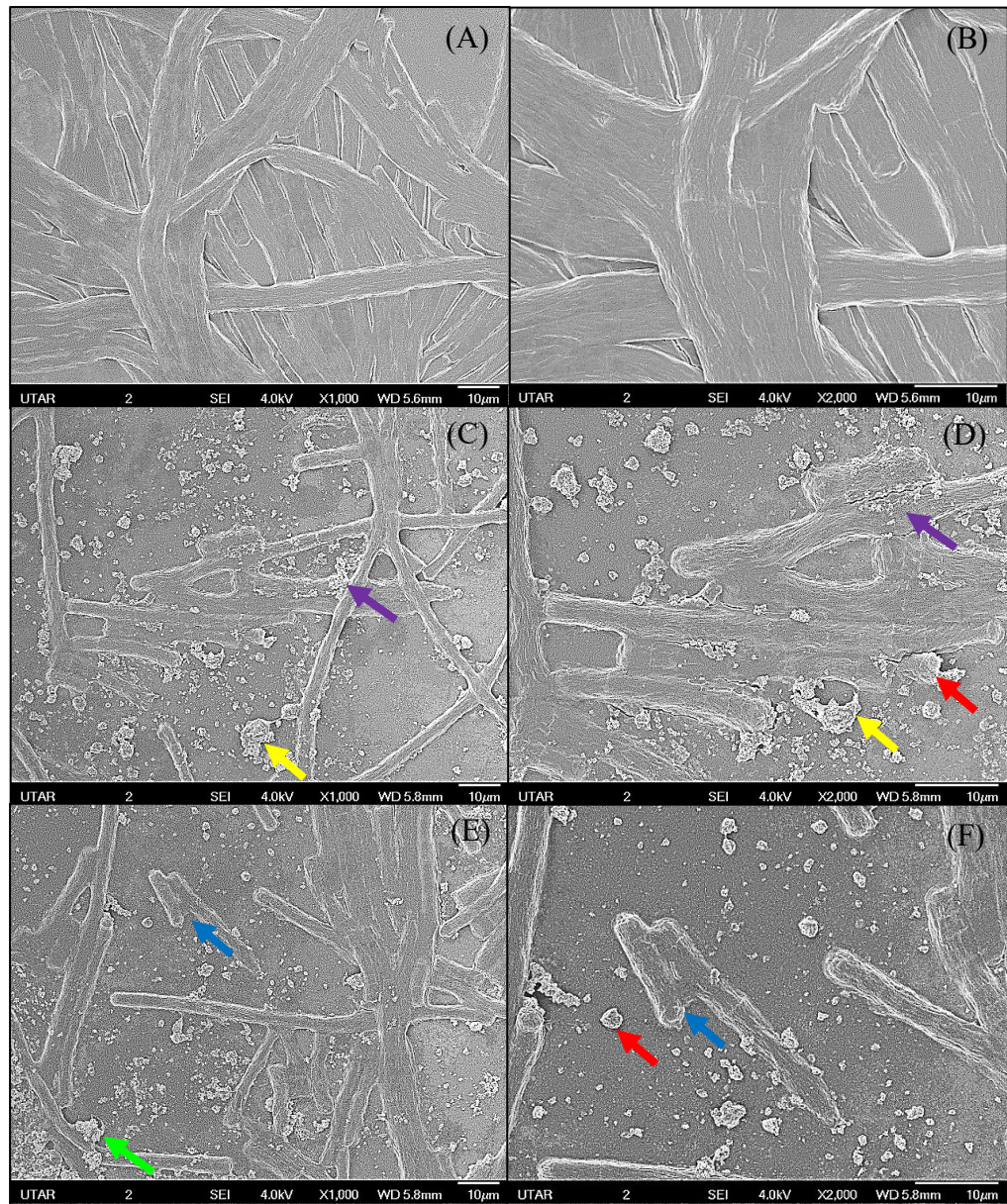


Figure 4.3: SEM images of control and 100 µg/mL Ag NPs treated *S. platensis* at 96 h. (A) control at 1000X magnification; (B) control at 2000X magnification; (C, E) 100 µg/mL Ag NPs treated *S. platensis* at 1000X magnification; (D, F) 100 µg/mL Ag NPs treated *S. platensis* at 2000X magnification. The agglomeration of Ag NPs (green arrow), short fragments of *S. platensis* cells (blue arrow), the attachment of Ag NPs on *S. platensis* (purple arrow), aggregates of distorted cells with Ag NPs (yellow arrow), and the breakage of *S. platensis* cells (red arrow) can be clearly observed.

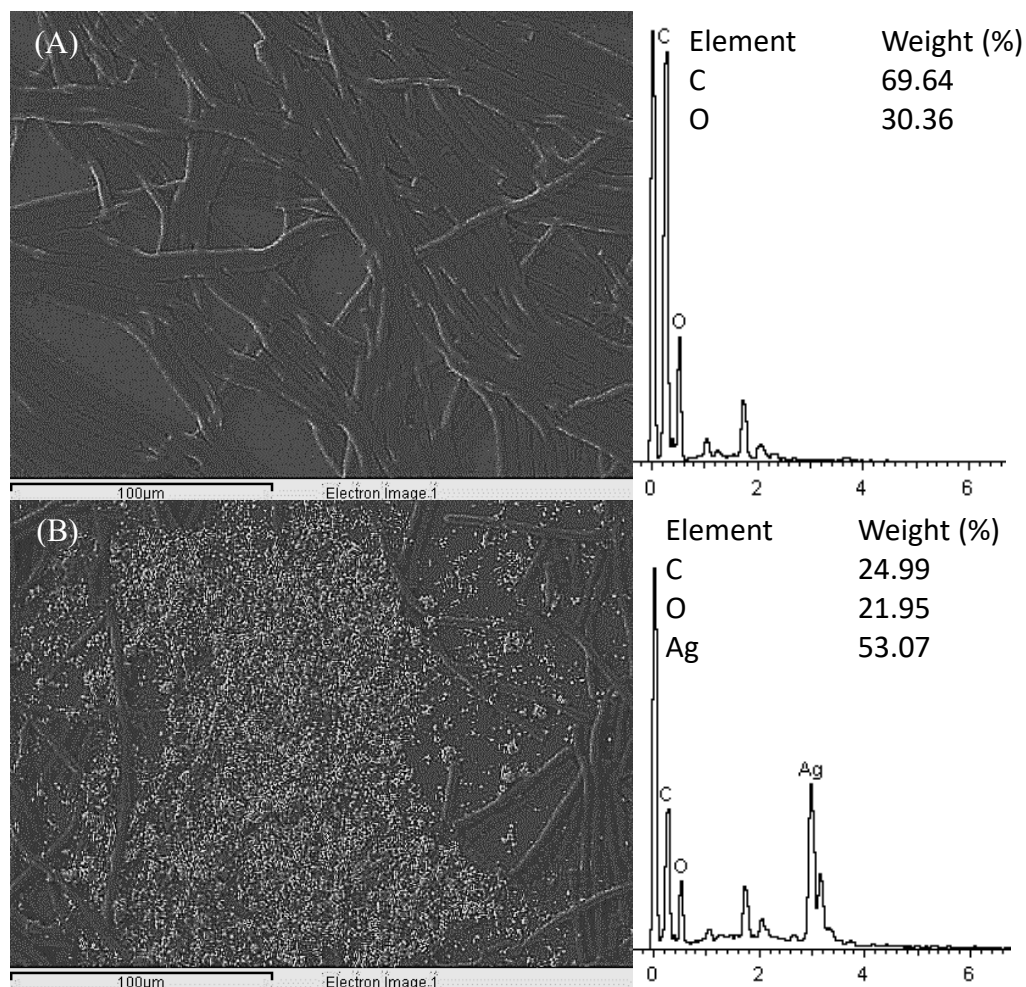


Figure 4.4: EDX image and spectrum of control (A) and 100 µg/mL Ag NPs treated *S. platensis* at 96 h (B).

4.3 Effects of Ag NPs on Growth Pattern and Biomass

The *S. platensis* cultures and growth pattern of *S. platensis* treated with different concentrations of Ag NPs at each time interval can be observed in Figure 4.5 and Figure 4.6. The biomass concentration of *S. platensis* decreased as the concentration of Ag NPs and the exposure time increased. Figure 4.7 shows the percentage loss in biomass concentration of *S. platensis* relative to control when treated with different concentration of Ag NPs from 24 to 96 h. The exposure of Ag NPs caused significant ($p < 0.05$) loss in the biomass of *S. platensis* for

concentrations $\geq 10 \mu\text{g/mL}$ at 24 and 48 h. While, significant ($p < 0.05$) loss in biomass can be observed for all tested concentrations from 5 to 100 $\mu\text{g/mL}$ at 72 and 96 h. The maximum loss in biomass of *S. platensis* happened in 96 h with the reported values of 5.86 ± 1.21 , 7.21 ± 1.51 , 33.13 ± 3.30 , 50.79 ± 3.22 , and $65.71 \pm 2.79\%$ for 5, 10, 25, 50, and 100 $\mu\text{g/mL}$ Ag NPs, respectively.

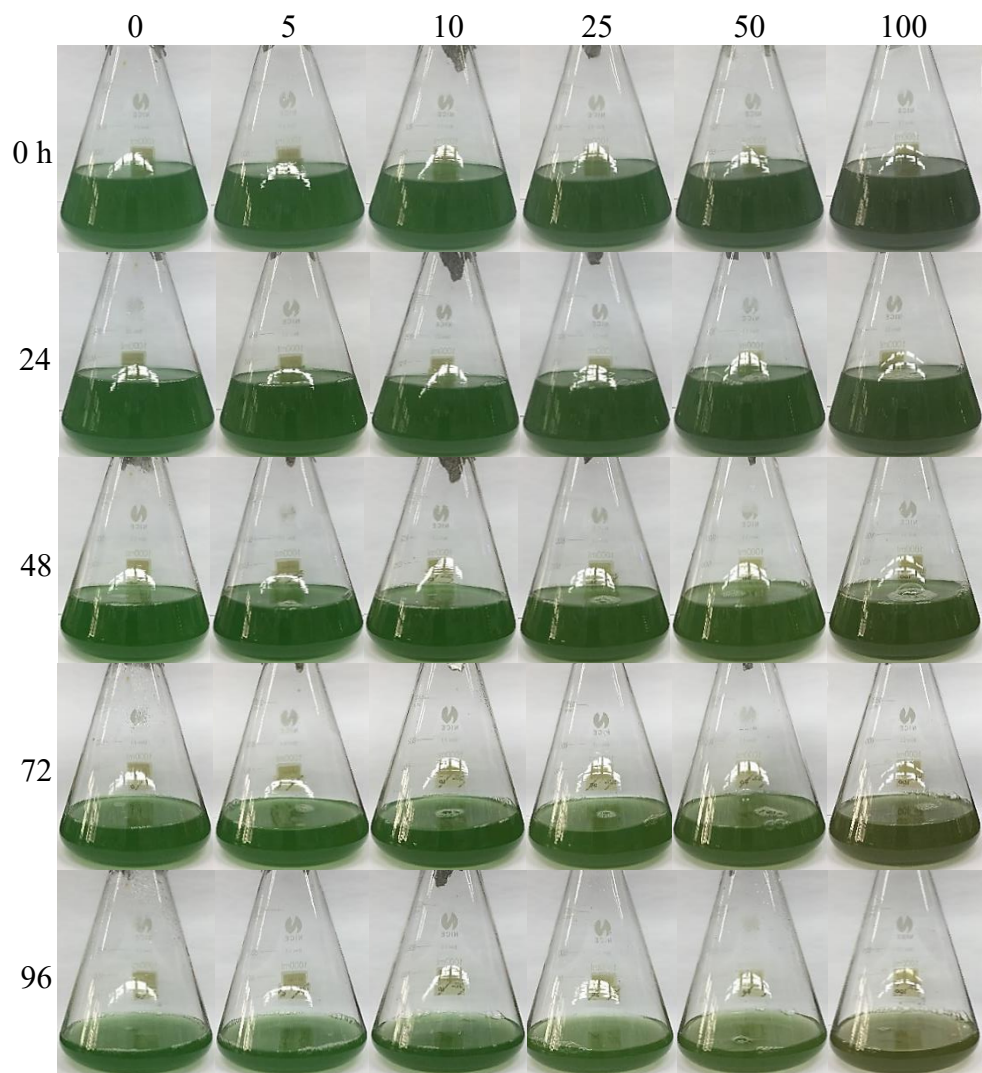


Figure 4.5: *S. platensis* cultures treated with different concentrations of Ag NPs at each time interval (24, 48, 72 and 96 h).

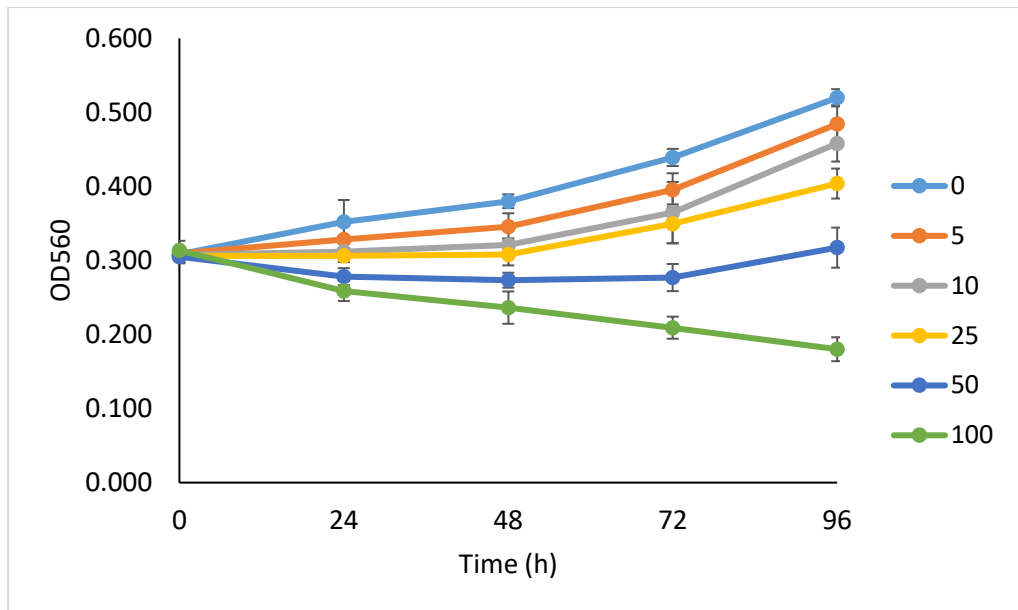


Figure 4.6: Growth pattern of *S. platensis* treated with different concentrations of Ag NPs at each time interval

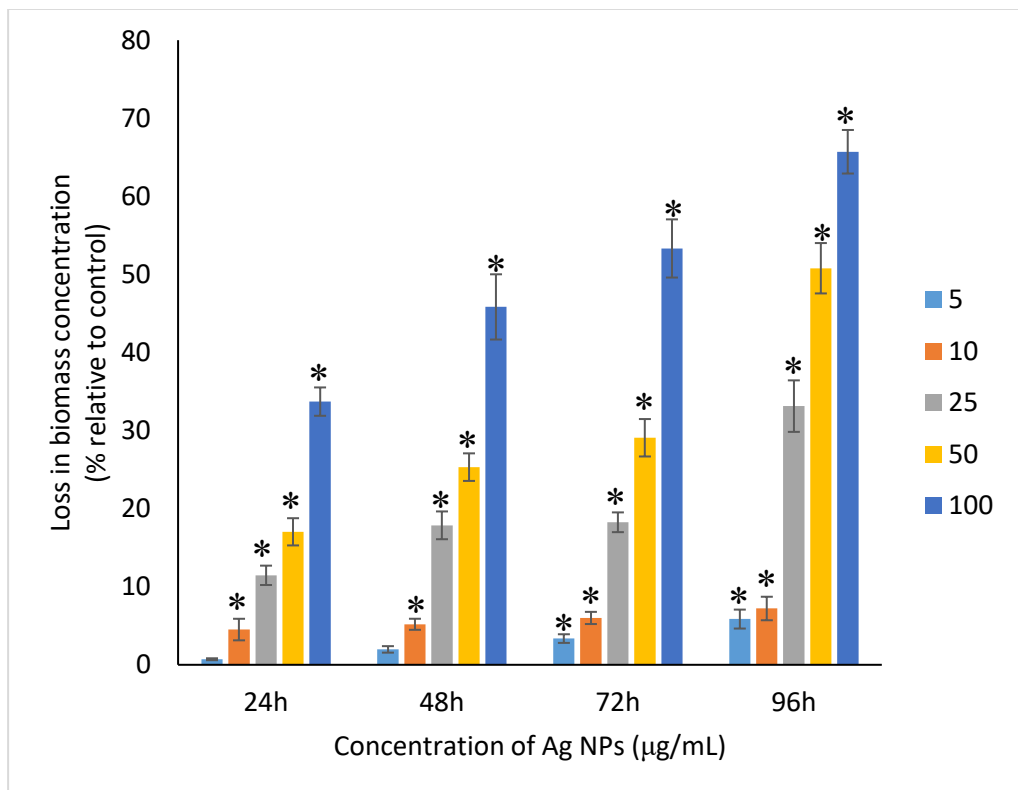


Figure 4.7: Percentage of loss in biomass concentration of *S. platensis* relative to control from 24 to 96 h upon treatment of Ag NPs. The values plotted are in mean \pm standard deviation. * indicates the significance difference at $p < 0.05$ between the control and Ag NPs treated algal suspension for each time interval.

4.4 Effects of Ag NPs to Proteins, Carbohydrates and Lipids

4.4.1 Proteins

The loss of protein in *S. platensis* can be observed in Figure 4.8 where the percentage of loss in protein increased as the dose of Ag NPs and time interval increased. All the tested concentrations of Ag NPs caused significant ($p < 0.05$) loss in the protein of *S. platensis* from 24 to 96 h. Maximum reduction in protein content was observed at 96 h with the resultant values of 23.27 ± 1.43 , 27.83 ± 2.10 , 34.45 ± 2.40 , 52.65 ± 2.98 , and $67.21 \pm 3.98\%$ for 5, 10, 25, 50, and 100 $\mu\text{g/mL}$ of Ag NPs, respectively.

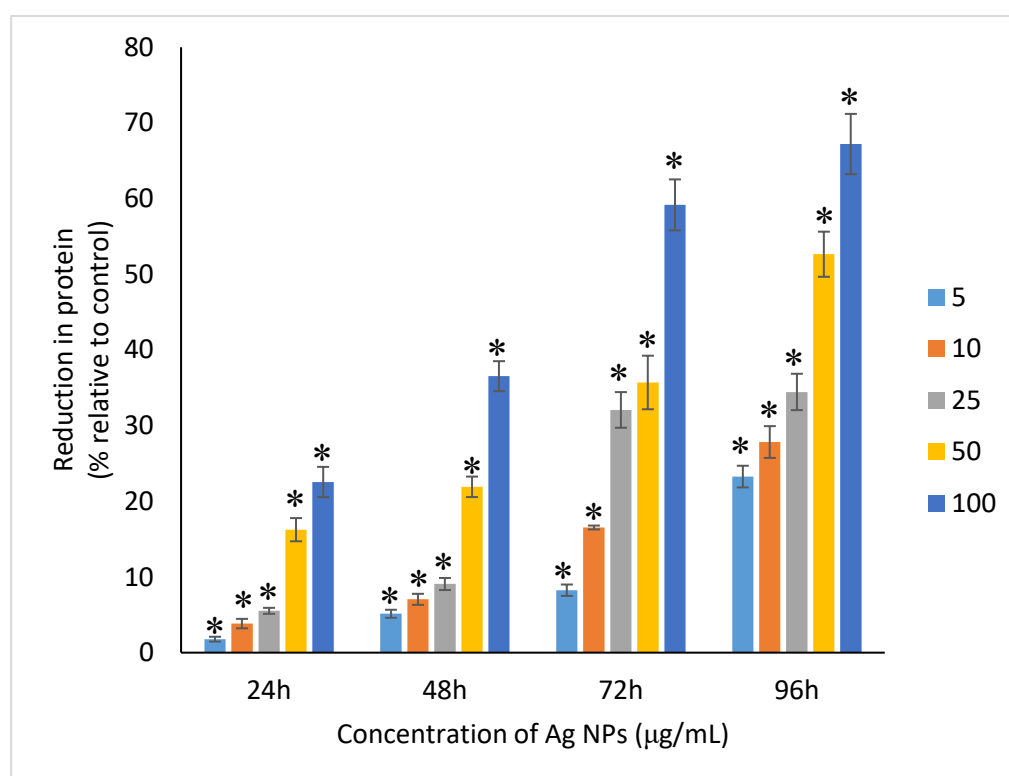


Figure 4.8: Percentage of loss in proteins of *S. platensis* relative to control from 24 to 96 h upon treatment of Ag NPs. The values plotted are in mean \pm standard deviation. * indicates the significance difference at $p < 0.05$ between the control and Ag NPs treated algal suspension for each time interval.

4.4.2 Carbohydrates

Figure 4.9 shows the percentage loss in carbohydrate of *S. platensis* relative to control when exposed to Ag NPs. The exposure of Ag NPs caused significant ($p < 0.05$) loss in carbohydrate of *S. platensis* for concentrations $\geq 10 \mu\text{g/mL}$ at 24 h. While, significant ($p < 0.05$) loss can be observed in all the tested concentrations of Ag NPs from 48 to 96 h. Maximum reduction in carbohydrate content was observed at 96 h with the resultant values of 9.68 ± 1.39 , 14.07 ± 1.77 , 28.78 ± 2.82 , 36.35 ± 2.10 , and $48.99 \pm 4.39\%$ for 5, 10, 25, 50, and 100 $\mu\text{g/mL}$ of Ag NPs, respectively.

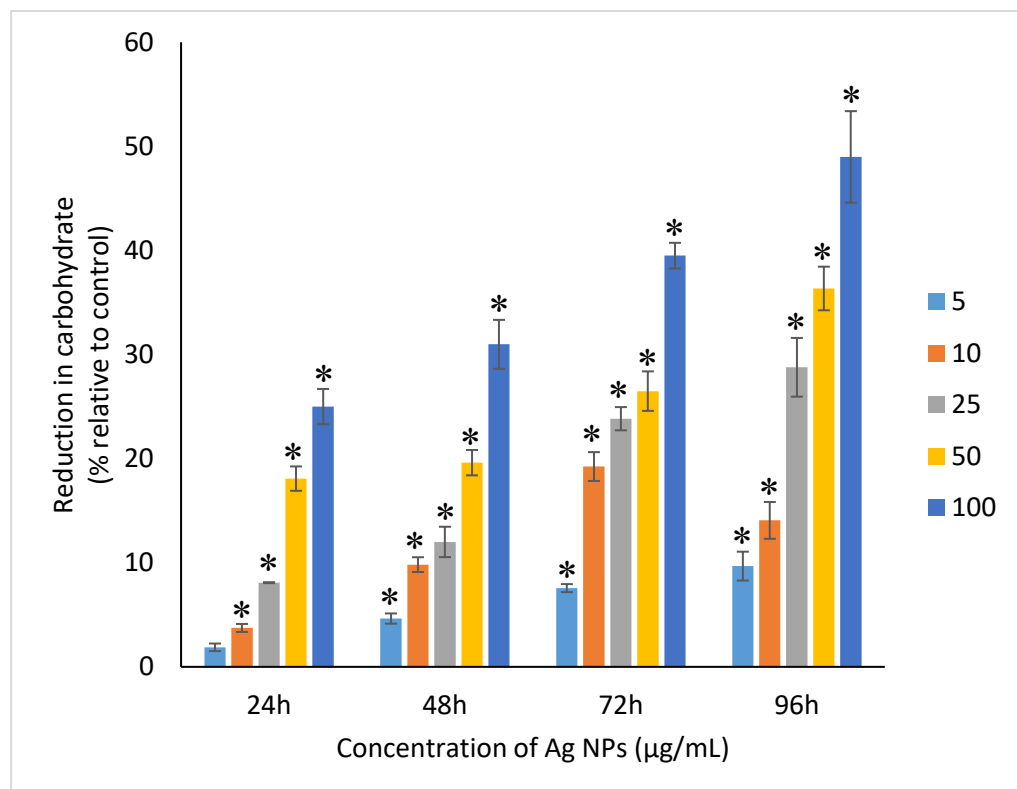


Figure 4.9: Percentage of loss in carbohydrates of *S. platensis* relative to control from 24 to 96 h upon treatment of Ag NPs. The values plotted are in mean \pm standard deviation. * indicates the significance difference at $p < 0.05$ between the control and Ag NPs treated algal suspension for each time interval.

4.4.3 Lipids

The loss of lipid in *S. platensis* can be observed in Figure 4.10 where the percentage of loss in lipid increased as the concentration of Ag NPs and time interval increased. All the tested concentrations of Ag NPs caused significant ($p < 0.05$) loss in the lipid of *S. platensis* from 24 to 96 h. Maximum reduction in protein content was observed at 96 h with the resultant values of 14.39 ± 0.78 , 22.34 ± 1.88 , 42.76 ± 2.09 , 55.92 ± 2.31 , and $59.62 \pm 3.96\%$ for 5, 10, 25, 50, and 100 $\mu\text{g/mL}$ of Ag NPs, respectively.

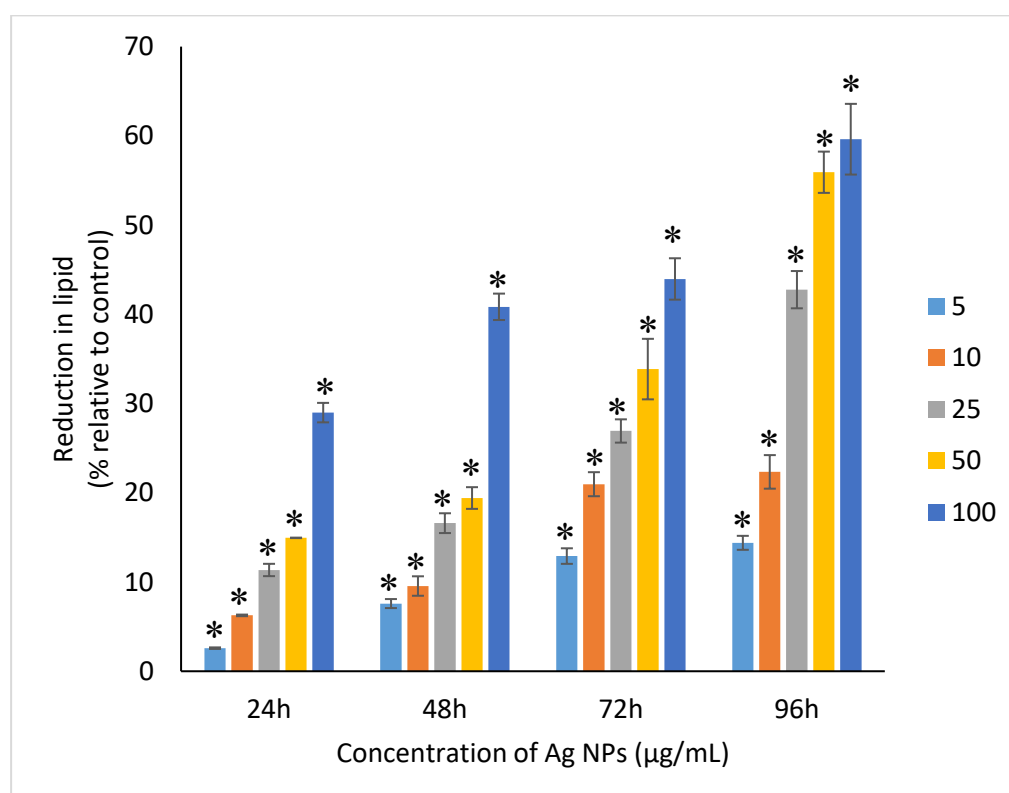


Figure 4.10: Percentage of loss in lipids of *S. platensis* relative to control from 24 to 96 h upon treatment of Ag NPs. The values plotted are in mean \pm standard deviation. * indicates the significance difference at $p < 0.05$ between the control and Ag NPs treated algal suspension for each time interval.

4.5 Effects of Ag NPs to Chlorophyll-*a*, Carotenoids and C-Phycocyanin

4.5.1 Chlorophyll-*a*

The loss of chlorophyll-*a* in *S. platensis* can be observed in Figure 4.11 where the percentage of loss in chlorophyll-*a* increased as the dose of Ag NPs and time interval increased. The exposure of Ag NPs caused significant ($p < 0.05$) loss in chlorophyll-*a* of *S. platensis* for concentrations ≥ 10 $\mu\text{g/mL}$ at 24 h. While, significant ($p < 0.05$) loss can be observed in all the tested concentrations of Ag NPs from 48 to 96 h. Maximum reduction in chlorophyll-*a* content was observed at 96 h with the resultant values of 28.63 ± 0.83 , 38.10 ± 0.70 , 53.81 ± 4.83 , 71.97 ± 5.94 , and $82.99 \pm 7.81\%$ for 5, 10, 25, 50, and 100 $\mu\text{g/mL}$ of Ag NPs, respectively.

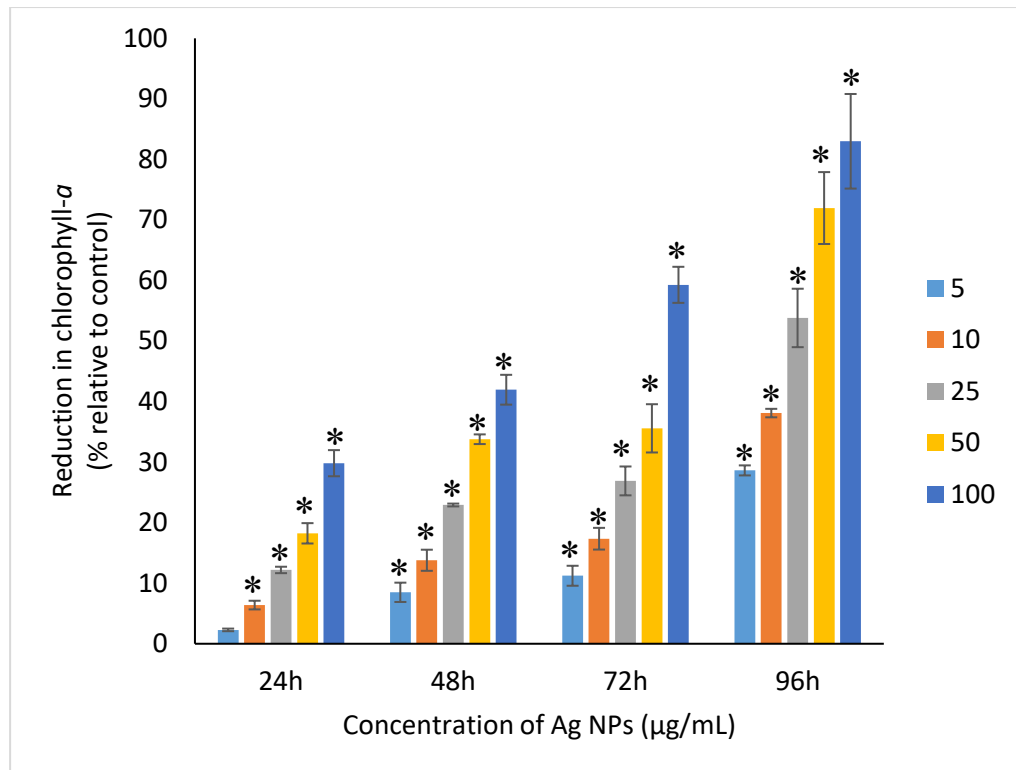


Figure 4.11: Percentage of loss in chlorophyll-*a* of *S. platensis* relative to control from 24 to 96 h upon treatment of Ag NPs. The values plotted are in mean \pm standard deviation. * indicates the significance difference at $p < 0.05$ between the control and Ag NPs treated algal suspension for each time interval.

4.5.2 Carotenoids

The loss of carotenoid in *S. platensis* can be observed in Figure 4.12 where the percentage of loss in carotenoid increased as the concentration of Ag NPs and time interval increased. All the tested concentrations of Ag NPs caused significant ($p < 0.05$) loss in the carotenoid of *S. platensis* from 24 to 96 h. Maximum reduction in carotenoid content was observed at 96 h with the resultant values of 22.44 ± 2.02 , 29.53 ± 1.84 , 44.67 ± 2.94 , 60.46 ± 4.95 , and $67.55 \pm 2.63\%$ for 5, 10, 25, 50, and 100 $\mu\text{g/mL}$ of Ag NPs, respectively.

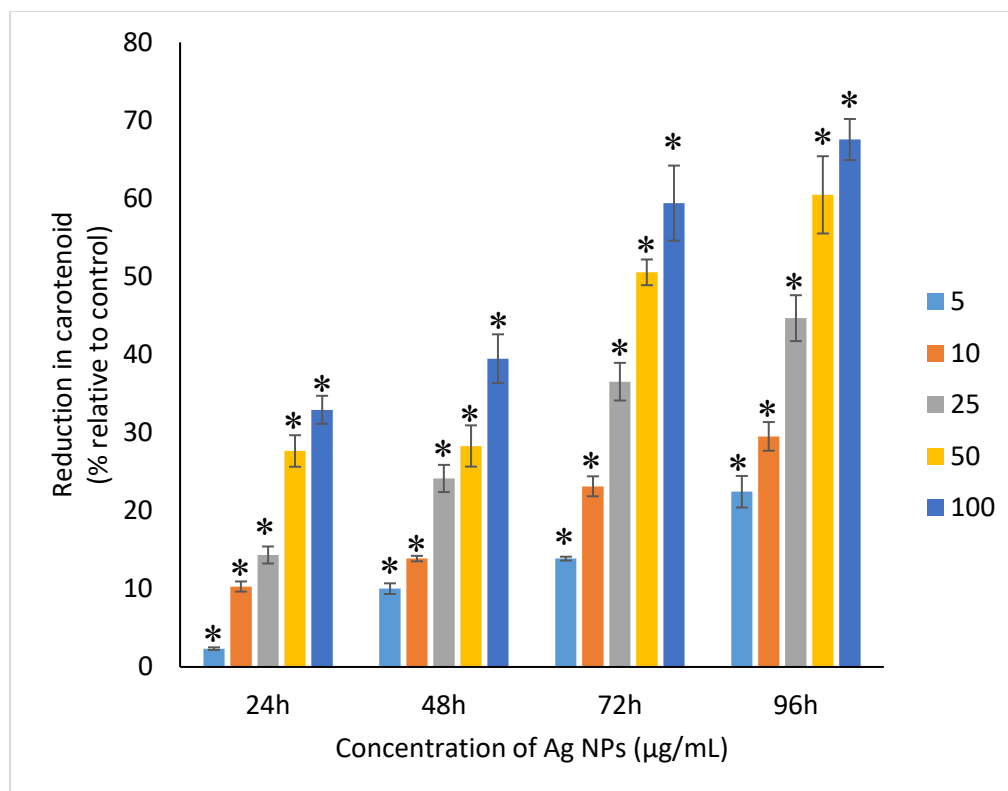


Figure 4.12: Percentage of loss in carotenoids of *S. platensis* relative to control from 24 to 96 h upon treatment of Ag NPs. The values plotted are in mean \pm standard deviation. * indicates the significance difference at $p < 0.05$ between the control and Ag NPs treated algal suspension for each time interval.

4.5.3 C-Phycocyanin

The loss of C-phycocyanin in *S. platensis* can be observed in Figure 4.13 where the percentage of loss in C-phycocyanin increased as the concentration of Ag NPs and time interval increased. The exposure of Ag NPs caused significant ($p < 0.05$) loss in C-phycocyanin of *S. platensis* for concentrations ≥ 10 $\mu\text{g/mL}$ at 24 h. While, significant ($p < 0.05$) loss can be observed in all the tested concentrations of Ag NPs from 48 to 96 h. Maximum reduction in C-phycocyanin content was observed at 96 h with the resultant values of 21.97 ± 1.57 , 28.18 ± 1.44 , 48.91 ± 1.28 , 65.85 ± 3.01 , and $75.03 \pm 1.55\%$ for 5, 10, 25, 50, and 100 $\mu\text{g/mL}$ of Ag NPs, respectively.

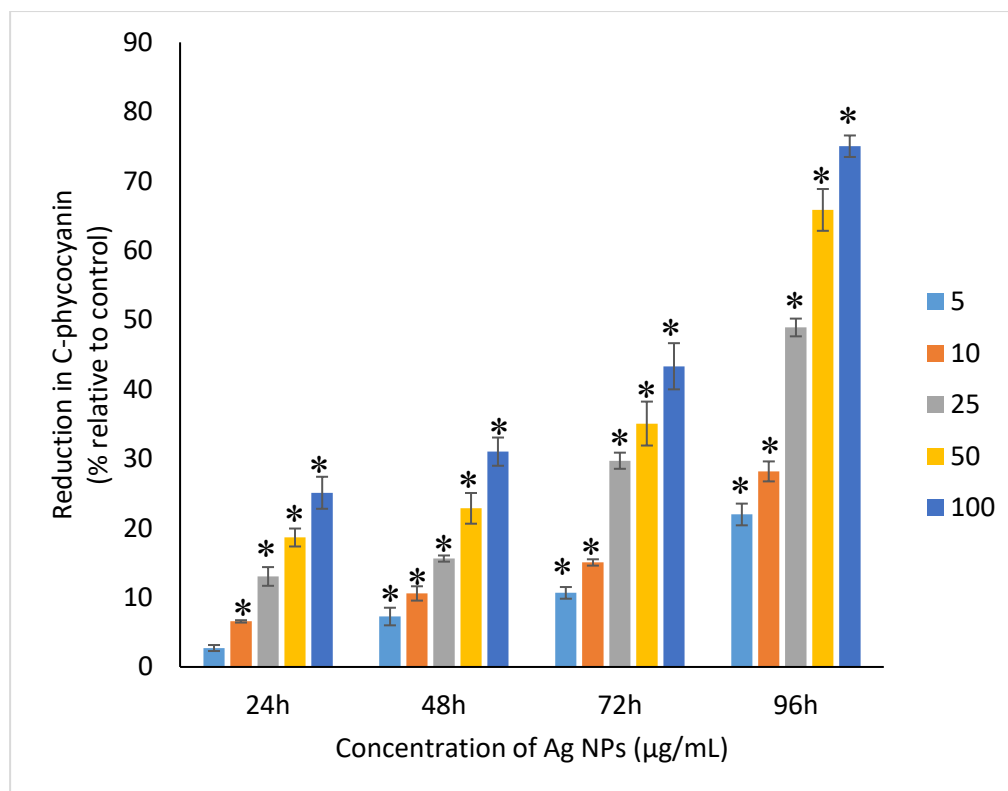


Figure 4.13: Percentage of loss in C-phycoerythrin of *S. platensis* relative to control from 24 to 96 h upon treatment of Ag NPs. The values plotted are in mean \pm standard deviation. * indicates the significance difference at $p < 0.05$ between the control and Ag NPs treated algal suspension for each time interval.

4.6 Effects of Ag NPs to Total Phenolic Compounds

The loss of phenolic content in *S. platensis* can be observed in Figure 4.14 where the percentage of loss in total phenolic compound increased as the concentration of Ag NPs and time interval increased. All the tested concentrations of Ag NPs caused significant ($p < 0.05$) loss in the total phenolic compound of *S. platensis* from 24 to 96 h. Maximum reduction in phenolic content was observed at 96 h with the resultant values of 17.27 ± 0.65 , 24.29 ± 1.82 , 41.96 ± 4.04 , 58.10 ± 4.99 , and $63.43 \pm 2.89\%$ for 5, 10, 25, 50, and 100 $\mu\text{g/mL}$ of Ag NPs, respectively.

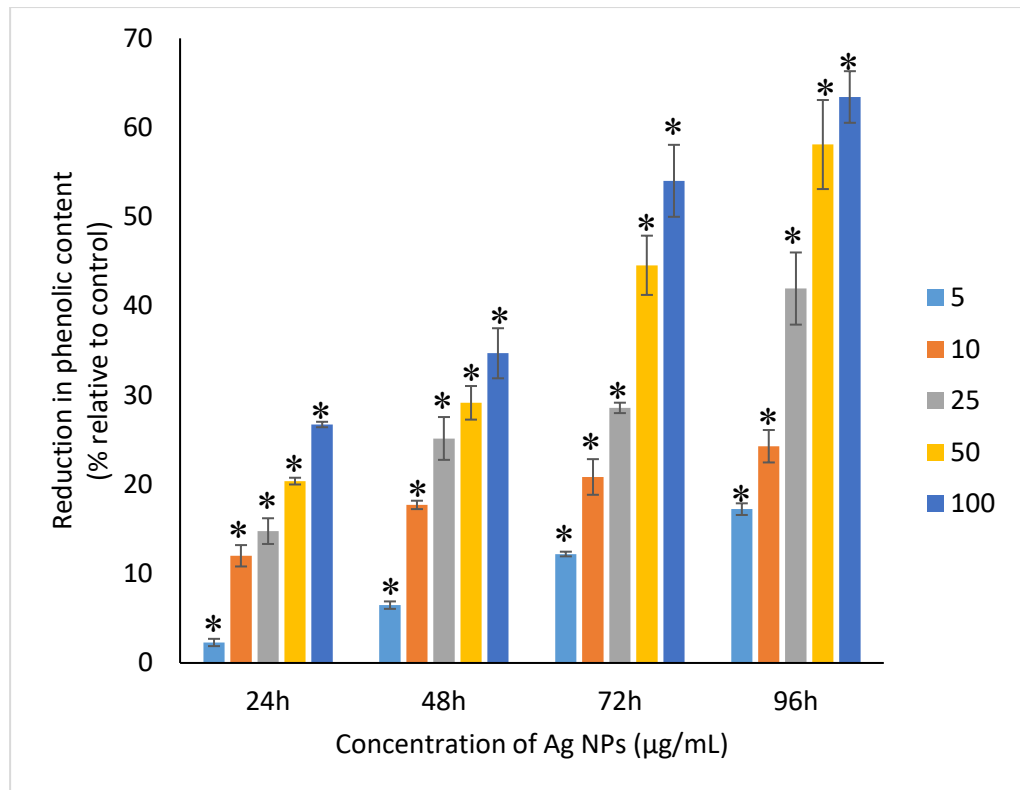


Figure 4.14: Percentage of loss in total phenolic compounds of *S. platensis* relative to control from 24 to 96 h upon treatment of Ag NPs. The values plotted are in mean \pm standard deviation. * indicates the significance difference at $p < 0.05$ between the control and Ag NPs treated algal suspension for each time interval.

CHAPTER 5

DISCUSSION AND CONCLUSION

5.1 Cellular Interaction and Cellular Accumulation of Ag NPs on Algal Cells

5.1.1 ATR-FTIR Spectroscopy

ATR-FTIR was done to determine the possible functional groups that are involved in the attachment of Ag NPs on the surface of the microalgae cell wall. The functional groups such as hydroxyl, amine, methyl, amide I, amide II, carboxyl, carbonyl and phosphate groups from the cell wall of *S. platensis* were identified to be possibly involved in the interaction of Ag NPs with *S. platensis*. The region between 3282 and 3279 cm^{-1} is relative to the symmetric –OH and –NH stretching of the hydroxyl and amide functional groups from water and protein (Ansari et al., 2019; Dotto et al., 2012; Zinicovscaia et al., 2020). The presence of asymmetric –CH₂ stretching vibration of methyl group was found between 2925 and 2923 cm^{-1} , which belongs to the long methylenic chains of lipidic fractions (Ansari et al., 2019; Ferreira et al., 2011). The peaks at 1644 and 1639 cm^{-1} were the symmetric C=O stretching of protein amide I, while, the symmetric deformation of N-H bend and C-N stretching of protein amide II can be found between 1537 and 1535 cm^{-1} (Ansari et al., 2019; Bataller and Capareda, 2018). The region between 1393 and 1387 cm^{-1} could be attributed to C=O stretching of aldehydes, ketones, and carboxylate (Çelekli et al., 2021, 2010). Peaks at 1239 and 1235 cm^{-1} were linked to asymmetrical P=O stretching of phosphodiester of nucleic acids and phospholipids (Ansari et al., 2019; Fang et al., 2011). Also, the region between 1157 and 1152 cm^{-1} was assigned as the

carbohydrate characteristic bands with C-O and C-C stretching (Bataller and Capareda, 2018; Ferreira et al., 2011). In contrast to the control cell, the peak at 1078 cm^{-1} which indicates the CO stretching of alcoholic group (Sheng et al., 2004) was shifted and formed a new band at 1024 cm^{-1} in the Ag NPs treated cell representing C-O, C-C, and C-OH stretching of the carboxyl and hydroxyl groups (Çelekli et al., 2021; Zinicovscaia et al., 2020). The peaks between 524 and 520 cm^{-1} were the $-\text{PO}$ and aromatic $-\text{CH}$ stretching of phosphate (Zinicovscaia et al., 2020).

Based on the results in Figure 4.2, the decreasing relative intensities of both the OH bands in the Ag NPs treated cells and also the NH bands, suggesting the interaction of ions with NH groups through the electron lone pairs of the nitrogen atom (Ferreira et al., 2011). The decreasing relative intensity of peaks between 1638 and 1387 cm^{-1} indicated the involvement of amide and carboxyl groups in the adsorption of NPs where it may be due to the amide group and cation interaction, which is characterized by electron lone pairs over oxygen and nitrogen atoms. The regions corresponding to the carbohydrate and phosphate functional groups did not appear to be appreciably impacted by the adsorption of NPs (Ferreira et al., 2011).

5.1.2 SEM-EDX Analysis

SEM-EDX analysis was conducted to determine the cellular accumulation of Ag NPs in the biomass and the subsequent morphological changes in *S. platensis* cells caused by the treatment of Ag NPs. Similar findings were reported on *S. platensis* treated with zinc oxide nanoparticles (ZnO NPs) (Djearmane et al.,

2018a) and *S. costatum* treated with Ag NPs (Huang et al., 2016). The physical barrier formed during the surface attachment of NPs on the cells was reported to inhibit the growth of photosynthetic microbes. The adsorption and accumulation of multiple layers of NPs on the cell surface might affect the transfer of nutrients and induce physical stress to the photosynthetic microbes (Metzler et al., 2011). The pore diameter in the cell wall of microalgae was found to be ranging from 5 to 20 nm (Navarro et al., 2008a), which is much smaller than the Ag NPs size used in this study and hence it is assumed that the Ag NPs were mainly adsorbed on the surface of *S. platensis*. The agglomeration of Ag NPs on the cell surface of microalgae was found to show a vital role in the toxicity of Ag NPs to the photosynthetic microbes grown in salt water (Sendra et al., 2017). The adsorption and aggregation of NPs on the cell surface can cause mechanical damage and affect the cellular metabolism (Hazeem et al., 2016) and thus can cause the growth inhibition and the corresponding drop in biomass concentration and photosynthetic pigments (Metzler et al., 2011).

5.2 Effects of Ag NPs on Growth Pattern and Biomass

The changes of *S. platensis* biomass due to the exposure of Ag NPs over 96 h was estimated through spectrophotometric method to study the effects of Ag NPs on the growth pattern and biomass of *S. platensis*. A concentration- and time-dependent loss was observed in the biomass concentration of *S. platensis* due to the exposure of Ag NPs. Researches conducted by Lone et al. (2013) and Comotto et al. (2014) confirmed the loss of biomass of *S. platensis* using different NPs. It was reported that 10 µg/mL of 50 nm ZnO NPs caused 41%

loss in biomass concentration of *S. platensis* when exposed for 10 days (Lone et al., 2013), and 74% loss in biomass concentration when treated with 100 µg/mL of 14 nm TiO₂ NPs for 15 days (Comotto et al., 2014). Previous studies have presented the growth inhibitory effect of Ag NPs on different photosynthetic microbes. For instance, 200 µg/mL of Ag NPs can cause a complete inhibition in *Scenedesmus* sp. and almost 100% inhibition in *Thalassiosira* sp. at 72 h with the EC₅₀ values of 89.92 and 107.21 µg/L for *Scenedesmus* sp. and *Thalassiosira* sp., respectively (Pham, 2019). Smaller size Ag NPs was found to cause higher growth inhibition on *C. reinhardtii* and as *C. reinhardtii* treated with 10 µg/L of Ag NPs with size of 4.5 and 16.7 nm showed more than 50% growth inhibition at 72 h with the EC₅₀ value of < 10 µg/L for Ag NPs, whereas the EC₅₀ value of > 300 µg/L was reported for Ag NPs with 46.7 nm (Sendra et al., 2017). Djearamane et al. (2019b) evidenced a significant reduction in the cell viability and the corresponding biomass concentration of *C. vulgaris* when exposed to ZnO NPs.

The growth rate of photosynthetic microbes exposed to Ag NPs might be affected by the shape, size, concentration, surface charge and also surface coatings (Cepoi et al., 2020). Many researchers suggested that the growth inhibition of cells was because of the production of ROS (Djearamane et al., 2020; Suman et al., 2015; Xia et al., 2015) or the mechanical damage caused by NPs on the cells (Castro-Bugallo et al., 2014). Other factors such as the light shading effect (Sadiq et al., 2011), release of metal ions (Aravantinou et al., 2015; Lee and An, 2013; Suman et al., 2015), interaction with the culture medium (Manier et al., 2013), and the synergistic effects of these different factors (Manzo et al., 2013) were also reported to affect the growth of the cells.

The destruction of cell membrane upon exposure to NPs is one of the factors that cause the growth inhibition, which leads to the uncontrolled release and intake of electrolytes and subsequently affect the photosynthesis apparatus and also the synthesis of macronutrients (Anusha et al., 2017a). The interaction of metal ions with the functional groups present on the surface of the cells would affect the growth rate as well (Balaji et al., 2014).

5.3 Effects of Ag NPs to Proteins, Carbohydrates and Lipids

The total proteins, carbohydrates and lipids of *S. platensis* were tested to determine the effect of the treatment of Ag NPs to the production of macronutrients of *S. platensis*. A dose and time-dependent decrease in the protein, carbohydrate and lipid content observed from this study may be due to the stress caused by Ag NPs present in the culture medium (Holan and Volesky, 1994). Similar results were shown when *S. platensis* was treated with different heavy metals and NPs. *S. platensis* treated with 10 µg/mL ZnO NPs was reported to have a 79% reduction in protein content when exposed for 10 days (Lone et al., 2013), while 32, 64 and 69% reduction was observed when treated with 100 µg/mL of Se metal at 24, 48 and 72 h (Zinicovscaia et al., 2017). Balaji et al. (2014) reported that the exposure of 42 mg/L of Ni and 48 mg/L of Zn to *S. platensis* for 18 days led to the highest reduction in protein content.

Similar to proteins, a dose and time-dependent reduction in the carbohydrates of *A. platensis* was observed in this study. A study by Zinicovscaia et al. (2017) reported 76% reduction in the carbohydrate content of *S. platensis* when treated with 100 µg/mL of Se at 72 h. However, another study on *S. costatum* using

0.05 to 50 µg/mL of Ag NPs evidence only a limited impact on the carbohydrate content when exposed for 24 h (Huang et al., 2016).

Finding of Zinicovscaia et al. (2017) stated that 100 µg/mL of Se metal caused 23, 50 and 80% reduction in lipid content of *S. platensis* when exposed to 24, 48 and 72 h, respectively. *S. platensis* treated with 100, 250 and 500 µg/mL of TiO₂ NPs stated to have 44, 53 and 66% reduction in lipid yield was reported in *S. platensis* when treated with 100, 250 and 500 µg/mL of TiO₂ NPs at Day 5 (Casazza et al., 2015a). On the other hand, Pham (2019) reported that Ag NPs at the concentrations of 5 to 200 µg/mL would raise the lipid yield from 11 to 17% at 72 h for *Thalassiosira* sp.. The lipid content in *Scenedesmus* sp. also showed increment of 8.1 and 7.6% with the presence of Ag NPs at the concentrations of 5 and 20 µg/mL, and then decreased at higher concentrations of 100 and 200 µg/mL.

The oxidation of the functional groups and structural elements of cyanobacteria is caused by the production of ROS and the release of metal from the treatment of NPs. The proteins, lipids, and carbohydrates are then broken down into smaller molecules up to monomers, small inorganic molecules, and water, which leads to the degradation of biomass (Khalifeh et al., 2022; Zinicovscaia et al., 2017). ROS can also lead to subsequent lipid peroxidation which will interrupt the cell metabolism (Wang et al., 2019). Cyanobacteria have the propensity to modify cellular metabolism by reducing the biosynthesis of metabolites under stress condition when exposed to NPs (Khalifeh et al., 2022; Pham, 2019).

The reduction in all these biological macromolecules of photosynthetic microbes may be because of the oxidative stress induced by the heavy metals or NPs that are present in the culture medium. A study reported that the cells that are growing under stress conditions were observed to have a lower protein synthesis capacity (Zeng and Vonshak, 1998). The high concentrations of NPs used during the exposure to the cells caused the damage in the cell membrane that led to the reduction in the synthesis of carbohydrates, which subsequently caused the uncontrolled release and intake of electrolytes (Anusha et al., 2017a). The decrease in carbohydrates may also be affected by the production of chlorophyll as carbohydrates are the main photosynthesis products that are kept in the chloroplasts (Huang et al., 2016). The change in the lipid content was due to the response to stress based on the condition and alteration in the physiological state of the cells as the phospholipids in the cell membrane play an important role in metabolism (Zinicovscaia et al., 2017).

Further, the researchers have also explained the mechanism for the depletion of macronutrients at the molecular level. A study investigated the gene expression of *C. reinhardtii* when exposed to Ag and reported that majority of the protein were significantly regulated but only observed at the transcriptome and not the proteome level, which may be the reason for the reduced synthesis of protein in microalgae (Pillai et al., 2014). The treatment of TiO₂ NPs was also reported to disrupt the material and energy metabolism in *Chlorella pyrenoidosa* at the molecular level, where the gene expression of lipid synthesis, carbohydrate synthesis and cell division were down regulated (Middepogu et al., 2018), indicating the inhibition of biosynthesis of lipid and carbohydrate and also the cell division of *C. pyrenoidosa* at the gene expression level. In short, the

attachment of NPs on the cell membrane leads to the damage in the cell membrane which poses a vital role in reducing the production of proteins, carbohydrates and lipids in the photosynthetic microbes.

5.4 Effects of Ag NPs to Chlorophyll-*a*, Carotenoids and C-Phycocyanin

Besides macronutrients, the effects of Ag NPS on the pigments (chlorophyll-*a*, carotenoids and C-phycocyanin) of *S. platensis* was also studied. A concentration and dose-dependent reduction in the chlorophyll-*a* content of *S. platensis* is related to the stress caused by Ag NPs (Holan and Volesky, 1994). Similar to the present study, study by Djearamane et al. (2018) stated 63, 75, 86, 88 and 93% reduction in chlorophyll-*a* of *S. platensis* when treated with 10, 50, 100, 150 and 200 µg/mL of ZnO NPs, respectively at 96 h. A study by Pham (2019) showed 21.5 and 14.5 % reduction in chlorophyll-*a* of *Scenedesmus* sp. and *Thalassiosira* sp. respectively, when exposed to 200 µg/mL Ag NPs at 72 h. Another study reported that the treatment of 0.05 µg/mL Ag NPs significantly increased the production of chlorophyll-*a* in *S. costatum* by 4.7% at 24 h, and decreased by 2.4% when the dose of Ag NPs was increased to 5 µg/mL. The maximum reduction in chlorophyll-*a* content of *S. costatum* was reported to be 35% when treated with 500 µg/mL of Ag NPs for 24 h (Huang et al., 2016).

Like chlorophyll-*a*, the carotenoids and C-phycocyanin of *S. platensis* cells exhibited a concentration and time-dependent reduction when exposed to Ag NPs. Similar to the present results, Djearamane et al. (2018) reported a maximum reduction of 76.2% in carotenoids and 74.1 % in C-phycocyanin when exposed to 200 µg/mL of ZnO NPs, respectively, at 96 h. Another study

stated that 10 µg/mL of ZnO NPs caused 50% reduction in *S. platensis* when exposed for 10 days (Lone et al., 2013). While, Zinicovscaia et al. (2017) stated that the C-phycoyanin concentration of *S. platensis* reduced from 6.9 to 2.4% at 24 h when exposed to Se ions. The lowest C-phycoyanin content was observed at 72 h with 0.66% C-phycoyanin in *Spirulina* biomass, which contained only about 10% of the original amount.

Chlorophyll-*a* is a useful indicator to determine the efficiency of photosynthesis and growth status of photosynthetic microbes. The inhibition of the biosynthesis of the key protein for photosynthesis might further affect the photosynthesis products (Huang et al., 2016). The reduction of chlorophyll-*a* might be due to the destruction in chloroplast ribosomes (Sendra et al., 2017), increased activity of chlorophyllase, the disruption of membrane system, and also the inactivation of electron transport functions in the photosystem (Holan and Volesky, 1994). The effective quantum yield of PSII was decreased in cyanobacteria when treated with NPs marks the decreased efficiency of the photochemical energy conversion process (Sendra et al., 2017). Carotenoids are the accessory photosynthetic pigments that primarily absorbs light in the blue-green region (Miazek et al., 2015). While, C-phycoyanin is a type of phycobilins that are present in cyanobacteria which helps to absorb the wavelengths of light between 595 and 640 nm to supplement the light-capturing ability of chlorophyll (Frank and Cogdell, 2012). The reduction in the accessory photosynthetic pigments (carotenoids and C-phycoyanin) under stress conditions affects the light-absorbing ability of chlorophyll which subsequently leads to the inhibition of growth. The exposure of NPs to cyanobacteria also leads to the destruction of thylakoids that causes the decrease in photosynthetic pigments which affects the

photosynthesis of cyanobacteria, resulting in the inhibition of growth and cell death (Arunakumara and Zhang, 2009). The attachment of Ag NPs on the surface of the cells can cause the physical shading and act as a photosynthesis barrier which in turn can result in the loss of biomass (Huang et al., 2016) and thus the macronutrients.

5.5 Effects of Ag NPs to Total Phenolic Compounds

The total phenolic compounds of *S. platensis* after the exposure of Ag NPs was estimated to determine the intracellular phenolic compound production which may be linked to the antioxidant activity of microalgae. A typical dose-dependent and time-dependent reduction was observed for the total phenolic contents of *S. platensis* when treated with Ag NPs. Earlier study by Fazelian et al. (2020) reported a significant decrease in phenolic compounds of *N. oculata* when exposed to 25 to 50 mg/L of Ag NPs, although all the concentrations tested in the study showed decrease in the phenolic compound even from 1 mg/L of Ag NPs. In another study, *C. vulgris* cells treated with 2 to 6 mg/L of microwave synthesized silver-reduced graphene oxide nanocomposites (Ag-rGO) were also reported to have significant decrease in the phenolic contents at 24 h as compared to the control (Nazari et al., 2020). Similar reduced production of phenolic content was also found when using hydrothermal synthesized Ag-rGO (Nazari et al., 2018). Casazza et al. (2015) reported that the *S. platensis* exposed to 100, 250 and 500 µg/mL of TiO₂ NPs caused 34.9, 27.9 and 24.5% reduction in intracellular phenolic content at Day 5. While, another study reported 12, 17 and 24% reduction in the intracellular phenolic content of *H.*

pluvialis, *C. vulgaris* and *S. platensis*, respectively when treated with 100 µg/mL of TiO₂ NPs at Day 15 as compared to the control (Comotto et al., 2014). Zaidi et al. (2014) also reported a decrease in the total phenolic compounds of *Chlorella* sp. when treated with 5 and 10 ppm of Ag NPs.

Photosynthetic microbes under stress conditions are likely to excrete compounds such as phenolic compounds which can detoxify the surrounding environment and act as an antioxidant. When microalgae are under ideal conditions, phenolic compounds are the secondary plant metabolites that are produced by the phenyl propanoid metabolism and the shikimic acid pathway. However, varied environmental challenges to the cells may alter the amount of phenolic content (Vogt, 2010). The increased production of phenolic compounds is stimulated by the cells in response to the stress conditions and released to the culture medium with a decrease in the intracellular concentration of phenolic compounds and increase in the extracellular phenolic content (Comotto et al., 2014). The reduction in total phenolic compounds in the photosynthetic microbes under the exposure of heavy metals may be due to the inhibition of photosynthesis which results in the reduced production of new phenolic compounds (Connan and Stengel, 2011). The decreased production of the total phenolic compounds can lead to a decreased antioxidant activity which can cause reduction in the biomass (Bello-Bello et al., 2017; Fazelian et al., 2020).

5.6 Toxicity Mechanism of NPs

Most researchers suggested that the physical constraints and oxidative stress are the primary cause of NPs to exhibit toxicity to microalgae. Large NPs aggregates trapping algal cells not only limits the amount of light accessible for photosynthesis but also hinders the intake of nutrients (Li et al., 2015; Li et al., 2018). Through the excessive accumulation of intracellular ROS caused by NPs exposure, oxidative stress is caused (Costa et al., 2016; Hazeem et al., 2016). According to Chen et al. (2019), which explore the mechanism of NPs through meta-analysis, revealed that the ROS remarkably increased by 90% in the presence of NPs, showing the buildup of excess ROS in microalgae cells which leads to subsequent oxidative stress. The ROS accumulation in microalgae induced by NPs is not remarkably influenced by NPs surface modification, however, is strongly related to the type of NPs and the microalgae species, and the dose of NPs used. As the exposure of NPs caused the formation of ROS, the defense mechanism of microalgae will be triggered, where the antioxidative enzymes superoxide dismutase (SOD) and peroxidase (POD) were synthesized to scavenge ROS. When the capacity of antioxidant enzymes was unable to remove the excessively generated ROS, the cell membrane of microalgae cells would be damaged by the excessive ROS, where membrane lipid peroxidation occurs. Lipid peroxidation may lead to an increase cell membrane permeability, which results in the loss of membrane selectivity, fluidity, and integrity (Lei et al., 2016). The damage to the microalgae cell membrane and the alteration in photosynthetic activity are the most frequent biological markers to determine the toxicity of NPs in microalgae (Sendra et al., 2018). Through a change in the lipid-to-protein ratio of the pigment-protein complexes, the built up ROS in

chloroplast could lower the amount of chlorophyll present in microalgae cells (Du et al., 2016; Huang et al., 2016; F. Li et al., 2015). The energy transfer in light responses is interrupted by a fall in chlorophyll level brought on by NPs, which also results the reduction in cell density and a delay in algal growth (Chen et al., 2019).

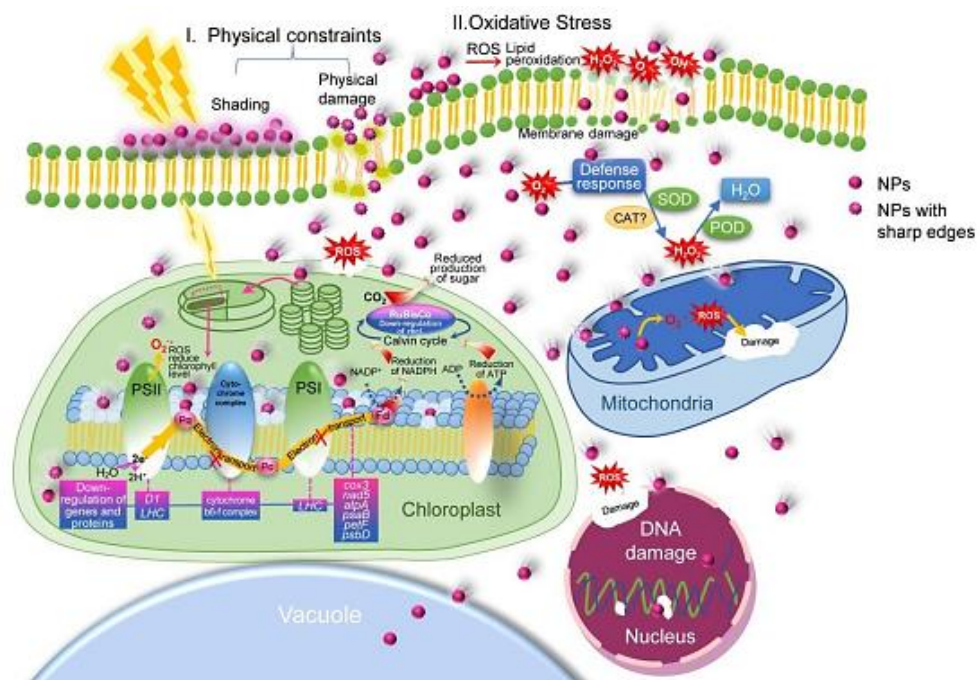


Figure 5.15: Toxicity mechanism of NPs to algal cell membrane and organelles (Chen et al., 2019).

5.7 Conclusion

The objectives of this study have been achieved. The results of the present study identified the possible involvement of the functional groups such as hydroxyl, amine, methyl, amide I, amide II, carboxyl, carbonyl, and phosphate groups from *S. platensis* cell wall in the interaction and accumulation of Ag NPs in *S. platensis*, causing surface alterations and damage of the Ag NPs treated *S.*

platensis. The exposure of Ag NPs to *S. platensis* lead to a dose and time-dependent reduction in the biomass, proteins, carbohydrates, lipids, chlorophyll-*a*, carotenoids, C-phycoyanin, and phenolic compounds. Significant results were observed even from the treatment of Ag NPs at lowest concentration of 10 µg/mL at 24 h, and the maximum effects were found at 100 µg/mL Ag NPs treated *S. platensis* for all the parameters tested. The interaction between Ag NPs and the functional groups on the cell wall can form a physical barrier and block the photosynthesis activity, the transfer of nutrients, and induced stress to the cells, which led to the growth inhibition and the corresponding reduction in biomass, macromolecules, pigments, and phenolic compounds. The findings of this study may be useful to design methods to detect the contamination of Ag NPs with *S. platensis* and thus will help to produce and provide the consumers with high-quality *Spirulina* nutritional supplements with uncompromised nutritional properties. Otherwise, the consumption of Ag NPs contaminated *S. platensis* supplements may not offer the consumers with the desired nutritional benefits and may even cause health risks due to Ag NPs contamination.

5.8 Limitation and Recommendation

There are some limitations in this study where firstly, inductively coupled plasma-optical emission spectroscopy (ICP-OES) was not able to be conducted to investigate the cellular accumulation of Ag NPs in *S. platensis*. Hence, ICP-OES is recommended to be carried out in the future study to quantify the amount of Ag NPs that has been absorbed by *S. platensis*. The internalization of Ag NPs

in *S. platensis* cells through TEM analysis was not able to confirm in this study. The toxicity of Ag ions to *S. platensis* was not tested in this study. Multiple literature claimed that Ag ion released from Ag NPs also exert toxicity to microalgae, although Ag NPs itself also can cause significant toxicity to aquatic organisms.

Since *S. platensis* has the ability to adsorb and absorb NPs in their biomass, methods to eliminate Ag NPs in NPs contaminated microalgae can be investigated to reverse the contamination of NPs in contaminated microalgae. Also, the toxicity of Ag NPs to human body can be carried out in the future to investigate the minimum concentration of Ag NPs that can exert toxicity effects to human cells.

REFERENCES

- Abdulqader, G., Barsanti, L., Tredici, M.R., 2000. Harvest of *Arthrospira platensis* from Lake Kossorom (Chad) and its household usage among the Kanembu. *J. Appl. Phycol.* 12, pp. 493–498.
- Agrawal, N., Minj, D.K., Rani, K., 2015. Estimation of total carbohydrate present in dryfruits. *IOSR-JESTFT* 1, pp. 24-27.
- Akbarnezhad, M., Mehrgan, M.S., Kamali, A., Baboli, M.J., 2016. Bioaccumulation of Fe⁺² and its effects on growth and pigment content of *Spirulina* (*Arthrospira platensis*). *AACL Bioflux* 9, pp. 227-238.
- Al-Dhabi, N.A., 2013. Heavy metal analysis in commercial *Spirulina* products for human consumption. *Saudi J. Biol. Sci.* 20, pp. 383–388.
- Al-Homaidan, A.A., Al-Houri, H.J., Al-Hazzani, A.A., Elgaaly, G., Moubayed, N.M.S., 2014. Biosorption of copper ions from aqueous solutions by *Spirulina platensis* biomass. *Arab. J. Chem.* 7, pp. 57–62.
- Ali, S., Saleh, A., 2012. *Spirulina*-an over view. *Int. J. Pharm. Pharm. Sci.* 4, pp. 9–15.
- Aliakbarian, B., Dehghani, F., Perego, P., 2009. The effect of citric acid on the phenolic contents of olive oil. *Food Chem.* 116, pp. 617–623.
- Anastopoulos, I., Kyzas, G.Z., 2015. Progress in batch biosorption of heavy metals onto algae. *J. Mol. Liq.* 209, pp. 77–86.
- Andersen, R.A., 2005. *Algal culturing techniques*. Burlington, Mass: Elsevier/Academic Press.
- Ansari, F.A., Ravindran, B., Gupta, S.K., Nasr, M., Rawat, I., Bux, F., 2019. Techno-economic estimation of wastewater phycoremediation and environmental benefits using *Scenedesmus obliquus* microalgae. *J. Environ. Manage.* 240, pp. 293–302.
- Anusha, L., Chingangbam, S.D., Sibi, G., 2017b. Inhibition Effects of Cobalt Nano Particles Against Fresh Water Algal Blooms Caused by *Microcystis* and *Oscillatoria*. *Am. J. Appl. Sci. Res.* 3, pp. 26.

Aravantinou, A.F., Tsarpali, V., Dailianis, S., Manariotis, I.D., 2015. Effect of cultivation media on the toxicity of ZnO nanoparticles to freshwater and marine microalgae. *Ecotoxicol. Environ. Saf.* 114, pp. 109–116.

Arunakumara, K.K.I.U., Zhang, X., 2009. Effects of heavy metals (Pb²⁺ and Cd²⁺) on the ultrastructure, growth and pigment contents of the unicellular cyanobacterium *Synechocystis* sp. PCC 6803. *Chin. J. Oceanol. Limnol.* 27, pp. 383–388.

Aruoja, V., Dubourguier, H.-C., Kasemets, K., Kahru, A., 2009. Toxicity of nanoparticles of CuO, ZnO and TiO₂ to microalgae *Pseudokirchneriella subcapitata*. *Sci. Total Environ.* 407, pp. 1461–1468.

Asharani, P.V., Lian Wu, Y., Gong, Z., Valiyaveetil, S., 2008. Toxicity of silver nanoparticles in zebrafish models. *Nanotechnology* 19, p. 255102.

Atiyeh, B.S., Costagliola, M., Hayek, S.N., Dibo, S.A., 2007. Effect of silver on burn wound infection control and healing: Review of the literature. *Burns* 33(2), pp. 139-148.

Balaji, S., Kalaivani, T., Rajasekaran, C., 2014. Biosorption of Zinc and Nickel and Its Effect on Growth of Different *Spirulina* Strains: Biosorption Potentials of *Spirulina* Strains. *CLEAN - Soil Air Water* 42, pp. 507–512.

Banerjee, A., Roychoudhury, A., 2019. Nanoparticle-Induced Ecotoxicological Risks in Aquatic Environments. In: *Nanomaterials in Plants, Algae and Microorganisms*. Elsevier, pp. 129–141.

Bataller, B.G., Capareda, S.C., 2018. A rapid and non-destructive method for quantifying biomolecules in *Spirulina platensis* via Fourier transform infrared – Attenuated total reflectance spectroscopy. *Algal Res.* 32, pp. 341–352.

Belay, A., 2007. *Spirulina (Arthrospira): Production and Quality Assurance*. In: Belay, A., Gershwin, M. (Eds.), *Spirulina in Human Nutrition and Health*. CRC Press, pp. 1–25.

Bello-Bello, J.J., Chavez-Santoscoy, R.A., Lecona-Guzmán, C.A., Bogdanchikova, N., Salinas-Ruíz, J., Gómez-Merino, F.C., Pestryakov, A., 2017. Hormetic Response by Silver Nanoparticles on In Vitro Multiplication of Sugarcane (*Saccharum* spp. Cv. Mex 69-290) Using a Temporary Immersion System. *Dose-Response* 15, 155932581774494.

Ben Hamissa, A.M., Seffen, M., Aliakbarian, B., Casazza, A.A., Perego, P., Converti, A., 2012. Phenolics extraction from *Agave americana* (L.) leaves using high-temperature, high-pressure reactor. *Food Bioprod. Process.* 90, pp. 17–21.

Bennett, A., Bogorad, L., 1973. Complementary chromatic adaptation in a filamentous blue-green alga. *J. Cell Biol.* 58, pp. 419–435.

Bensehaila, S., Doumandji, A., Boutekrabt, L., Manafikhi, H., Peluso, I., Bensehaila, K., Kouache, A., Bensehaila, A., 2015. The nutritional quality of *Spirulina platensis* of Tamenrasset, Algeria. *Afr. J. Biotechnol.* 14, pp. 1649–1654.

Bilberg, K., Hovgaard, M.B., Besenbacher, F., Baatrup, E., 2012. In Vivo Toxicity of Silver Nanoparticles and Silver Ions in Zebrafish (*Danio rerio*). *J. Toxicol.* 2012, pp. 1–9.

Blaser, S.A., Scheringer, M., MacLeod, M., Hungerbühler, K., 2008. Estimation of cumulative aquatic exposure and risk due to silver: Contribution of nano-functionalized plastics and textiles. *Sci. Total Environ.* 390, pp. 396–409.

Bolaños-Benítez, V., McDermott, F., Gill, L., Knappe, J., 2020. Engineered silver nanoparticle (Ag-NP) behaviour in domestic on-site wastewater treatment plants and in sewage sludge amended-soils. *Sci. Total Environ.* 722, p. 137794.

Bolouri-Moghaddam, M.R., Le Roy, K., Xiang, L., Rolland, F., Van den Ende, W., 2010. Sugar signalling and antioxidant network connections in plant cells: Sugar signalling and antioxidant networks in plants. *FEBS J.* 277, pp. 2022–2037.

Bothe, H., Schmitz, O., Yates, M.G., Newton, W.E., 2010. Nitrogen Fixation and Hydrogen Metabolism in Cyanobacteria. *Microbiol. Mol. Biol. Rev.* 74, pp. 529–551.

Boussiba, S., Richmond, A.E., 1980. C-phycocyanin as a storage protein in the blue-green alga *Spirulina platensis*. *Arch. Microbiol.* 125, pp. 143–147.

Burchardt, A.D., Carvalho, R.N., Valente, A., Nativo, P., Gilliland, D., García, C.P., Passarella, R., Pedroni, V., Rossi, F., Lettieri, T., 2012. Effects of Silver Nanoparticles in Diatom *Thalassiosira pseudonana* and Cyanobacterium *Synechococcus* sp. *Environ. Sci. Technol.* 46, pp. 11336–11344.

Cardozo, K.H.M., Guaratini, T., Barros, M.P., Falcão, V.R., Tonon, A.P., Lopes, N.P., Campos, S., Torres, M.A., Souza, A.O., Colepicolo, P., Pinto, E., 2007. Metabolites from algae with economical impact. *Comp. Biochem. Physiol. Part C Toxicol. Pharmacol.* 146, pp. 60–78.

Carlson, C., Hussain, S.M., Schrand, A.M., K. Braydich-Stolle, L., Hess, K.L., Jones, R.L., Schlager, J.J., 2008. Unique Cellular Interaction of Silver Nanoparticles: Size-Dependent Generation of Reactive Oxygen Species. *J. Phys. Chem. B* 112, pp. 13608–13619.

Casazza, A.A., Ferrari, P.F., Aliakbarian, B., Converti, A., Perego, P., 2015a. Effect of UV radiation or titanium dioxide on polyphenol and lipid contents of *Arthrospira (Spirulina) platensis*. *Algal Res.* 12, pp. 308–315.

Castro-Bugallo, A., González-Fernández, Á., Guisande, C., Barreiro, A., 2014. Comparative Responses to Metal Oxide Nanoparticles in Marine Phytoplankton. *Arch. Environ. Contam. Toxicol.* 67, pp. 483–493.

Çelekli, A., Gün, D., Bozkurt, H., 2021. Bleaching of olive pomace oil with *Spirulina platensis* as an eco-friendly process. *Algal Res.* 54, p. 102210.

Çelekli, A., Yavuzatmaca, M., Bozkurt, H., 2010. An eco-friendly process: Predictive modelling of copper adsorption from aqueous solution on *Spirulina platensis*. *J. Hazard. Mater.* 173, pp. 123–129.

Cepoi, L., Zinicovscaia, I., Rudi, L., Chiriac, T., Rotari, I., Turchenko, V., Djur, S., 2020. Effects of PEG-Coated Silver and Gold Nanoparticles on *Spirulina platensis* Biomass during Its Growth in a Closed System. *Coatings* 10, p. 717.

Chen, F., Xiao, Z., Yue, L., Wang, J., Feng, Y., Zhu, X., Wang, Z., Xing, B., 2019. Algae response to engineered nanoparticles: current understanding, mechanisms and implications. *Environ. Sci. Nano* 6, pp. 1026–1042.

Chen, X., Schluesener, H.J., 2008. Nanosilver: A nanoparticle in medical application. *Toxicol. Lett.* 176, pp. 1–12

Cho, Y.M., Mizuta, Y., Akagi, J., Toyoda, T., Sone, M., Ogawa, K., 2018. Size-dependent acute toxicity of silver nanoparticles in mice. *J. Toxicol. Pathol.* 31, pp. 73–80.

Ciferri, O., 1983. *Spirulina*, the edible microorganism. *Microbiol. Rev.* 47, pp. 551–578.

Comotto, M., Casazza, A.A., Aliakbarian, B., Caratto, V., Ferretti, M., Perego, P., 2014. Influence of TiO₂ Nanoparticles on Growth and Phenolic Compounds Production in Photosynthetic Microorganisms. *Sci. World J.* 2014, pp. 1–9.

Connan, S., Stengel, D.B., 2011. Impacts of ambient salinity and copper on brown algae: 2. Interactive effects on phenolic pool and assessment of metal binding capacity of phlorotannin. *Aquat. Toxicol.* 104, pp. 1–13.

Costa, C.H. da, Perreault, F., Oukarroum, A., Melegari, S.P., Popovic, R., Matias, W.G., 2016. Effect of chromium oxide (III) nanoparticles on the production of reactive oxygen species and photosystem II activity in the green alga *Chlamydomonas reinhardtii*. *Sci. Total Environ.* 565, pp. 951–960.

Croteau, M.-N., Misra, S.K., Luoma, S.N., Valsami-Jones, E., 2011. Silver Bioaccumulation Dynamics in a Freshwater Invertebrate after Aqueous and Dietary Exposures to Nanosized and Ionic Ag. *Environ. Sci. Technol.* 45, pp. 6600–6607.

Cunningham, B., Engstrom, A.M., Harper, B.J., Harper, S.L., Mackiewicz, M.R., 2021. Silver Nanoparticles Stable to Oxidation and Silver Ion Release Show Size-Dependent Toxicity In Vivo. *Nanomaterials* 11, p. 1516.

da Costa, G.M., Hussain, C.M., 2020. Safety risk, ELSI (ethical, legal, social issues), and economics of nanomaterials, in: Handbook of Nanomaterials in Analytical Chemistry. *Elsevier*, pp. 435–446.

Dalai, S., Pakrashi, S., Kumar, R.S.S., Chandrasekaran, N., Mukherjee, A., 2012. A comparative cytotoxicity study of TiO₂ nanoparticles under light and dark conditions at low exposure concentrations. *Toxicol. Res.* 1, p. 116.

Dazhi, W., Zhaodi, C., Shaojing, L., Yahui, G., 2003. Toxicity and accumulation of selenite in four microalgae. *Chin. J. Oceanol. Limnol.* 21, pp. 280–285.

de Marco Castro, E., Shannon, E., Abu-Ghannam, N., 2019. Effect of Fermentation on Enhancing the Nutraceutical Properties of *Arthrospira platensis* (*Spirulina*). *Fermentation* 5, p. 28.

del Rio-Chanona, E.A., Zhang, D., Xie, Y., Manirafasha, E., Jing, K., 2015. Dynamic Simulation and Optimization for *Arthrospira platensis* Growth and C-Phycocyanin Production. *Ind. Eng. Chem. Res.* 54, pp. 10606–10614.

Deng, R., Chow, T.-J., 2010. Hypolipidemic, Antioxidant, and Antiinflammatory Activities of Microalgae *Spirulina*: Hypolipidemic, Antioxidant, and Antiinflammatory Activities of Microalgae *Spirulina*. *Cardiovasc. Ther.* 28, pp. e33–e45.

Deniz, F., Saygideger, S.D., Karaman, S., 2011. Response to Copper and Sodium Chloride Excess in *Spirulina* sp. (Cyanobacteria). *Bull. Environ. Contam. Toxicol.* 87, pp. 11–15.

Devi, K.U., Swapna, G., Suneetha, S., 2014. Microalgae in Bioremediation. In: *Microbial Biodegradation and Bioremediation*. Elsevier, pp. 433–454.

Dewez, D., Oukarroum, A., 2012. Silver nanoparticles toxicity effect on photosystem II photochemistry of the green alga *Chlamydomonas reinhardtii* treated in light and dark conditions. *Toxicol. Environ. Chem.* 94, pp. 1536–1546.

Djearamane, S., Lim, Y.M., Wong, L.S., Lee, P.F., 2019a. Cellular accumulation and cytotoxic effects of zinc oxide nanoparticles in microalga *Haematococcus pluvialis*. *PeerJ* 7, p. e7582.

Djearamane, S., Lim, Y.M., Wong, L.S., Lee, P.F., 2018a. Cytotoxic effects of zinc oxide nanoparticles on cyanobacterium *Spirulina (Arthrospira) platensis*. *PeerJ* 6, p. e4682.

Djearamane, S., Wong, L.S., Lim, Y.M., Lee, P.F., 2020. Oxidative stress effects of zinc oxide nanoparticles on fresh water microalga *Haematococcus pluvialis*. *Ecol. Environ. Conserv.* 26, pp. 663–668.

Djearamane, S., Wong, L.S., Lim, Y.M., Lee, P.F., 2019b. Cytotoxic effects of zinc oxide nanoparticles on *Chlorella vulgaris*. *Pollut. Res.* 38, pp. 479–484.

Dotto, G.L., Cadaval, T.R.S., Pinto, L.A.A., 2012. Use of *Spirulina platensis* micro and nanoparticles for the removal synthetic dyes from aqueous solutions by biosorption. *Process Biochem.* 47, pp. 1335–1343.

Du, S., Zhang, P., Zhang, R., Lu, Q., Liu, L., Bao, X., Liu, H., 2016. Reduced graphene oxide induces cytotoxicity and inhibits photosynthetic performance of the green alga *Scenedesmus obliquus*. *Chemosphere* 164, pp. 499–507.

Durán, N., Nakazato, G., Seabra, A.B., 2016. Antimicrobial activity of biogenic silver nanoparticles, and silver chloride nanoparticles: an overview and comments. *Appl. Microbiol. Biotechnol.* 100, pp. 6555–6570.

Elechiguerra, J.L., Burt, J.L., Morones, J.R., Camacho-Bragado, A., Gao, X., Lara, H.H., Yacaman, M.J., 2005. Interaction of silver nanoparticles with HIV-1. *J. Nanobiotechnology* 3, p. 6.

El-Sheekh, M.M., El-Naggar, A.H., Osman, M.E.H., El-Mazaly, E., 2003. Effect of cobalt on growth, pigments and the photosynthetic electron transport in *Monoraphidium minutum* and *Nitzschia perminuta*. *Braz. J. Plant Physiol.* 15, pp. 159–166.

Fais, G., Manca, A., Bolognesi, F., Borselli, M., Concas, A., Busutti, M., Broggi, G., Sanna, P., Castillo-Aleman, Y.M., Rivero-Jiménez, R.A., Bencomo-Hernandez, A.A., Ventura-Carmenate, Y., Altea, M., Pantaleo, A., Gabrielli, G., Biglioli, F., Cao, G., Giannaccare, G., 2022. Wide Range Applications of *Spirulina*: From Earth to Space Missions. *Mar. Drugs* 20, p. 299.

Fang, L., Zhou, C., Cai, P., Chen, W., Rong, X., Dai, K., Liang, W., Gu, J.-D., Huang, Q., 2011. Binding characteristics of copper and cadmium by cyanobacterium *Spirulina platensis*. *J. Hazard. Mater.* 190, pp. 810–815.

Fazelian, N., Movafeghi, A., Yousefzadi, M., Rahimzadeh, M., 2019. Cytotoxic impacts of CuO nanoparticles on the marine microalga *Nannochloropsis oculata*. *Environ. Sci. Pollut. Res.* 26, pp. 17499–17511.

Fazelian, N., Movafeghi, A., Yousefzadi, M., Rahimzadeh, M., Zarei, M., 2020. Impact of silver nanoparticles on the growth, fatty acid profile, and antioxidative response of *Nannochloropsis oculata*. *Acta Physiol. Plant.* 42, P. 126.

Ferreira, L.S., Rodrigues, M.S., de Carvalho, J.C.M., Lodi, A., Finocchio, E., Perego, P., Converti, A., 2011. Adsorption of Ni²⁺, Zn²⁺ and Pb²⁺ onto dry biomass of *Arthrospira (Spirulina) platensis* and *Chlorella vulgaris*. I. Single metal systems. *Chem. Eng. J.* 173, pp. 326–333.

Frank, H.A., Cogdell, R.J., 2012. 8.6 Light Capture in Photosynthesis. In: *Comprehensive Biophysics*. Elsevier, pp. 94–114.

Furno, F., Morley, K.S., Wong, B., Sharp, B.L., Arnold, P.L., Howdle, S.M., Bayston, R., Brown, P.D., Winship, P.D., Reid, H.J., 2004. Silver nanoparticles and polymeric medical devices: a new approach to prevention of infection? *J. Antimicrob. Chemother.* 54, pp. 1019–1024.

George, B., Pancha, I., Desai, C., Chokshi, K., Paliwal, C., Ghosh, T., Mishra, S., 2014. Effects of different media composition, light intensity and photoperiod on morphology and physiology of freshwater microalgae *Ankistrodesmus falcatus* – A potential strain for bio-fuel production. *Bioresour. Technol.* 171, pp. 367–374.

Gong, N., Shao, K., Feng, W., Lin, Z., Liang, C., Sun, Y., 2011. Biototoxicity of nickel oxide nanoparticles and bio-remediation by microalgae *Chlorella vulgaris*. *Chemosphere* 83, pp. 510–516.

Govindaraju, K., Basha, S.K., Kumar, V.G., Singaravelu, G., 2008. Silver, gold and bimetallic nanoparticles production using single-cell protein (*Spirulina platensis*) Geitler. *J. Mater. Sci.* 43, pp. 5115–5122.

Granqvist, C.G., Buhrman, R.A., 1976. Ultrafine metal particles. *J. Appl. Phys.* 47, pp. 2200–2219.

Griffitt, R.J., Hyndman, K., Denslow, N.D., Barber, D.S., 2009. Comparison of Molecular and Histological Changes in Zebrafish Gills Exposed to Metallic Nanoparticles. *Toxicol. Sci.* 107, pp. 404–415.

Griffitt, R.J., Luo, J., Gao, J., Bonzongo, J.-C., Barber, D.S., 2008. Effects of particle composition and species on toxicity of metallic nanomaterials in aquatic organisms. *Environ. Toxicol. Chem.* 27, p. 1972.

Gupta, S., Sharma, S., Singh, S., 2014. Hexavalent chromium toxicity to cyanobacterium *Spirulina platensis*. *Int. Res. J. Pharm.* 5, pp. 910–914.

Habib, M.A., Parvin, M., Huntington, T., Hasan, M. (Eds.), 2008. *A review on culture, production and use of Spirulina as food for humans and feeds for domestic animals and fish, FAO fisheries and aquaculture circular*. Food and Agriculture Organization of the United Nations, Rome.

Hajimahmoodi, M., Faramarzi, M.A., Mohammadi, N., Soltani, N., Oveisi, M.R., Nafissi-Varcheh, N., 2010. Evaluation of antioxidant properties and total phenolic contents of some strains of microalgae. *J. Appl. Phycol.* 22, pp. 43–50.

Hazeem, L.J., Bououdina, M., Rashdan, S., Brunet, L., Slomianny, C., Boukherroub, R., 2016. Cumulative effect of zinc oxide and titanium oxide nanoparticles on growth and chlorophyll a content of *Picochlorum* sp. *Environ. Sci. Pollut. Res.* 23, pp. 2821–2830.

He, M., Yan, Y., Pei, F., Wu, M., Gebreluel, T., Zou, S., Wang, C., 2017. Improvement on lipid production by *Scenedesmus obliquus* triggered by low dose exposure to nanoparticles. *Sci. Rep.* 7, p. 15526.

Holan, Z.R., Volesky, B., 1994. Biosorption of lead and nickel by biomass of marine algae. *Biotechnol. Bioeng.* 43, pp. 1001–1009.

Huang, J., Cheng, J., Yi, J., 2016. Impact of silver nanoparticles on marine diatom *Skeletonema costatum*: Silver nanoparticles are phototoxic to marine diatom. *J. Appl. Toxicol.* 36, pp. 1343–1354.

Hussain, S.M., Hess, K.L., Gearhart, J.M., Geiss, K.T., Schlager, J.J., 2005. In vitro toxicity of nanoparticles in BRL 3A rat liver cells. *Toxicol. In Vitro* 19, pp. 975–983.

Jaime, L., Mendiola, J.A., Herrero, M., Soler-Rivas, C., Santoyo, S., Señorans, F.J., Cifuentes, A., Ibáñez, E., 2005. Separation and characterization of antioxidants from *Spirulina platensis* microalga combining pressurized liquid extraction, TLC, and HPLC-DAD. *J. Sep. Sci.* 28, pp. 2111–2119.

Jibri, S.M., Jakada, B.H., Umar, H.Y., Ahmad, T.A., 2016. Importance of Some Algal Species as a Source of Food and Supplement. *Int. J. Curr. Microbiol. Appl. Sci.* 5, pp. 186–193.

Jung, C.H.G., Braune, S., Waldeck, P., Küpper, J.-H., Petrick, I., Jung, F., 2021. Morphology and Growth of *Arthrospira platensis* during Cultivation in a Flat-Type Bioreactor. *Life* 11, p. 536.

Jung, F., Krüger-Genge, A., Waldeck, P., Küpper, J.-H., 2019. *Spirulina platensis*, a super food? *J. Cell. Biotechnol.* 5, pp. 43–54.

Kameshwari, V., Selvaraj, S., Sundaramoorthy, S., 2020. Single Cell Protein *Spirulina*-A Nutrient Treasure. *Res. J. Pharmacol. Pharmacodyn.* 12, p. 49.

Karlsson, H.L., Toprak, M.S., Fadeel, B., 2015. Toxicity of Metal and Metal Oxide Nanoparticles. In: *Handbook on the Toxicology of Metals*. Elsevier, pp. 75–112.

Khalifeh, F., Salari, H., Zamani, H., 2022. Mechanism of MnO₂ nanorods toxicity in marine microalgae *Chlorella sorokiniana* during long-term exposure. *Mar. Environ. Res.* 179, p. 105669.

Khorrami, S., Zarrabi, A., Khaleghi, M., Danaei, M., Mozafari, M., 2018. Selective cytotoxicity of green synthesized silver nanoparticles against the MCF-7 tumor cell line and their enhanced antioxidant and antimicrobial properties. *Int. J. Nanomedicine* 13, pp. 8013–8024.

Kleiven, M., Macken, A., Oughton, D.H., 2019. Growth inhibition in *Raphidocelis subcapita* – Evidence of nanospecific toxicity of silver nanoparticles. *Chemosphere* 221, pp. 785–792.

Kondzior, P., Butarewicz, A., 2018. Effect of Heavy Metals (Cu and Zn) on the Content of Photosynthetic Pigments in the Cells of Algae *Chlorella vulgaris*. *J. Ecol. Eng.* 19, pp. 18–28.

Koru, E., 2012. Earth Food *Spirulina (Arthrospira)*: Production and Quality Standarts. In: El-Samragy, Y. (Ed.), *Food Additive*. InTech.

Koyande, A.K., Chew, K.W., Rambabu, K., Tao, Y., Chu, D.-T., Show, P.-L., 2019. Microalgae: A potential alternative to health supplementation for humans. *Food Sci. Hum. Wellness* 8, pp. 16–24.

Książyk, M., Asztemborska, M., Stęborowski, R., Bystrzejewska-Piotrowska, G., 2015. Toxic Effect of Silver and Platinum Nanoparticles Toward the Freshwater Microalga *Pseudokirchneriella subcapitata*. *Bull. Environ. Contam. Toxicol.* 94, pp. 554–558.

Kumar, A., Dixit, C.K., 2017. Methods for characterization of nanoparticles. In: *Advances in Nanomedicine for the Delivery of Therapeutic Nucleic Acids*. Elsevier, pp. 43–58.

Laban, G., Nies, L.F., Turco, R.F., Bickham, J.W., Sepúlveda, M.S., 2010. The effects of silver nanoparticles on fathead minnow (*Pimephales promelas*) embryos. *Ecotoxicology* 19, pp. 185–195.

Lane, T.W., 2022. Barriers to microalgal mass cultivation. *Curr. Opin. Biotechnol.* 73, pp. 323–328.

Lansdown, A.B.G., 2006. Silver in Health Care: Antimicrobial Effects and Safety in Use. In: Hipler, U.-C., Elsner, P. (Eds.), *Current Problems in Dermatology*. KARGER, Basel, pp. 17–34.

Lau, Z.L., Low, S.S., Ezeigwe, E.R., Chew, K.W., Chai, W.S., Bhatnagar, A., Yap, Y.J., Show, P.L., 2022. A review on the diverse interactions between microalgae and nanomaterials: Growth variation, photosynthetic performance and toxicity. *Bioresour. Technol.* 351, p. 127048.

Lee, K.J., Nallathamby, P.D., Browning, L.M., Osgood, C.J., Xu, X.-H.N., 2007. In Vivo Imaging of Transport and Biocompatibility of Single Silver Nanoparticles in Early Development of Zebrafish Embryos. *ACS Nano* 1, pp. 133–143.

Lee, W.M., An, Y.J., 2013. Effects of zinc oxide and titanium dioxide nanoparticles on green algae under visible, UVA, and UVB irradiations: No evidence of enhanced algal toxicity under UV pre-irradiation. *Chemosphere* 91, pp. 536–544.

Lei, C., Zhang, L., Yang, K., Zhu, L., Lin, D., 2016. Toxicity of iron-based nanoparticles to green algae: Effects of particle size, crystal phase, oxidation state and environmental aging. *Environ. Pollut.* 218, pp. 505–512.

Li, C., Shuford, K.L., Park, Q.-H., Cai, W., Li, Y., Lee, E.J., Cho, S.O., 2007. High-Yield Synthesis of Single-Crystalline Gold Nano-octahedra. *Angew. Chem. Int. Ed.* 46, pp. 3264–3268.

Li, F., Liang, Z., Zheng, X., Zhao, W., Wu, M., Wang, Z., 2015. Toxicity of nano-TiO₂ on algae and the site of reactive oxygen species production. *Aquat. Toxicol.* 158, pp. 1–13.

Li, Lin, Li, Lu, Zhou, X., Yu, Y., Li, Z., Zuo, D., Wu, Y., 2019. Silver nanoparticles induce protective autophagy via Ca²⁺/CaMKK β /AMPK/mTOR pathway in SH-SY5Y cells and rat brains. *Nanotoxicology* 13, pp. 369–391.

Li, M., Chen, D., Liu, Y., Chuang, C.Y., Kong, F., Harrison, P.J., Zhu, X., Jiang, Y., 2018. Exposure of engineered nanoparticles to *Alexandrium tamarens* (Dinophyceae): Healthy impacts of nanoparticles via toxin-producing dinoflagellate. *Sci. Total Environ.* 610–611, pp. 356–366.

Li, M., Hu, C., Zhu, Q., Chen, L., Kong, Z., Liu, Z., 2006. Copper and zinc induction of lipid peroxidation and effects on antioxidant enzyme activities in the microalga *Pavlova viridis* (Prymnesiophyceae). *Chemosphere* 62, pp. 565–572.

Li, X., Chen, Y., Ye, J., Fu, F., Pokhrel, G.R., Zhang, H., Zhu, Y., Yang, G., 2017. Determination of different arsenic species in food-grade spirulina powder by ion chromatography combined with inductively coupled plasma mass spectrometry. *J. Sep. Sci.* 40, pp. 3655–3661.

Li, X., Lan, T.H., Tien, C.-H., Gu, M., 2012. Three-dimensional orientation-unlimited polarization encryption by a single optically configured vectorial beam. *Nat. Commun.* 3, p. 998.

Li, X., Lenhart, J.J., 2012. Aggregation and Dissolution of Silver Nanoparticles in Natural Surface Water. *Environ. Sci. Technol.* 46, pp. 5378–5386.

Li, Y., Kröger, M., Liu, W.K., 2015. Shape effect in cellular uptake of PEGylated nanoparticles: comparison between sphere, rod, cube and disk. *Nanoscale* 7, pp. 16631–16646.

Li, Y., Zhou, W., Hu, B., Min, M., Chen, P., Ruan, R.R., 2012. Effect of light intensity on algal biomass accumulation and biodiesel production for mixotrophic strains *Chlorella kessleri* and *Chlorella protothecoide* cultivated in highly concentrated municipal wastewater. *Biotechnol. Bioeng.* 109, pp. 2222–2229.

Liang, S.X.T., Wong, L.S., Dhanapal, A.C.T.A., Djearmane, S., 2020. Toxicity of Metals and Metallic Nanoparticles on Nutritional Properties of Microalgae. *Water. Air. Soil Pollut.* 231, p. 52.

Liu, S., Lu, Y., Chen, W., 2018. Bridge knowledge gaps in environmental health and safety for sustainable development of nano-industries. *Nano Today* 23, pp. 11–15.

Lohse, S.E., Abadeer, N.S., Zoloty, M., White, J.C., Newman, L.A., Murphy, C.J., 2017. Nanomaterial Probes in the Environment: Gold Nanoparticle Soil Retention and Environmental Stability as a Function of Surface Chemistry. *ACS Sustain. Chem. Eng.* 5, pp. 11451–11458.

Lone, J.A., Kumar, A., Kundu, S., Lone, F.A., Suseela, M.R., 2013. Characterization of Tolerance Limit in *Spirulina platensis* in Relation to Nanoparticles. *Water. Air. Soil Pollut.* 224, p. 1670.

Loo, Y.Y., Rukayadi, Y., Nor-Khaizura, M.A.R., Kuan, C.H., Chieng, B.W., Nishibuchi, M., Radu, S., 2018. In Vitro Antimicrobial Activity of Green Synthesized Silver Nanoparticles Against Selected Gram-negative Foodborne Pathogens. *Front. Microbiol.* 9, p. 1555.

Maadane, A., Merghoub, N., Ainane, T., El Arroussi, H., Benhima, R., Amzazi, S., Bakri, Y., Wahby, I., 2015. Antioxidant activity of some Moroccan marine microalgae: Pufa profiles, carotenoids and phenolic content. *J. Biotechnol.* 215, pp. 13–19.

Machu, L., Misurcova, L., Vavra Ambrozova, J., Orsavova, J., Mlcek, J., Sochor, J., Jurikova, T., 2015a. Phenolic Content and Antioxidant Capacity in Algal Food Products. *Molecules* 20, pp. 1118–1133.

Mahana, A., Guliy, O.I., Mehta, S.K., 2021. Accumulation and cellular toxicity of engineered metallic nanoparticle in freshwater microalgae: Current status and future challenges. *Ecotoxicol. Environ. Saf.* 208, p. 111662.

Manier, N., Bado-Nilles, A., Delalain, P., Aguerre-Chariol, O., Pandard, P., 2013. Ecotoxicity of non-aged and aged CeO₂ nanomaterials towards freshwater microalgae. *Environ. Pollut.* 180, pp. 63–70.

Manzo, S., Miglietta, M.L., Rametta, G., Buono, S., Di Francia, G., 2013. Toxic effects of ZnO nanoparticles towards marine algae *Dunaliella tertiolecta*. *Sci. Total Environ.* 445–446, pp. 371–376.

Marin, S., Vlasceanu, G., Tiplea, R., Bucur, I., Lemnar, M., Marin, M., Grumezescu, A., 2015. Applications and Toxicity of Silver Nanoparticles: A Recent Review. *Curr. Top. Med. Chem.* 15, pp. 1596–1604.

Mary Leema, J.T., Kirubakaran, R., Vinithkumar, N.V., Dheen, P.S., Karthikayulu, S., 2010. High value pigment production from *Arthrospira (Spirulina) platensis* cultured in seawater. *Bioresour. Technol.* 101, pp. 9221–9227.

Metsoviti, M.N., Katsoulas, N., Karapanagiotidis, I.T., Papapolymerou, G., 2019. Effect of nitrogen concentration, two-stage and prolonged cultivation on growth rate, lipid and protein content of *Chlorella vulgaris*. *J. Chem. Technol. Biotechnol.* 94, pp. 1466–1473.

Metsoviti, M.N., Papapolymerou, G., Karapanagiotidis, I.T., Katsoulas, N., 2019. Comparison of Growth Rate and Nutrient Content of Five Microalgae Species Cultivated in Greenhouses. *Plants* 8, p. 279.

Metzler, D.M., Li, M., Erdem, A., Huang, C.P., 2011. Responses of algae to photocatalytic nano-TiO₂ particles with an emphasis on the effect of particle size. *Chem. Eng. J.* 170, pp. 538–546.

Miao, A.J., Luo, Z., Chen, C.-S., Chin, W.-C., Santschi, P.H., Quigg, A., 2010. Intracellular Uptake: A Possible Mechanism for Silver Engineered Nanoparticle Toxicity to a Freshwater Alga *Ochromonas danica*. *PLoS ONE* 5, p. e15196.

Miao, A.J., Schwehr, K.A., Xu, C., Zhang, S.-J., Luo, Z., Quigg, A., Santschi, P.H., 2009. The algal toxicity of silver engineered nanoparticles and detoxification by exopolymeric substances. *Environ. Pollut.* 157, pp. 3034–3041.

Miazek, K., Iwanek, W., Remacle, C., Richel, A., Goffin, D., 2015. Effect of Metals, Metalloids and Metallic Nanoparticles on Microalgae Growth and Industrial Product Biosynthesis: A Review. *Int. J. Mol. Sci.* 16, pp. 23929–23969.

Middepogu, A., Hou, J., Gao, X., Lin, D., 2018. Effect and mechanism of TiO₂ nanoparticles on the photosynthesis of *Chlorella pyrenoidosa*. *Ecotoxicol. Environ. Saf.* 161, pp. 497–506.

Mody, V., Siwale, R., Singh, A., Mody, H., 2010. Introduction to metallic nanoparticles. *J. Pharm. Bioallied Sci.* 2, p. 282.

Mohanraj, V.J., Chen, Y., 2007. Nanoparticles - A review. *Trop. J. Pharm. Res.* 5, pp. 561–573.

Molino, A., Iovine, A., Casella, P., Mehariya, S., Chianese, S., Cerbone, A., Rimauro, J., Musmarra, D., 2018. Microalgae Characterization for Consolidated and New Application in Human Food, Animal Feed and Nutraceuticals. *Int. J. Environ. Res. Public Health* 15, p. 2436.

Moon, J., Kwak, J.I., An, Y.-J., 2019. The effects of silver nanomaterial shape and size on toxicity to *Caenorhabditis elegans* in soil media. *Chemosphere* 215, pp. 50–56.

Moon, S., Narune, A., Prasad, E., 2022. Silver Nanoparticles Market by Synthesis Method (Wet Chemistry, Ion Implantation, and Biological Synthesis), Shape (Spheres, Platelets, Rods, Colloidal Silver Particles, and Others), and Application (Healthcare & Life science, Textile, Electronics & IT, Food & Beverages, Pharmaceuticals, Cosmetics, Water Treatment, and Others): Global Opportunity Analysis and Industry Forecast 2021-2030 (No. A06923). *Allied Market Research*.

Moraes, I. de O., Arruda, R. de O.M., Maresca, N.R., Antunes, A. de O., Moraes, R. de O., 2013. *Spirulina platensis*: process optimization to obtain biomass. *Ciênc. E Tecnol. Aliment.* 33, pp. 179–183.

Morones, J.R., Elechiguerra, J.L., Camacho, A., Holt, K., Kouri, J.B., Ramírez, J.T., Yacaman, M.J., 2005. The bactericidal effect of silver nanoparticles. *Nanotechnology* 16, pp. 2346–2353.

Moroney, J.V., Bartlett, S.G., Samuelsson, G., 2001. Carbonic anhydrases in plants and algae: Carbonic anhydrases in plants and algae. *Plant Cell Environ.* 24, pp. 141–153.

Mueller, N.C., Nowack, B., 2008. Exposure Modeling of Engineered Nanoparticles in the Environment. *Environ. Sci. Technol.* 42, pp. 4447–4453.

Mühling, M., Harris, N., Belay, A., Whitton, B.A., 2003. Reversal of helix orientation in the cyanobacterium *Arthrospira*. *J. Phycol.* 39, pp. 360–367.

Nagasamy Venkatesh, H., Bhowmik, H., Kuila, A., 2018. Metallic Nanoparticle: A Review. *Biomed. J. Sci. Tech. Res.* 4, pp. 3765–3775.

Narsing Rao, M.P., Dhulappa, A., 2022. Synthesis of silver nanoparticles using Actinobacteria. In: *Green Synthesis of Silver Nanomaterials*. Elsevier, pp. 479–492.

Navarro, E., Baun, A., Behra, R., Hartmann, N.B., Filser, J., Miao, A.-J., Quigg, A., Santschi, P.H., Sigg, L., 2008a. Environmental behavior and ecotoxicity of engineered nanoparticles to algae, plants, and fungi. *Ecotoxicology* 17, pp. 372–386.

Navarro, E., Piccapietra, F., Wagner, B., Marconi, F., Kaegi, R., Odzak, N., Sigg, L., Behra, R., 2008b. Toxicity of Silver Nanoparticles to *Chlamydomonas reinhardtii*. *Environ. Sci. Technol.* 42, pp. 8959–8964.

Nazari, F., Jafarirad, S., Movafeghi, A., Kosari-Nasab, M., Kazemi, E.M., 2020. Toxicity of microwave-synthesized silver-reduced graphene oxide nanocomposites to the microalga *Chlorella vulgaris*: Comparison with the hydrothermal method synthesized counterparts. *J. Environ. Sci. Health Part A* 55, pp. 639–649.

Nazari, F., Movafeghi, A., Jafarirad, S., Kosari-Nasab, M., Divband, B., 2018. Synthesis of Reduced Graphene Oxide-Silver Nanocomposites and Assessing Their Toxicity on the Green Microalga *Chlorella vulgaris*. *BioNanoScience* 8, pp. 997–1007.

Neale, P.A., Jämting, Å.K., O'Malley, E., Herrmann, J., Escher, B.I., 2015. Behaviour of titanium dioxide and zinc oxide nanoparticles in the presence of wastewater-derived organic matter and implications for algal toxicity. *Environ. Sci. Nano* 2, pp. 86–93.

Nielsen, S.S., 2010. Phenol-Sulfuric Acid Method for Total Carbohydrates. In: Nielsen, S.S. (Ed.), *Food Analysis Laboratory Manual, Food Science Texts Series*. Springer US, Boston, MA, pp. 47–53.

Oukarroum, A., Bras, S., Perreault, F., Popovic, R., 2012. Inhibitory effects of silver nanoparticles in two green algae, *Chlorella vulgaris* and *Dunaliella tertiolecta*. *Ecotoxicol. Environ. Saf.* 78, pp. 80–85.

Palmieri, D., Aliakbarian, B., Casazza, A.A., Ferrari, N., Spinella, G., Pane, B., Cafueri, G., Perego, P., Palombo, D., 2012. Effects of polyphenol extract from olive pomace on anoxia-induced endothelial dysfunction. *Microvasc. Res.* 83, pp. 281–289.

Panda, B.S., 2021. A Review on Synthesis of Silver Nanoparticles and their Biomedical Applications. *Lett. Appl. NanoBioScience* 11, pp. 3218–3231.

Pandurangan, M., Kim, D.H., 2015. In vitro toxicity of zinc oxide nanoparticles: a review. *J. Nanoparticle Res.* 17, 158.

Papapolymerou, G., Karayannis, V., Besios, A., Riga, A., Gougoulis, N., Spiliotis, X., 2018. Scaling-up sustainable *Chlorella vulgaris* microalgal biomass cultivation from laboratory to pilot-plant photobioreactor, towards biofuel. *Glob. NEST J.* 21, pp. 37–42.

Park, M.-H., Kim, K.-H., Lee, H.-H., Kim, J.-S., Hwang, S.-J., 2010. Selective inhibitory potential of silver nanoparticles on the harmful cyanobacterium *Microcystis aeruginosa*. *Biotechnol Lett* 6.

Pham, T.-L., 2019. Effect of Silver Nanoparticles on Tropical Freshwater and Marine Microalgae. *J. Chem.* 2019, pp. 1–7.

Pillai, S., Behra, R., Nestler, H., Suter, M.J.-F., Sigg, L., Schirmer, K., 2014. Linking toxicity and adaptive responses across the transcriptome, proteome, and phenotype of *Chlamydomonas reinhardtii* exposed to silver. *Proc. Natl. Acad. Sci.* 111, pp. 3490–3495.

Precedence Research, 2022. Nanomaterials Market (By Product: Carbon Nanotubes, Titanium Nanoparticles, Silver Nanoparticles, Aluminum Oxide Nanomaterials, Gold (Au), Iron (Fe), Copper (Cu), Platinum (Pt), Nickel (Ni), Antimony Tin Oxide, Bismuth Oxide, Others; By Application: Aerospace, Automotive, Medical, Energy & power, Electronics, Paints & Coatings, Others) - Global Industry Analysis, Size, Share, Growth, Trends, Regional Outlook, and Forecast 2022 – 2030 (No. 1752).

Puspitasari, R., Suratno, Purbonegoro, T., Agustin, A.T., 2018. Cu toxicity on growth and chlorophyll-a of *Chaetoceros* sp. *IOP Conf. Ser. Earth Environ. Sci.* 118, p. 012061.

Qin, Y., 2005. Silver-containing alginate fibres and dressings. *Int. Wound J.* 2, pp. 172–176.

Ramkumar, V.S., Pugazhendhi, A., Gopalakrishnan, K., Sivagurunathan, P., Saratale, G.D., Dung, T.N.B., Kannapiran, E., 2017. Biofabrication and characterization of silver nanoparticles using aqueous extract of seaweed *Enteromorpha compressa* and its biomedical properties. *Biotechnol. Rep.* 14, pp. 1–7.

Reboleira, J., Freitas, R., Pinteus, S., Silva, J., Alves, C., Pedrosa, R., Bernardino, S., 2019. Spirulina. In: *Nonvitamin and Nonmineral Nutritional Supplements*. Elsevier, pp. 409–413.

Ribeiro, F., Gallego-Urrea, J.A., Goodhead, R.M., Van Gestel, C.A.M., Moger, J., Soares, A.M.V.M., Loureiro, S., 2015. Uptake and elimination kinetics of silver nanoparticles and silver nitrate by *Raphidocelis subcapitata*: The influence of silver behaviour in solution. *Nanotoxicology* 9, pp. 686–695.

Richmond, A. (Ed.), 2003. *Handbook of Microalgal Culture*. Blackwell Publishing Ltd, Oxford, UK.

Rizwan, M., Mujtaba, G., Lee, K., 2017. Effects of iron sources on the growth and lipid/carbohydrate production of marine microalga *Dunaliella tertiolecta*. *Biotechnol. Bioprocess Eng.* 22, pp. 68–75.

Rolland, J.P., Maynor, B.W., Euliss, L.E., Exner, A.E., Denison, G.M., DeSimone, J.M., 2005. Direct Fabrication and Harvesting of Monodisperse, Shape-Specific Nanobiomaterials. *J. Am. Chem. Soc.* 127, pp. 10096–10100.

Romero, N., Visentini, F.F., Márquez, V.E., Santiago, L.G., Castro, G.R., Gagneten, A.M., 2020. Physiological and morphological responses of green microalgae *Chlorella vulgaris* to silver nanoparticles. *Environ. Res.* 189, p. 109857.

Ruangsomboon, S., 2012. Effect of light, nutrient, cultivation time and salinity on lipid production of newly isolated strain of the green microalga, *Botryococcus braunii* KMITL 2. *Bioresour. Technol.* 109, pp. 261–265.

Rzymiski, P., Budzulak, J., Niedzielski, P., Klimaszuk, P., Proch, J., Kozak, L., Poniedziałek, B., 2019. Essential and toxic elements in commercial microalgal food supplements. *J. Appl. Phycol.* 31, pp. 3567–3579.

Saçan, M.T., Oztay, F., Bolkent, S., 2007. Exposure of *Dunaliella tertiolecta* to Lead and Aluminum: Toxicity and Effects on Ultrastructure. *Biol. Trace Elem. Res.* 120, pp. 264–272.

Sadiq, I.M., Pakrashi, S., Chandrasekaran, N., Mukherjee, A., 2011. Studies on toxicity of aluminum oxide (Al₂O₃) nanoparticles to microalgae species: *Scenedesmus* sp. and *Chlorella* sp. *J. Nanoparticle Res.* 13, pp. 3287–3299.

Sathasivam, R., Radhakrishnan, R., Hashem, A., Abd_Allah, E.F., 2019. Microalgae metabolites: A rich source for food and medicine. *Saudi J. Biol. Sci.* 26, pp. 709–722.

Schultz, S., Smith, D.R., Mock, J.J., Schultz, D.A., 2000. Single-target molecule detection with nonbleaching multicolor optical immunolabels. *Proc. Natl. Acad. Sci.* 97, pp. 996–1001.

Sendra, M., Blasco, J., Araújo, C.V.M., 2018. Is the cell wall of marine phytoplankton a protective barrier or a nanoparticle interaction site? Toxicological responses of *Chlorella autotrophica* and *Dunaliella salina* to Ag and CeO₂ nanoparticles. *Ecol. Indic.* 95, pp. 1053–1067.

Sendra, M., Yeste, M.P., Gatica, J.M., Moreno-Garrido, I., Blasco, J., 2017. Direct and indirect effects of silver nanoparticles on freshwater and marine microalgae (*Chlamydomonas reinhardtii* and *Phaeodactylum tricorutum*). *Chemosphere* 179, pp. 279–289.

Shao, W., Ebaid, R., El-Sheekh, M., Abomohra, A., Eladel, H., 2019. Pharmaceutical applications and consequent environmental impacts of *Spirulina* (*Arthrospira*): An overview. *Grasas Aceites* 70, p. 292.

Sharma, J., Kumar, S.S., Bishnoi, N.R., Pugazhendhi, A., 2019. Screening and enrichment of high lipid producing microalgal consortia. *J. Photochem. Photobiol. B* 192, pp. 8–12.

Sheng, P.X., Ting, Y.-P., Chen, J.P., Hong, L., 2004. Sorption of lead, copper, cadmium, zinc, and nickel by marine algal biomass: characterization of biosorptive capacity and investigation of mechanisms. *J. Colloid Interface Sci.* 275, pp. 131–141.

Sibi, G., Ananda Kumar, D., Gopal, T., Harinath, K., Banupriya, S., Chaitra, S., 2017. Metal Nanoparticle Triggered Growth and Lipid Production in *Chlorella vulgaris*. *Int. J. Sci. Res. Environ. Sci. Toxicol.* 2, pp. 1–8.

Siddiqui, M.W., Prasad, K. (Eds.), 2017. *Plant Secondary Metabolites, Volume One: Biological and Therapeutic Significance*, 0 ed. Apple Academic Press, New Jersey: Apple Academic Press, Inc.

Sondi, I., Salopek-Sondi, B., 2004. Silver nanoparticles as antimicrobial agent: a case study on *E. coli* as a model for Gram-negative bacteria. *J. Colloid Interface Sci.* 6.

Sørensen, S.N., Baun, A., 2015. Controlling silver nanoparticle exposure in algal toxicity testing – A matter of timing. *Nanotoxicology* 9, pp. 201–209.

Stanic-Vucinic, D., Minic, S., Nikolic, M.R., Velickovic, T.C., 2018. Spirulina Phycobiliproteins as Food Components and Complements. In: Jacob-Lopes, E., Zepka, L.Q., Queiroz, M.I. (Eds.), *Microalgal Biotechnology*. InTech.

Stepanov, A.L., Popok, V.N., Hole, D.E., 2002. Formation of Metallic Nanoparticles in Silicate Glass through Ion Implantation. *Glass Phys. Chem.* 28, pp. 90–95.

Sufian, M.M., Khattak, J.Z.K., Yousaf, S., Rana, M.S., 2017. Safety issues associated with the use of nanoparticles in human body. *Photodiagnosis Photodyn. Ther.* 19, pp. 67–72.

Sukenik, A., Carmeli, Y., Berner, T., 1989. Regulation of fatty acid composition by irradiance level in the eustigmatophyte *Nannochloropsis* sp.1. *J. Phycol.* 25, pp. 686–692.

Suman, T.Y., Radhika Rajasree, S.R., Kirubakaran, R., 2015. Evaluation of zinc oxide nanoparticles toxicity on marine algae *Chlorella vulgaris* through flow cytometric, cytotoxicity and oxidative stress analysis. *Ecotoxicol. Environ. Saf.* 113, pp. 23–30.

Sunda, W.G., 2012. Feedback Interactions between Trace Metal Nutrients and Phytoplankton in the Ocean. *Front. Microbiol.* 3, p. 204.

Syafiuddin, A., Salmiati, S., Hadibarata, T., Kueh, A.B.H., Salim, M.R., Zaini, M.A.A., 2018. Silver Nanoparticles in the Water Environment in Malaysia: Inspection, characterization, removal, modeling, and future perspective. *Sci. Rep.* 8, p. 986.

Tan, C.H., Show, P.L., Lam, M.K., Fu, X., Ling, T.C., Chen, C.-Y., Chang, J.-S., 2020. Examination of indigenous microalgal species for maximal protein synthesis. *Biochem. Eng. J.* 154, p. 107425.

Tang, Y., Xin, H., Yang, S., Guo, M., Malkoske, T., Yin, D., Xia, S., 2018. Environmental risks of ZnO nanoparticle exposure on *Microcystis aeruginosa*: Toxic effects and environmental feedback. *Aquat. Toxicol.* 204, pp. 19–26.

Tibbetts, S.M., Milley, J.E., Lall, S.P., 2015. Chemical composition and nutritional properties of freshwater and marine microalgal biomass cultured in photobioreactors. *J. Appl. Phycol.* 27, pp. 1109–1119.

Tolaymat, T.M., El Badawy, A.M., Genaidy, A., Scheckel, K.G., Luxton, T.P., Suidan, M., 2010. An evidence-based environmental perspective of manufactured silver nanoparticle in syntheses and applications: A systematic review and critical appraisal of peer-reviewed scientific papers. *Sci. Total Environ.* 408, pp. 999–1006.

Urnuksaikhhan, E., Bold, B.E., Gunbileg, A., Sukhbaatar, N., Mishig-Ochir, T., 2021. Antibacterial activity and characteristics of silver nanoparticles biosynthesized from *Carduus crispus*. *Sci. Rep.* 11, p. 21047.

van Eykelenburg, C., 1979. The ultrastructure of *Spirulina platensis* in relation to temperature and light intensity. *Antonie Van Leeuwenhoek* 45, pp. 369–390.

Vance, M.E., Kuiken, T., Vejerano, E.P., McGinnis, S.P., Hochella, M.F., Rejeski, D., Hull, M.S., 2015. Nanotechnology in the real world: Redeveloping the nanomaterial consumer products inventory. *Beilstein J. Nanotechnol.* 6, pp. 1769–1780.

Vega, J.M., Herrera, J., Aparicio, P.J., Paneque, A., Losada, M., 1971. Role of Molybdenum in Nitrate Reduction by *Chlorella*. *Plant Physiol.* 48, pp 294–299.

Venkataraman, L.V., 1997. *Spirulina platensis* (*Arthrospira*): Physiology, Cell Biology and Biotechnologym. *J. Appl. Phycol.* 9, pp. 295–296.

Vogt, T., 2010. Phenylpropanoid Biosynthesis. *Mol. Plant* 3, pp. 2–20.

Wan, D., Wu, Q., Kuča, K., 2021. Spirulina. In: *Nutraceuticals*. Elsevier, pp. 959–974.

Wang, F., Guan, W., Xu, L., Ding, Z., Ma, H., Ma, A., Terry, N., 2019. Effects of Nanoparticles on Algae: Adsorption, Distribution, Ecotoxicity and Fate. *Appl. Sci.* 9, p. 1534.

Wen, L.-S., Santschi, P.H., Gill, G.A., Paternostro, C.L., Lehman, R.D., 1997. Colloidal and Particulate Silver in River and Estuarine Waters of Texas. *Environ. Sci. Technol.* 31, pp. 723–731.

Wijffels, R.H., Barbosa, M.J., Eppink, M.H.M., 2010. Microalgae for the production of bulk chemicals and biofuels. *Biofuels Bioprod. Biorefining* 4, pp. 287–295.

Wong, S.W.Y., Leung, P.T.Y., Djurišić, A.B., Leung, K.M.Y., 2010. Toxicities of nano zinc oxide to five marine organisms: influences of aggregate size and ion solubility. *Anal. Bioanal. Chem.* 396, pp. 609–618.

Xia, B., Chen, B., Sun, X., Qu, K., Ma, F., Du, M., 2015. Interaction of TiO₂ nanoparticles with the marine microalga *Nitzschia closterium*: Growth inhibition, oxidative stress and internalization. *Sci. Total Environ.* 508, pp. 525–533.

Yeo, M., Pak, S., 2008. Exposing zebrafish to silver nanoparticles during caudal fin regeneration disrupts caudal fin growth and p53 signaling. *Mol. Cell. Toxicol.* 4, pp. 311–317.

Yeo, M., Yoon, J., 2009. Comparison of the Effects of Nano-silver Antibacterial Coatings and Silver Ions on Zebrafish Embryogenesis. *Mol. Cell. Toxicol.* 5, pp. 23–31.

Zaidi, S., Maurya, C., Shankhadarwar, S., Pius, J., 2014. Silver nanoparticles – chlorella interaction: effect on metabolites. In: *Bioscience Discovery*, 1-I. Presented at the National Conference on Conservation of Natural Resources & Biodiversity for Sustainable Development, RUT Printer and Publisher, pp. 62–65.

Zeng, M.-T., Vonshak, A., 1998. Adaptation of *Spirulina platensis* to salinity-stress. *Comp. Biochem. Physiol. A. Mol. Integr. Physiol.* 120, pp. 113–118.

Zhang, H., Huang, Q., Xu, A., Wu, L., 2016. Spectroscopic probe to contribution of physicochemical transformations in the toxicity of aged ZnO NPs to *Chlorella vulgaris*: new insight into the variation of toxicity of ZnO NPs under aging process. *Nanotoxicology* 10, pp. 1177–1187.

Zhao, C.-M., Wang, W.-X., 2010. Biokinetic Uptake and Efflux of Silver Nanoparticles in *Daphnia magna*. *Environ. Sci. Technol.* 44, pp. 7699–7704.

Zhu, S., Wang, Y., Shang, C., Wang, Z., Xu, J., Yuan, Z., 2015. Characterization of lipid and fatty acids composition of *Chlorella zofingiensis* in response to nitrogen starvation. *J. Biosci. Bioeng.* 120, pp. 205–209.

Zhurkov, V.S., Savostikova, O.N., Yurchenko, V.V., Krivtsova, E.K., Kovalenko, M.A., Murav'eva, L.V., Alekseeva, A.V., Belyaeva, N.N., Mikhailova, R.I., Sycheva, L.P., 2017. Features of the Mutagenic and Cytotoxic Effects of Nanosilver and Silver Sulfate in Mice. *Nanotechnologies Russ.* 12, pp. 667–672.

Zinicovscaia, I., Chiriac, T., Cepoi, L., Rudi, L., Culicov, O., Frontasyeva, M., Rudic, V., 2017. Selenium uptake and assessment of the biochemical changes in *Arthrospira (Spirulina) platensis* biomass during the synthesis of selenium nanoparticles. *Can. J. Microbiol.* 63, pp. 27–34.

Zinicovscaia, I., Yushin, N., Pantelica, A., Demčák, Š., Mitu, A., Apostol, A.I., 2020. Lithium Biosorption by *Arthrospira (Spirulina) platensis* Biomass. *Ecol. Chem. Eng. S* 27, pp. 271–280.

LIST OF PUBLICATIONS AND CONFERENCE PRESENTATIONS

PUBLICATIONS

1. Liang, S.X.T., Wong, L.S., Antony Dhanapal, A.C.T. and Djearamane, S., 2020. Toxicity of metals and metallic nanoparticles on nutritional properties of microalgae. *Water, Air, & Soil Pollution*, 231(2), pp. 1-14.

Water Air Soil Pollut (2020) 231:52
<https://doi.org/10.1007/s11270-020-4413-5>

Toxicity of Metals and Metallic Nanoparticles on Nutritional Properties of Microalgae

Sharolynne Xiao Tong Liang · Ling Shing Wong ·
Anto Cordelia Tanislaus Antony Dhanapal ·
Sinouvassane Djearamane

Received: 7 October 2019 / Accepted: 10 January 2020
© Springer Nature Switzerland AG 2020

Abstract Microalgae has been utilized as food and supplement by humans for more than thousands of years due to their high nutritional properties such as proteins, vitamins, minerals, and other nutrients. However, the improvement in the modern society caused increased release of metals and metallic nanoparticles (MNPs) into the freshwater that might cause toxicity to the marine and freshwater microalgae. Although low concentration of these metals and MNPs will not affect the metabolism of microalgae, high concentration of metals and MNPs, on the other hand, can cause toxicity to microalgae. Studies have been done to evaluate the toxicity mechanism of metals and MNPs and the effect of these metals

(pigments, biological macromolecules, and phenolic compounds) of microalgae are summarized as well.

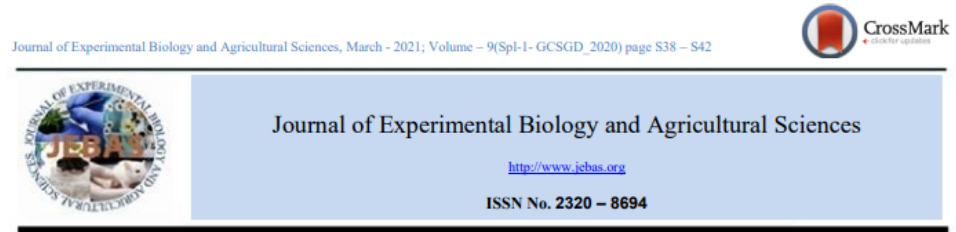
Keywords Nutritional properties · Microalgae · Metallic nanoparticles · Toxicity · Metal stress

1 Introduction

Microalgae are photosynthetic unicellular organisms that use light energy to convert carbon dioxide from the surrounding to produce organic carbon, with short



2. Liang, S.X.T., Wong, L.S., Antony Dhanapal, A.C.T., Balu, P. and Djearmane, S., 2021. Therapeutic applications of spirulina against human pathogenic viruses. *Journal of Experimental Biology and Agricultural Sciences*, 9, pp. S38-S42.



THERAPEUTIC APPLICATIONS OF *Spirulina* AGAINST HUMAN PATHOGENIC VIRUSES

Sharolynne Xiao Tong Liang¹, Ling Shing Wong², Anto Cordelia Tanislaus Antony Dhanapal³, Prakash Balu⁴, Sinouvassane Djearmane^{1*}

¹Department of Biomedical Science, Faculty of Science, Universiti Tunku Abdul Rahman, Kampar, 31900 Malaysia

²Life Science Division, Faculty of Health and Life Sciences, INTI International University, Nilai, 71800 Malaysia

³Department of Chemical Science, Faculty of Science, Universiti Tunku Abdul Rahman, Kampar, 31900 Malaysia

⁴Department of Biotechnology, School of Life Sciences, Vels Institute of Science, Technology and Advanced Studies (VISTAS), Chennai, Tamil Nadu, 600117, India

Received – July 18, 2020; Revision – September 17, 2020; Accepted – January 03, 2021

Available Online – March 25, 2021

DOI: [http://dx.doi.org/10.18006/2021.9\(Spl-1-GCSGD_2020\).S38.S42](http://dx.doi.org/10.18006/2021.9(Spl-1-GCSGD_2020).S38.S42)

KEYWORDS

Spirulina

Cyanobacteria

ABSTRACT

Viruses can spread worldwide and the early detection of emerging infectious diseases and outbreaks in humans and animals is important for effective surveillance and prevention. Viruses such as human immunodeficiency virus (HIV), swine flu, and influenza virus are some of the viruses that spread

ACCEPTED PAPER

1. Liang, S.X.T., Wong, L.S., Antony Dhanapal, A.C.T., Balu, P. and Djearamane, S., 2022. Impact of Silver Nanoparticles on the Nutritional Properties of *Spirulina platensis*. *PeerJ*.

Decision on your PeerJ submission: "Impact of silver nanoparticles on the nutritional properties of *Arthrospira platensis*" (#2022:02:70828:2:0:REVIEW) ▸ Inbox x

→ PeerJ <peer.review@peerj.com>
to me ▾

Wed, Aug 10, 12:25 AM

PeerJ

Dear Dr. Liang,

Thank you for your submission to PeerJ.

I am writing to inform you that your manuscript - **Impact of silver nanoparticles on the nutritional properties of *Arthrospira platensis*** - has been **Accepted** for publication. Congratulations!

This is an editorial acceptance; publication is dependent on authors meeting all journal policies and guidelines.

CONFERENCE PRESENTATIONS

1. Liang, S.X.T., Djearamane, S., Antony Dhanapal, A.C.T., Wong, L.S. “Toxic effects of silver nanoparticles on the nutritional properties of *Spirulina platensis*”. *International Conference on Green Sustainable Technology and Management (ICGSTM) 2022* held by INTI International University on 10 – 11 June 2022. (Oral presentation)



2. Liang, S.X.T., Djearamane, S., Antony Dhanapal, A.C.T., Wong, L.S. "Impact of silver nanoparticles *Spirulina platensis*". 12th MIFT National Food Science and Technology Competition 2021 held by the Malaysia Institute of Food Technology (MIFT) and Tunku Abdul Rahman University College (TARUC) on 4-5 August 2021. (Poster presentation)



3. Liang, S.X.T., Djearamane, S., Antony Dhanapal, A.C.T., Wong, L.S., Balu, P. “Therapeutic applications of *Spirulina* against human pathogenic viruses” *1st Postgraduate Colloquium on Science Technology, Engineering & Mathematics (STEM) 2021* held by Universiti Tunku Abdul Rahman, Kampar Campus, Perak, Malaysia on 27 May 2021. (Oral presentation)



Certificate of Participation

This is to certify that

SHAROLYNNE LIANG XIAO TONG
(Oral Presenter)

Hereby recognized for participation in the
1st Postgraduate Colloquium on Science, Technology, Engineering & Mathematics (STEM) 2021

Co-organised by
Faculty of Information and Communication Technology (FICT), Faculty of Engineering and Green Technology (FEGT),
Faculty of Science (FSc), Centre for Agriculture and Food Research (CAFR) & Centre of Internet of Things and Big Data (CIoTBD)
held on **27th May 2021**
Universiti Tunku Abdul Rahman, Kampar Campus, Perak, Malaysia

Ms Wong Li Min
Chairperson of the event

Ts Dr Goh Hock Guan
Deputy Dean, FICT

Dr Lo Po Kim
Deputy Dean, FEGT

Dr Phoon Lee Quen
Deputy Dean, FSc

APPENDIX A

Chemical and Reagent Preparation

Culture medium for *Spirulina*

Culture medium for *Spirulina* was prepared according to Table 3.1 to Table 3.4. Working culture medium for *Spirulina* was prepared by combining Solution 1 and Solution 2 in 1:1 ratio, producing 1 L of the medium. Stock culture medium was autoclaved (HVE-50, Hirayama, Japan) at 121°C for 30 minutes under 15 psi.

Table 1: Recipe for Solution 1.

Component	Amount
NaHCO ₃ (Gene Chemicals, Malaysia)	13.61 g/0.5 L
Na ₂ CO ₃ (QRec, Malaysia)	4.03 g/0.5 L
K ₂ HPO ₄ (QRec, Malaysia)	0.50 g/0.5 L

Table 2: Recipe for Solution 2.

Component	Amount
NaNO ₃ (Gene Chemicals, Malaysia)	2.50 g/0.5 L
K ₂ SO ₄ (Merck, Malaysia)	1.00 g/0.5 L
NaCl (Merck, Malaysia)	1.00 g/0.5 L
MgSO ₄ ·7H ₂ O (Merck, Malaysia)	0.20 g/0.5 L
CaCl ₂ ·2H ₂ O (Sigma-Aldrich, Malaysia)	0.04 g/0.5 L
P-IV metal solution	6 mL/0.5 L
Chu micronutrient solution	1 mL/0.5 L

Table 3: Recipe for P-IV metal solution.

Component	Amount
Na ₂ EDTA·2H ₂ O (Merck, Malaysia)	0.750 g/L
FeCl ₃ ·6H ₂ O (Merck, Malaysia)	0.097 g/L
MnCl ₂ ·4H ₂ O (Merck, Malaysia)	0.041 g/L
ZnCl ₂ (Sigma-Aldrich, Malaysia)	0.005 g/L
CoCl ₂ ·6H ₂ O (Sigma-Aldrich, Malaysia)	0.002 g/L
Na ₂ MoO ₄ ·2H ₂ O (Merck, Malaysia)	0.004 g/L

Table 4: Recipe for Chu micronutrient solution.

Component	Amount
CuSO ₄ ·5H ₂ O (Merck, Malaysia)	0.020 g/L
ZnSO ₄ ·7H ₂ O (Sigma-Aldrich, Malaysia)	0.044 g/L
CoCl ₂ ·6H ₂ O (Sigma-Aldrich, Malaysia)	0.020 g/L
MnCl ₂ ·4H ₂ O (Merck, Malaysia)	0.012 g/L
Na ₂ MoO ₄ ·2H ₂ O (Merck, Malaysia)	0.012 g/L
H ₃ BO ₃ (R&M Chemicals, Malaysia)	0.620 g/L
Na ₂ EDTA·2H ₂ O (Merck, Malaysia)	0.050 g/L

Culture medium with silver nanoparticles (Ag NPs)

Ag NPs was purchased from Sigma-Aldrich, Malaysia. Stock culture solution with Ag NPs (200 µg/mL) was prepared by adding 0.16 g of Ag NPs powder into 800 mL of *Spirulina* medium and ultra-sonicated (Tru-Sweep Ultrasonic Cleaner, Crest Ultrasonics, Malaysia) at 40 kHz until the NPs were homogenously dispersed in the medium. The stock solution was then diluted with *Spirulina* medium to prepare the working concentrations of 100 µg/mL (1:2 dilution), 50 µg/mL (1:4 dilution), 25 µg/mL (1:8 dilution), 10 µg/mL (1:20 dilution), and 5 µg/mL (1:40 dilution) of Ag NPs.

Phosphate buffered saline (PBS), 1x

Phosphate buffered saline stock solution (10x) was purchased from Sigma-Aldrich, Malaysia. A 10-fold dilution was done to prepare 1x PBS from 10x PBS by diluting 100 mL of 10x PBS with 900 mL of distilled water.

Protein Assay

Bovine serum albumin (BSA, 100 µg/mL) powder was obtained from Sigma-Aldrich, Malaysia. NaOH and NaK tartrate·4H₂O were purchased from Sigma-Aldrich, Malaysia and Fisher Chemical, Malaysia, respectively. Folin-Ciocalteu phenol reagent was provided by R&M Chemicals, Malaysia. Stock solution of bovine serum albumin (BSA, 100 µg/mL) was prepared by dissolving 5 mg of BSA powder in 50 mL of distilled water. The stock solution of BSA was then diluted with distilled water to prepare the working concentrations of 10, 20, 30,

40 and 50 µg/mL. Sodium hydroxide (NaOH, 0.5 N) solution was prepared by dissolving 20 g of NaOH pellet in 1000 mL distilled water. Lowry solution was made up freshly for every use using Lowry reagents A (2% (w/v) Na₂CO₃ in 0.1 N NaOH), B (1% (w/v) NaK tartrate·4H₂O), and C (0.5% (w/v) CuSO₄·4H₂O) with the ratio of reagent A:B:C = 48:1:1. The preparation for Lowry reagent A, B, and C were as follows: Lowry reagent A: 2 g of sodium carbonate (Na₂CO₃) and 0.4 g of NaOH in 100 mL of distilled water; Lowry reagent B: 1 g of potassium sodium tartrate tetrahydrate (NaK tartrate·4H₂O) in 99 mL of distilled water; Lowry reagent C: 0.5 g of copper sulphate (CuSO₄) in 99.5 mL distilled water. Folin-Ciocalteu phenol reagent (FCR, 1 N) was prepared freshly by dissolving FCR with distilled water in 1:1 ratio.

Lipid Assay

Chloroform was purchased from Fisher Chemical, Malaysia and methanol was purchased from RCI Labscan, Malaysia. Chloroform/methanol/water (1/2/0.8, v/v/v) was prepared by mixing 200 mL of chloroform, 400 mL of methanol and 160 mL of distilled water to produce 760 mL of the solution.

Carbohydrate Assay

Glucose and hydrochloric acid (HCl, 2.5M) were obtained from Fisher Chemical, Malaysia and QRë, Malaysia. Stock solution for glucose (100 µg/mL) was prepared by dissolving 5 mg of glucose powder in 50 mL of distilled water. The stock solution was diluted with distilled water to obtain the working concentrations of 10, 20, 30, 40 and 50 µg/mL. Hydrochloric acid (HCl, 2.5 N)

was prepared by dissolving 41 mL of 37% HCl in 159 mL of distilled water. Phenol (80%, w/w) was prepared by dissolving 40 g of phenol in 10 g of distilled water.

Chlorophyll-*a* and Carotenoid Assay

A 900 mL methanol was diluted in 100 mL of distilled water to obtain 1 L of 90% methanol solution.

C-phycoyanin Assay

Sodium phosphate dibasic heptahydrate ($\text{Na}_2\text{HPO}_4 \cdot 7\text{H}_2\text{O}$) and sodium phosphate monobasic monohydrate ($\text{NaH}_2\text{PO}_4 \cdot \text{H}_2\text{O}$) are supplied by R&M Chemicals, Malaysia. Phosphate buffer (0.05 M, pH 6.7) was prepared by adding 5.971 g of sodium phosphate dibasic heptahydrate ($\text{Na}_2\text{HPO}_4 \cdot 7\text{H}_2\text{O}$) and 3.826 g of sodium phosphate monobasic monohydrate ($\text{NaH}_2\text{PO}_4 \cdot \text{H}_2\text{O}$) into 800 mL of distilled water. The pH of the solution was adjusted using NaOH/HCl to 6.7 and topped up to 1 L with distilled water.

Total Phenolic Compound Assay

Gallic acid powder was obtained from R&M Chemicals, Malaysia. Stock solution of gallic acid (100 $\mu\text{g}/\text{mL}$) was prepared by dissolving 5 mg of gallic acid powder in 50 mL of distilled water. The stock solution was diluted with distilled water to obtain the working concentrations of 10, 20, 30, 40 and 50

$\mu\text{g/mL}$. Sodium carbonate (Na_2CO_3 , 20%) was prepared by dissolving 20 g of Na_2CO_3 powder in 100 mL of distilled water.

APPENDIX B

Turnitin Report

Turnitin Originality Report

Processed on: 29-Jan-2023 20:14 +08
ID: 2001486168
Word Count: 16194
Submitted: 2

Document Viewer



Impact of Silver Nanoparticles on the Nutri... By Sharolynne Liang

Similarity Index 18%	Similarity by Source	
	Internet Sources:	8%
	Publications:	14%
	Student Papers:	4%